

# **Characterization of Interply Shear Behaviour of Out-of-Autoclave Thermosetting Prepreg Composites**

Harinderpal Singh Grewal

A thesis

in

The Department

of

Mechanical and Industrial Engineering

Presented in Partial Fulfillment of the Requirements

for the Degree of Master of Applied Science (Mechanical Engineering)

at Concordia University

Montreal, Quebec, Canada

September 2015

© Harinderpal Singh Grewal, 2015

**CONCORDIA UNIVERSITY**

**School of Graduate Studies**

This is to certify that the thesis prepared

By: Harinderpal Singh Grewal

Entitled: Characterization of Interply Shear Behaviour of Out-of-Autoclave Thermosetting Prepreg Composites

and submitted in partial fulfillment of the requirements for the degree of

**Master of Applied Science (Mechanical Engineering)**

complies with the regulations of the University and meets the accepted standards with respect to originality and quality.

Signed by the final Examining Committee:

\_\_\_\_\_  
Chair  
Dr. R. Bhat

\_\_\_\_\_  
Examiner  
Dr. S. V. Hoa

\_\_\_\_\_  
External Examiner  
Dr. C. Marsden

\_\_\_\_\_  
Examiner and Supervisor  
Dr. M. Hojjati

Approved by \_\_\_\_\_

Dr. S. Narayanswamy, MASC Program Director

Department of Mechanical and Industrial Engineering

\_\_\_\_\_  
Dr. Amir Asif  
Dean, Faculty of Engineering and Computer Science

Date: September 17<sup>th</sup>, 2015

## ABSTRACT

### **Characterization of Interply Shear Behaviour of Out-of-Autoclave Thermosetting Prepreg Composites**

Harinderpal Singh Grewal

Thermoforming of composite materials includes deforming the flat sheets of prepreg laminates into complex shaped composite parts. This deformation of flat laminates into complex shapes can cause wrinkles in the final part. External processing conditions of forming process must be chosen in a way to minimize wrinkles. This dissertation describes the experimental technique to measure friction between two plies of thermoset prepreg. A test rig was designed and constructed which can provide different temperatures and different normal pressures to the prepreg sample. This test rig was installed on a tensile testing machine which can provide different pulling rates and measure the frictional resistance between prepreg layers. It was observed that a yield shear stress level associated with each set of external processing conditions exists which has to be overcome to begin the layer slippage. Further continuing the slippage requires less force than the initial yield shear force. The results show that the temperature is the most influencing external processing parameter as the coefficient of friction decreases significantly with increase in temperature. This is due to the resin viscosity reduction. Forming rate which was simulated by pulling velocity in experimental set up has less effect on the interply friction. Larger friction coefficient was found at higher pulling velocities and vice versa. With the increase in normal pressure, the coefficient of friction decreases. By comparing the 8HS, 5HS and UD prepregs, frictional resistance was found to be the largest in unidirectional composites, followed by 8-harness and 5-harness composites respectively. It was observed that change in the fabric (fiber) orientation of the prepreg plies has effect on interply friction. Interestingly, experimental results show that friction mechanism between prepreg plies is mixed friction i.e. it is dominated by coulomb friction as well as hydrodynamic friction. To draw Stribeck curves, Hersey number was calculated and plotted against the coefficient of friction. A friction model was developed based on the linear relationship between friction coefficient and Hersey number. By deriving the relationship between angle  $\theta$  and the two variables from linear equations, a general equation was developed which could be used to predict coefficient of friction for any set of processing conditions at any fabric (fiber) orientation. A design of experiments

technique, Taguchi method, was adopted to find the optimum processing parameters in thermoforming of composites. Analysis of Variance was used to find the contribution of each parameter.

**Keywords:** Composite Forming, Thermosetting Composite, Out-of-Autoclave Prepreg, Interply Friction, Hersey Number, Stribeck Curve, Taguchi Method.

## ACKNOWLEDGEMENTS

I would like to express my sincere gratitude to my supervisor, Dr. Mehdi Hojjati, for his relentless support and unconventional patience in helping me throughout the course of the thesis project.

I would like to thank Dr. Suong Van Hoa for allowing me to access the facilities in the CONCOM laboratories. I am very thankful to Natural Sciences and Engineering Research Council of Canada (NSERC) and Bombardier Aerospace for providing me the financial support and the required material throughout this project.

I am extremely grateful to Mr. Dainius Juras and Dr. Iosif Daniel Rosca for their guidance and technical support. I would also like to thank Mr. Henry and Mr. Heng Wang for their timely help regarding my experimental work.

Finally, I would like to take this opportunity to extend my deep appreciation to my family and friends, for their unconditional love and support during the course of the project. The deepest appreciation is expressed to my mother for her encouragement and endless love throughout my course of study. I would like to dedicate this thesis to my parents, Mr. Gurdip Singh and Mrs. Narinder Kaur.

## TABLE OF CONTENTS

Chapter 1 : Introduction .....	1
1.1 Thesis Organization .....	3
1.2 Introduction to Forming Operations .....	4
1.3 Pre-impregnated composites (Prepregs) .....	5
1.4 Diaphragm Forming.....	6
1.5 Motive.....	7
1.6 Thesis Objectives and Challenges .....	7
Chapter 2 : Literature Review.....	9
2.1 Composite forming mechanisms.....	9
2.2 Inter-ply Slippage.....	12
2.3 Inter-ply Friction test methodology .....	14
2.3.1 Pull-out rig .....	15
2.3.2 Pull-through rig.....	16
2.4 Out-of-Autoclave curing.....	17
2.5 Stribeck Curve .....	17
Chapter 3 : Materials and Test Apparatus.....	20
3.1 Material Selection .....	20
3.1.1 CYCOM 5320-1 Resin System.....	22
3.2 Rheological characterization of the prepreg .....	22
3.3 Sample Preparation .....	23
3.4 Design of Friction Test Rig.....	25
3.4.1 Schematic of Test Rig.....	26
3.4.2 Temperature Control.....	27

3.4.3 Temperature Distribution.....	28
3.4.4 Pressure Control.....	30
3.5 Summary.....	32
Chapter 4 : Experiments, Results and Discussions.....	33
4.1 Experimentation and Results .....	33
4.2 Test Conditions .....	36
4.3 Influence of Temperature.....	37
4.4 Influence of Pulling Rate .....	40
4.5 Influence of Normal Pressure .....	43
4.6 Influence of Fiber Orientation .....	47
4.7 Microscopic Analysis.....	51
4.8 Unidirectional Prepreg Analysis .....	54
4.9 Investigation of Tool/Ply Friction.....	58
4.10 Investigation of 5HS/8HS Friction .....	61
4.11 Summary.....	64
Chapter 5 : Modelling and Optimization .....	65
5.1 Stribeck Analysis .....	65
5.2 Modelling of Unidirectional Prepregs .....	74
5.3 Friction Models of Other Prepreg Configurations.....	80
5.4 Optimization Techniques .....	81
5.5 Taguchi Method .....	82
5.5.1 Standard Procedure .....	83
5.5.2 Selection of Process Parameters .....	83
5.5.3 Selection of Orthogonal Array.....	84
5.5.4 Signal-to-Noise (S/N) Ratios.....	86

5.5.5 Influence of Processing Parameters .....	86
5.6 Analysis of Variance (ANOVA).....	90
5.6.1 Confirmation Test .....	91
5.7 Summary.....	92
Chapter 6 : Conclusions and Contributions .....	93
Chapter 7 : Future Scope.....	95
REFERENCES .....	96
APPENDICES .....	101

## List of Figures

Figure 1.1 Aircraft Composite Content [2].....	2
Figure 1.2 Sequence of steps involved in forming operation .....	4
Figure 1.3 Schematics of two common forms of prepregs (a) Unidirectional prepregs, (b) Fabric prepregs [6] .....	5
Figure 1.4 Schematic of double diaphragm forming [11].....	6
Figure 2.1 Deformation mechanisms for fabric type composite materials during forming (a) Intra-ply shear (b) Intra-ply tensile loading (c) Consolidation (d) Tool/ply or ply/ply shear (e) Ply bending [4] .....	9
Figure 2.2 The fabric angle, $\phi$ , changes during intra-ply shear [12].....	10
Figure 2.3 Test set-ups to measure intra-ply friction (a) Bias-extension set-up (b) Picture-frame set-up [15] .....	11
Figure 2.4 Deformation of prepreg laminate under pressure [21] .....	12
Figure 2.5 Schematic of Pull-out test rig [5].....	15
Figure 2.6 Schematic of Pull-through test rig for ply/tool friction measurement [4] .....	16
Figure 2.7 Stribeck Curve [30] .....	18
Figure 3.1 Pictures of OOA prepregs as seen under microscope (a) 8-Harness (8HS), (b) 5-Harness (5HS), (c) Unidirectional (UD).....	21
Figure 3.2 Final samples for friction test (a) 8-Harness prepreg, (b) 5-Harness prepreg and (c) Unidirectional prepreg .....	24
Figure 3.3 Friction Test Rig.....	25
Figure 3.4 Schematic of the cross-section of Test Rig .....	26
Figure 3.5 Benchtop temperature controller by Omega.....	27
Figure 3.6 Working of PID Controller [3] .....	28
Figure 3.7 Infrared images showing temperature gradient of (a) Middle Plate, (b) Platen .....	29
Figure 3.8 Measurement of the Spring Constant (a) Start and (b) End of the test.....	30
Figure 3.9 Force-Displacement graph for calculation of spring constant.....	31
Figure 4.1 (a) Start, (b) Mid and (c) End of the test .....	33
Figure 4.2 Load-Displacement graphs at 50 °C, 0.5 mm/sec and 0.5 atm.....	34
Figure 4.3 Testing Region.....	35

Figure 4.4 Comparison between coefficients of friction for 8HS and 5HS at 50 °C, 0.5 mm/sec and 0.5 atm.....	36
Figure 4.5 Influence of temperature on Inter-Ply friction at 0.5 mm/sec, 0.5 atm and 0° fiber orientation for 8-harness carbon/epoxy prepregs [47] .....	38
Figure 4.6 Influence of temperature on Inter-Ply friction at 0.5 mm/sec, 0.5 atm and 0° fiber orientation for 5-harness carbon/epoxy prepregs [48] .....	38
Figure 4.7 Comparison of coefficients of friction at elevated temperatures for 8HS prepregs ....	39
Figure 4.8 Comparison of coefficients of friction at elevated temperatures for 5HS prepregs ....	39
Figure 4.9 Influence of pulling rate on inter-ply friction at 50 °C, 0.5 atm and 0° fiber orientation for 8-harness carbon/epoxy prepregs .....	41
Figure 4.10 Influence of pulling rate on inter-ply friction at 50 °C, 0.5 atm and 0° fiber orientation for 5-harness carbon/epoxy prepregs .....	41
Figure 4.11 Comparison of coefficients of friction at different pulling rates for 8HS prepregs ..	42
Figure 4.12 Comparison of coefficients of friction at different pulling rates for 5HS prepregs ..	42
Figure 4.13 Influence of pressure on inter-ply friction at 50 °C, 0.5 mm/sec for 8HS .....	43
Figure 4.14 Influence of pressure on inter-ply friction at 50 °C, 0.5 mm/sec for 5HS .....	43
Figure 4.15 Fiber deformations under different loading magnitude [29] .....	44
Figure 4.16 Comparison of coefficients of friction at different normal pressures for 8HS .....	45
Figure 4.17 Comparison of coefficients of friction at different normal pressures for 5HS .....	45
Figure 4.18 Relationship between Load, Normal Pressure and Friction Coefficient for 8HS .....	46
Figure 4.19 Relationship between Load, Normal Pressure and Friction Coefficient for 5HS .....	46
Figure 4.20 Fiber Orientation in a prepreg laminate [7] .....	47
Figure 4.21 Plot of load versus pulling rate for 8HS at different fiber orientations .....	48
Figure 4.22 Plot of load versus pulling rate for 5HS at different fiber orientations .....	48
Figure 4.23 Fiber Yarn rotation and deformation [29] .....	49
Figure 4.24 Influence of fiber orientation on friction coefficients for 8HS at 50°C, 0.5 mm/sec and 0.5 atm.....	50
Figure 4.25 Influence of fiber orientation on friction coefficients for 5HS at 50°C, 0.5 mm/sec and 0.5 atm.....	51
Figure 4.26 Mecatech 234 polishing machine .....	52
Figure 4.27 Tow geometry parameters [50] .....	52

Figure 4.28 Microscopic view of 8-Harness carbon/epoxy composite laminate.....	53
Figure 4.29 Microscopic view of 5-Harness carbon/epoxy composite laminate.....	53
Figure 4.30 Influence of temperature on inter-ply friction between UD prepregs at 0.5 mm/sec, 0.5 atm and 0° fiber orientation .....	55
Figure 4.31 Influence of temperature on coefficients of friction for 8HS, 5HS and UD's at 0.5 mm/sec, 0.5 atm and 0° fiber orientation.....	56
Figure 4.32 Influence of pulling rate on inter-ply friction of UD's at 50 °C and 0.5 mm/sec.....	57
Figure 4.33 Comparison of friction coefficients for 8HS, 5HS and UD's at different pulling rates, 50°C, 0.5 atm and 0° fiber orientation .....	57
Figure 4.34 Influence of normal pressure on interply friction for UD's at 50 °C, 0.5 mm/sec and 0° fiber orientation.....	58
Figure 4.35 Influence of temperature on tool-ply friction for 8HS and 5HS at 0.5 mm/sec, 0.5 atm and 0° fiber orientation .....	59
Figure 4.36 Influence of pulling rate on tool-ply friction for 8HS and 5HS at 50 °C, 0.5 atm and 0° fiber orientation .....	60
Figure 4.37 Influence of normal pressure on tool-ply friction for 8HS and 5HS at 50 °C, 0.5 mm/sec and 0° fiber orientation .....	61
Figure 4.38 Load vs. Temperature graphs for 5HS/8HS friction at 0.5 mm/sec, 0.5 atm and 0° fiber orientation .....	62
Figure 4.39 Load vs. Pulling Rate graphs for 5HS/8HS friction at 50 °C, 0.5 atm and 0° fiber orientation .....	63
Figure 4.40 Load vs. Normal Pressure graphs for 5HS/8HS friction at 50 °C, 0.5 mm/sec and 0° fiber orientation.....	63
Figure 5.1 Experimental Stribeck curve for 8-harness satin carbon/epoxy prepreg oriented at 0° to the direction of slippage.....	66
Figure 5.2 Experimental Stribeck curve for 8-harness satin carbon/epoxy prepreg oriented at 15° to the direction of slippage.....	67
Figure 5.3 Experimental Stribeck curve for 8-harness satin carbon/epoxy prepreg oriented at 30° to the direction of slippage.....	67
Figure 5.4 Experimental Stribeck curve for 8-harness satin carbon/epoxy prepreg oriented at 45° to the direction of slippage.....	68

Figure 5.5 Relationship between “a” and fabric angle “ $\theta$ ” for 8HS .....	69
Figure 5.6 Relationship between “b” and fabric angle “ $\theta$ ” for 8HS.....	69
Figure 5.7 Experimental Stribeck curve for 5-harness satin carbon/epoxy prepreg oriented at 0° to the direction of slippage.....	70
Figure 5.8 Experimental Stribeck curve for 5-harness satin carbon/epoxy prepreg oriented at 15° to the direction of slippage.....	71
Figure 5.9 Experimental Stribeck curve for 5-harness satin carbon/epoxy prepreg oriented at 30° to the direction of slippage.....	71
Figure 5.10 Experimental Stribeck curve for 5-harness satin carbon/epoxy prepreg oriented at 45° to the direction of slippage.....	72
Figure 5.11 Relationship between “a” and fabric angle “ $\theta$ ” for 5HS .....	73
Figure 5.12 Relationship between “b” and fabric angle “ $\theta$ ” for 5HS.....	73
Figure 5.13 Experimental Stribeck curve for unidirectional carbon/epoxy prepreg oriented at 0° to the direction of slippage.....	75
Figure 5.14 Experimental Stribeck curve for unidirectional carbon/epoxy prepreg oriented at 15° to the direction of slippage.....	75
Figure 5.15 Experimental Stribeck curve for unidirectional carbon/epoxy prepreg oriented at 30° to the direction of slippage.....	76
Figure 5.16 Experimental Stribeck curve for unidirectional carbon/epoxy prepreg oriented at 45° to the direction of slippage.....	76
Figure 5.17 Experimental Stribeck curve for unidirectional carbon/epoxy prepreg oriented at 60° to the direction of slippage.....	77
Figure 5.18 Experimental Stribeck curve for unidirectional carbon/epoxy prepreg oriented at 75° to the direction of slippage.....	77
Figure 5.19 Experimental Stribeck curve for unidirectional carbon/epoxy prepreg oriented at 90° to the direction of slippage.....	78
Figure 5.20 Relationship between “a” and fabric angle “ $\theta$ ” for UD .....	79
Figure 5.21 Relationship between “b” and fabric angle “ $\theta$ ” for UD.....	79
Figure 5.22 Experimental Stribeck curve for 8HS/Vacuum Bag .....	80
Figure 5.23 Experimental Stribeck curve for 5HS/Vacuum Bag .....	80
Figure 5.24 Experimental Stribeck curve for 5HS/8HS prepregs.....	81

Figure 5.25 Signal-to-noise (S/N) response graph for 8HS at different levels of (a) Normal Pressure  
(b) Temperature and (c) Pulling Rate ..... 88

Figure 5.26 Signal-to-noise (S/N) response graph for 5HS at different levels of (a) Normal Pressure  
(b) Temperature and (c) Pulling Rate ..... 89

## List of Tables

Table 3.1 Material properties of the composite materials used in this study .....	20
Table 3.2 Gel time at different temperatures [9] .....	23
Table 4.1 Test Conditions .....	36
Table 4.2 Maximum frictional loads for 8HS and 5HS at different rates .....	40
Table 4.3 Microscopic observations of 8HS and 5HS laminates .....	54
Table 5.1 Viscosity Values of Epoxy Resin .....	65
Table 5.2 Linear equations for 8HS at 15°, 30°, 45°, 60°, 75° and 90° fabric orientation .....	66
Table 5.3 Linear equations for 5HS at 0°, 15°, 30°, 45°, 60°, 75° and 90° fabric orientation .....	70
Table 5.4 Linear equations for UD at 0°, 15°, 30°, 45°, 60°, 75° and 90° fiber orientation .....	74
Table 5.5 Linear equations for 8HS/Vacuum Bag, 5HS/Vacuum Bag and 5HS/8HS .....	81
Table 5.6 Different levels for each parameter .....	83
Table 5.7 L <sub>9</sub> Orthogonal Array .....	84
Table 5.8 Signal-To-Noise (S/N) Ratio for Each Experiment .....	85
Table 5.9 Signal-To-Noise (S/N) Response for Each Parameter for 8HS .....	86
Table 5.10 Signal-To-Noise (S/N) Response for Each Parameter for 5HS .....	87
Table 5.11 Optimum process parameter combinations .....	87
Table 5.12 ANOVA Table for 8HS .....	91
Table 5.13 ANOVA Table for 5HS .....	91

# Chapter 1 : Introduction

With the advancement in the technology, composite materials are replacing metals in more and more sectors of aerospace and automobile industries. Their superior properties like high specific stiffness, high strength to weight ratio, low thermal expansion, corrosion resistance etc. make them more versatile. Composite materials basically consist of fibre reinforcements bonded together with a matrix material. Some naturally occurring composites are our bones, wood, horns etc. Composite structures allow the strength and stiffness of the material to change with the direction of loading.

The increasing demand of composite materials in aerospace industry has resulted in great developments in the field of composites with the improvement in manufacturing technologies and materials used. It has become a necessity for aerospace industries to improve their manufacturing methods to achieve less manufacturing time and less cost to meet the present needs. From traditional forming techniques like hand lay-up to advanced forming techniques like Automated Tape Laying (ATL) or Automated Fiber Placement (AFP), a wide range of forming methods are available for making composite components. However, traditional techniques are very time consuming and labor intensive. Advanced techniques like ATL or AFP are more efficient way of laying-up, but automated manufacturing methods require more sophisticated and highly productive equipment.

Additionally, overall manufacturing cost can be reduced by avoiding autoclave based curing process. This need is satisfied by the use of Out-of-Autoclave (OOA) prepregs manufacturing technology. The use of out-of-autoclave (OOA) prepregs can reduce cost as well as production time. The OOA prepregs can be formed by the application of temperature and vacuum only, without the need of high pressure and thus, saving the expenses for costly autoclave. Void contents can be eliminated in OOA prepregs by the use of tooling of appropriate type and identifying a maximum corner angle for a laminate of given thickness and a desired thickness uniformity [1].

Historically, composite materials are used more in military aircrafts than in civil aircrafts. But, since 2005 civil aircrafts have dramatically increased the use of composites. Composite by weight has increased from 12% in Boeing 777 to 50% in Boeing 787 [2]. Airbus A530 XWB is manufactured by using 53% composite materials by weight, which is more than composite by

weight in Boeing 787 and Airbus 380 [3]. Figure 1 shows the use of composite materials by weight in both military and civil aircrafts.

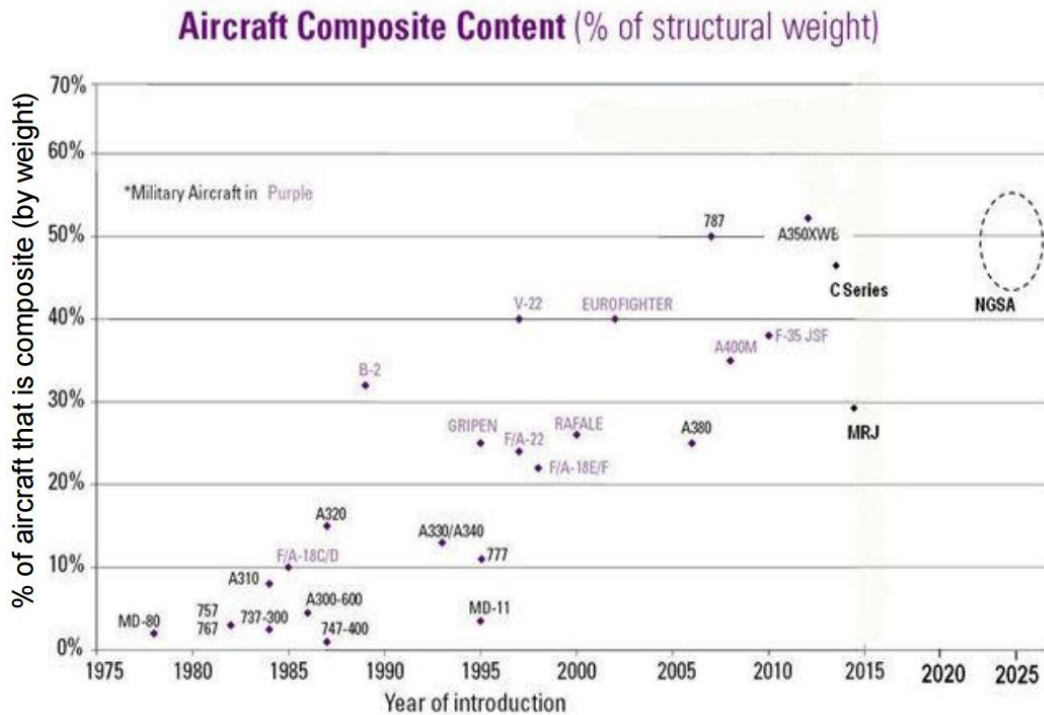


**Figure 1.1 Aircraft Composite Content [2]**

The use of various thermoforming techniques like hot drape forming can be integrated with automated fiber placement technique to get superior quality composite products. In thermoforming of composites many deformation mechanisms take place, such as intra-ply shear, inter-ply slippage, ply-bending, intra-ply tensile loading, etc., [4]. Inter-ply slippage plays the most important role in forming of prepreg plies and deciding the quality of the final product.

The focus of this research is on deformation mechanisms which occur during forming operation, especially Inter-Ply slippage deformation. The influence of processing parameters like temperature, forming rate, normal pressure and fiber orientation on inter-ply friction is investigated by using friction tests. Additionally, use of Stribeck curve to create a model of inter-ply friction phenomenon has been studied.

## 1.1 Thesis Organization

This thesis has been divided into 7 chapters and brief explanation of each chapter has been written below.

**Chapter 1** gives the brief description of use of composite materials in automotive and aerospace industries. It describes the use of AFP in coalition with diaphragm forming technique and use of out-of-autoclave prepreg technologies.

**Chapter 2** discusses the previous work done by researchers regarding different deformation mechanisms which occur during forming of prepreg plies. Specially, regarding inter-ply friction mechanism and different techniques used to measure it.

**Chapter 3** explains the material selection and manufacturing techniques. It describes the design and fabrication of friction test rig. This chapter explains the material properties of 5-harness (5HS), 8-harness (8HS) and unidirectional (UD) out-of-autoclave (OOA) carbon/epoxy prepreg. It describes the use of FLIR Infrared camera to determine the temperature distribution across the prepreg ply surface. It also explains the calibration of springs by calculating the spring constant by using MTS machine.

**Chapter 4** discusses the influence of various processing parameters like temperature, normal pressure and pulling rate on inter-ply shear of 5-harness, 8-harness and unidirectional prepreg plies using friction test rig. The effect of change in fibre orientation on the inter-ply friction is described in this chapter. It also describes the microscopic analysis of the interaction between different layers of prepreg.

**Chapter 5** introduces the modelling of inter-ply friction phenomenon by the use of Stribeck Analysis. The relation of Coefficient of friction ( $\mu$ ) with Hersey number ( $H$ ) is discussed in this chapter. The use of Taguchi method and Analysis of Variance (ANOVA) to find the optimum processing conditions to reduce inter-ply friction is also explained.

**Chapter 6** discusses the conclusions of the research work presented in this dissertation.

**Chapter 7** presents the future scope in the forming techniques and recommendations given regarding the inter-ply shear mechanism.

## 1.2 Introduction to Forming Operations

In forming of composite materials, several steps are involved starting from prepreg to the final product. Automated fiber placement technique could be integrated with diaphragm forming to speed up the process. Flat laminates are produced with the use of automated fiber placement machine which can place fibers at desired angle in each layer of the laminate. The process of laying-up prepreg plies at different angles can also be accomplished by hand lay-up technique, but it will take more time than automated process. Flat laminate is then deformed into desired shape using diaphragm forming technique. In diaphragm forming method, prepreg laminate is placed between two diaphragm membranes and with the combined application of vacuum from bottom and air pressure from the top it is deformed into tool geometry.

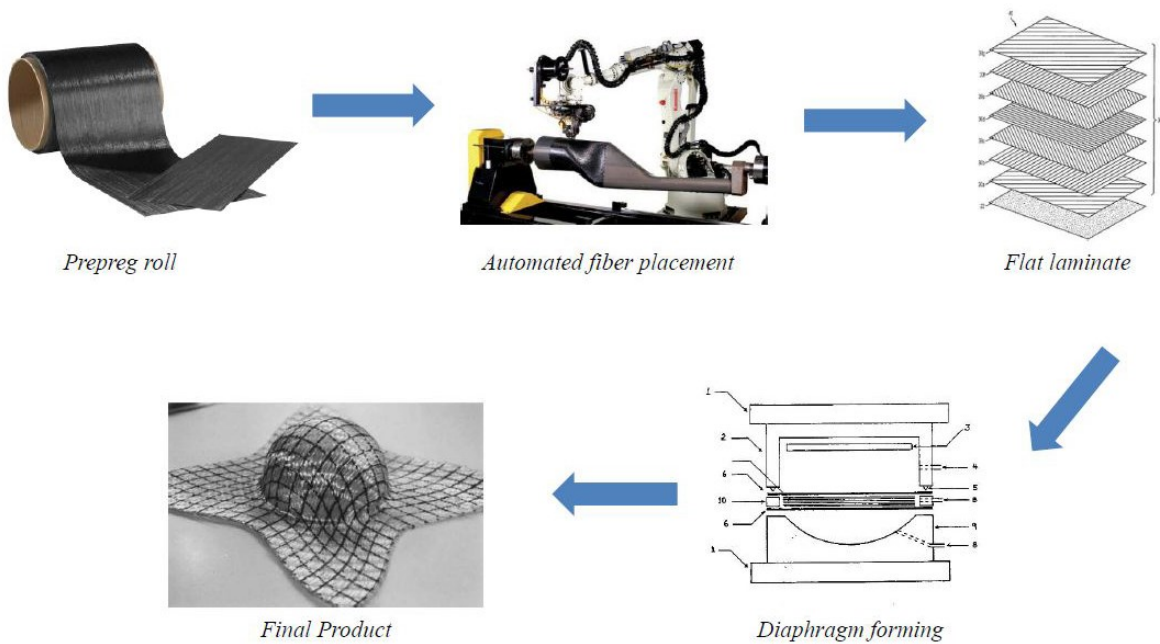


**Figure 1.2 Sequence of steps involved in forming operation**

In the forming process many deformation mechanisms take place, such as intra-ply shear, inter-ply slippage, ply-bending, intra-ply tensile loading, etc. [4]. Inter-ply slippage plays the most important role in forming of prepreg plies and deciding the quality of the final product [5]. Unwanted friction between layers of composite can lead to various defects, such as wrinkling, delaminating etc.

### 1.3 Pre-impregnated composites (Prepregs)

Pre-impregnated composites are made up of fibre reinforcements impregnated with matrix material which can be thermoset or thermoplastic [6]. Matrix serves the purpose of bonding the fibres together and providing transverse strength to final product. The shelf life of prepregs varies from few weeks to few months depending upon the conditions of storage. Thermoplastic matrix have unlimited shelf life due to their special chemical properties. A cured thermoplastic matrix can be molded again to a new shape by heating it. In thermosets chemical reactions take place all the time, even if stored at very low temperature, which makes them unusable after a certain period of time. Figure 1.3 shows the schematics of two commonly used prepregs, with unidirectional reinforcements and with fabric reinforcements.

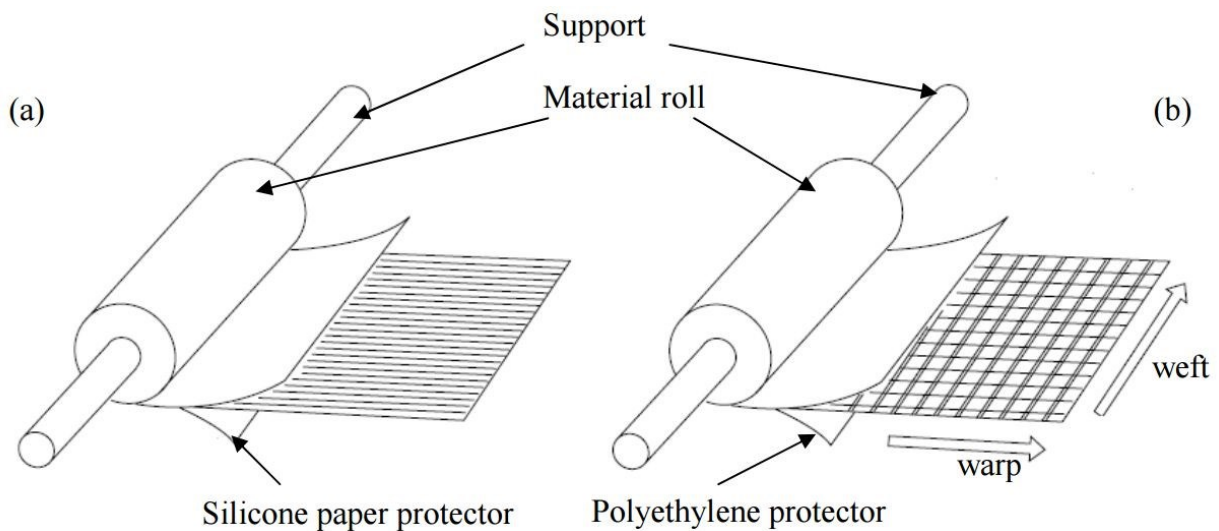


**Figure 1.3 Schematics of two common forms of prepregs (a) Unidirectional prepregs, (b) Fabric prepregs [6]**

Most commonly used matrix is epoxy which is thermosetting in nature. Resins are usually partially cured for thermoset matrices. Matrix materials helps in keeping the fibres aligned, helps in transferring the load between the fibres to utilize their strength effectively. Matrix assists the fibres in providing compression strength, shear strength and modulus to the composites; and protects the fibres from environmental attacks [7].

Prepregs have several advantages over other composites forms, such as fibre/resin ratios are very precisely controlled, less production cost, more control over fibre placement and angle, good

mechanical properties etc. Prepregs can be utilized in many processes such as hand lay-up technique, automated fiber placement technique, automated tape laying technique etc. Products made from prepregs range from sports to aerospace [6].

## 1.4 Diaphragm Forming

In diaphragm forming, flat composite laminate is deformed to a desired shape using one or two deformable membranes, called diaphragms [8]. Diaphragm forming can be classified into two types, Single diaphragm forming and Double diaphragm forming. In single diaphragm forming technique, prepreg is placed over the mold with sheets of release film above and below it [9]. After that, diaphragm is sealed at the top of the laminate. Vacuum is applied from the bottom of the mold and air pressure is applied from the top which molds the laminate to the shape of the tool [10]. Figure 1.4 shows the schematic of double diaphragm forming process.

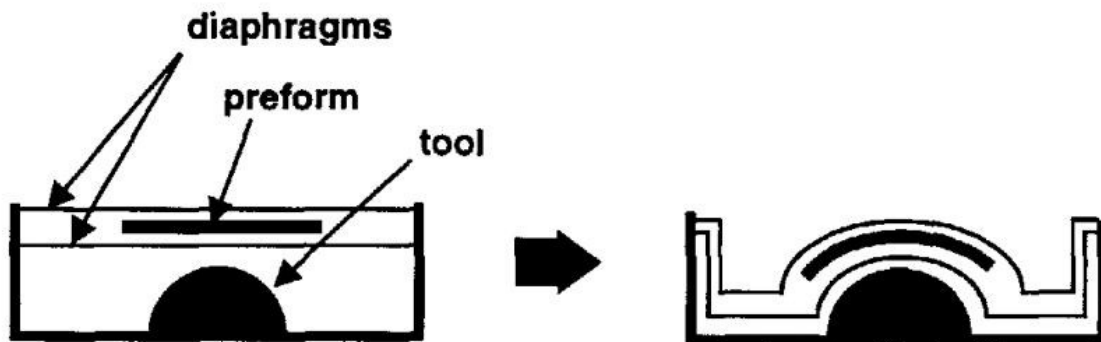


**Figure 1.4 Schematic of double diaphragm forming [11]**

The advantage of diaphragm forming is that deformable membrane stretch during the forming operation which keeps the composite laminate under tension and reduces the wrinkles in the final product. The disadvantage of diaphragm forming is high production time which is usually around one hour and high cost as for each composite part new diaphragm membrane is required [8].

## **1.5 Motive**

The main motive behind this research is to understand the inter-ply friction mechanism of out-of-autoclave carbon/epoxy prepreg. The proper understanding of various deformation mechanisms that take place during the forming of OOA prepreg could help in improving the quality of composite parts by reducing the defects like wrinkling, residual stresses etc. The aim of producing defect free complex shaped composite parts could be accomplished by this. The out-of-autoclave (OOA) technology can eliminate the requirement of costly autoclaves. Diaphragm forming method can be combined with OOA technology to reduce the production cost and to produce a high quality composite parts with negligible voids. To achieve this aim, influence of various processing parameters such as, temperature, normal pressure, rate, fiber orientation etc. were studied using a friction test rig which is capable of simulating the actual forming process. Recent advancements in composite technologies were studied.

The other motive for this study is to make data available for the optimum conditions required for a forming operation to make the final product defect free. To study this, various friction experiments were performed at different values of processing parameters. The effect of one parameter was studied by varying that processing parameter while keeping all others constant.

## **1.6 Thesis Objectives and Challenges**

The main objective of this project is to characterize the inter-ply shear properties of out-of-autoclave carbon/epoxy thermoset prepreg. In past decades, many researchers have done experimental and analytical works to characterize the inter-ply shear behaviour of woven composites using pull-out and pull-through experiments. The present research uses experimental and statistical data to characterize the drapability of out-of-autoclave composites before performing the actual forming operation.

In this thesis, the goal of finding the optimum processing conditions to perform the forming operation to achieve wrinkle free part has been addressed. The influence of each processing parameter on inter-ply shear and percentage contribution of every parameter in forming operation has been studied in this thesis.

In this project, the three main challenges linked with the manufacturing of defect free composite part that were recognized and must be resolved before actual operation are written as follow,

- To characterize the influences of various processing parameters such as, temperature, normal pressure, displacement rate, fiber orientation on the inter-ply shear behaviour of the out-of-autoclave prepreg by performing friction tests. The effect of these parameters on the coefficient of friction between prepreg plies is studied.
- To develop a model of inter-ply friction mechanism for OOA prepregs with the help of Stribeck curves. The objective of including processing parameters in the model was served by Hersey number which is the function of viscosity (temperature), pulling rate and normal pressure.
- To develop a general equation which could be used to predict coefficient of friction for any set of processing conditions at any fabric (fiber) orientation.
- To develop a technique to determine the optimum processing conditions which can facilitate defect free forming of laminate by using statistical approach. The most influencing parameter which effect the inter-ply friction the most is studied.

## Chapter 2 : Literature Review

In last few decades, many researchers have studied the forming techniques of prepreg composites. The various deformation mechanisms that take place during the forming had been studied in detail. Various defects that occur during forming were analysed and models were developed to eliminate those defects. Both quality and quantity of composite parts were improved by the development of new techniques.

### 2.1 Composite forming mechanisms

During the thermoforming of composites many forming mechanisms takes place, such as intra-ply shear, intra-ply tensile loading, tool/ply or ply/ply slippage, ply bending, consolidation, etc., [4]. Inter-ply slippage and intra-ply shear plays the most important role in forming of prepreg plies and deciding the quality of the final product [8]. Figure 2.1 shows deformation mechanisms for fabric type composite materials during forming.

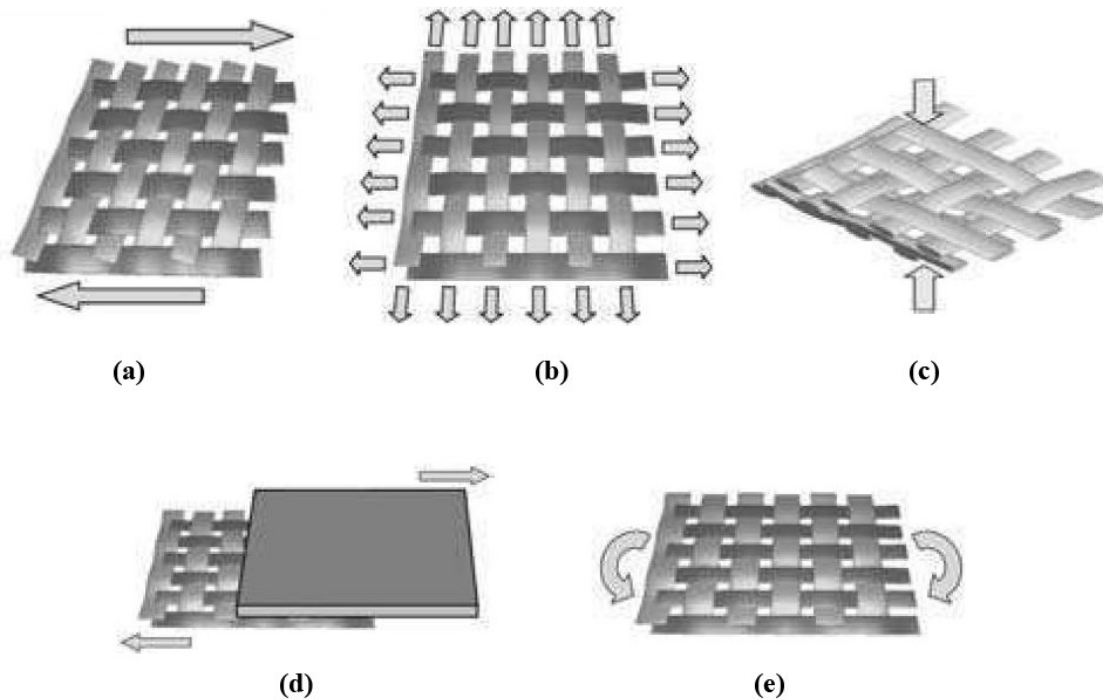


**Figure 2.1 Deformation mechanisms for fabric type composite materials during forming (a) Intra-ply shear (b) Intra-ply tensile loading (c) Consolidation (d) Tool/ply or ply/ply shear (e) Ply bending [4]**

From all of the deformation mechanisms, inter-ply friction is considered the most important and most dominating mechanism in the forming of prepreg plies [5]. Inter-ply friction mechanism involves the relative movement between the individual layers of prepreg [4], as shown in the figure 2.1 (d). American Society for Testing and Materials (ASTM) has no standard test to measure Inter-ply friction behaviour of composites. The most commonly used test method by the previous researchers is by the use of custom-designed friction test rig which is explained in the chapter 4. A brief summary of the previous work done by researchers on inter-ply shear behaviour is discussed in section 2.2.

Intra-ply shear is one of the principal deformation mechanisms which tend to happen when prepreg laminate is subjected to in-plane shear loading. It is the rotation between parallel tows and at tow crossovers, followed by inter tow consolidation [4]. In intra-ply shear or “trellis-effect” the fabric angle between warp and weft direction changes [12]. Figure 2.2 shows the change in the fabric angle during the intra-ply shear deformation of textile composites.

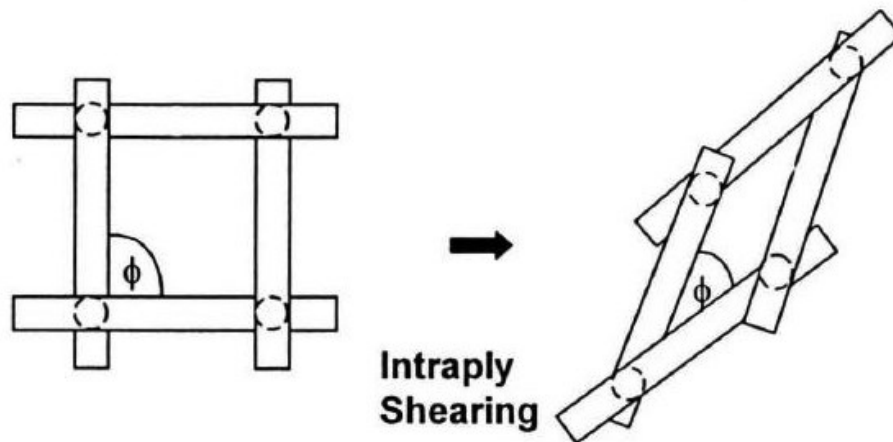


**Figure 2.2 The fabric angle,  $\phi$ , changes during intra-ply shear [12]**

The pin-jointed net (PJM) approximation theory is assumed to be working behind the deformation of the woven fabric which was originally proposed by Mack and Taylor [13]. Zhu et al. used bias-extension method to investigate large deformation and slippage mechanism of plain woven composite [14]. The measurement of intra-ply shear properties was done using bias-extension and picture-frame test methods by Lebrun et al. [15]. According to PJM approximation theory, during deformation of prepreg plies, yarns are inextensible without the possibility of slippage at

crossovers, but rotation of fibers is allowed [9,12]. The unidirectional (UD) prepregs have different deformation mechanism than fabric prepregs. In unidirectional prepregs deformation is parallel along the axis instead of adjacent yarns crossing over each other [4]. Aono et al. [16] studied the mapping algorithms for fitting the woven cloth to the curved surfaces.

Although there is no standardised test to measure intra-ply shear deformation, the picture-frame and bias-extension tests are the two tests which are most commonly used to measure intra-ply shear of prepreg plies [17]. The bias-extension and picture-frame test set-ups shown in figure 2.3 are used to measure the force needed to shear the prepreg sample and the angle at which it tends to lock.

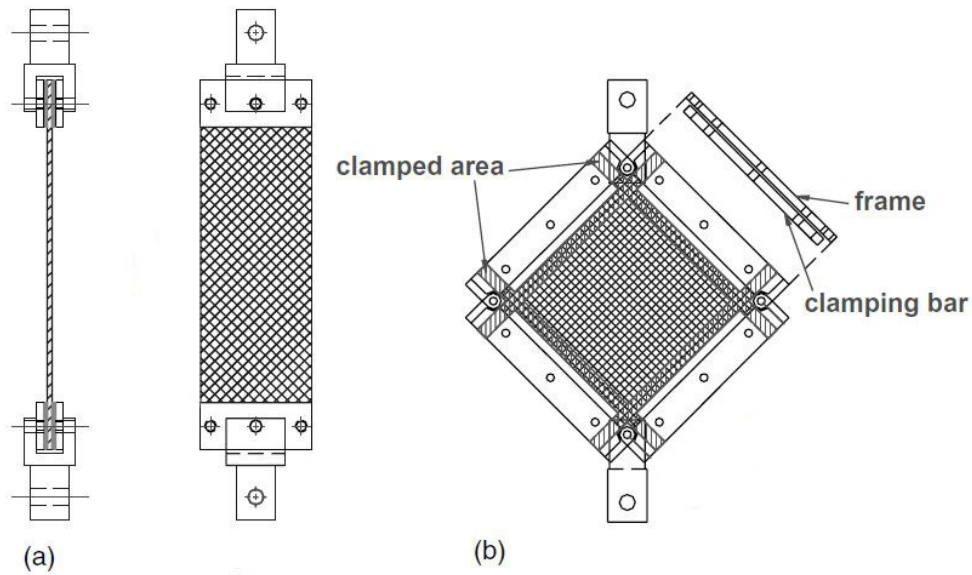


**Figure 2.3 Test set-ups to measure intra-ply friction (a) Bias-extension set-up (b) Picture-frame set-up [15]**

Besides inter-ply slippage and intra-ply shear, intra-ply bending is also one of the main deformation mechanisms which takes place during the deformation of prepreg plies according to the shape of the tool [4]. Ply bending is the only mechanism needed for the forming of single curvatures and required critically for double curvatures. Bilbao et al. used a standard cantilever bend test to study the bending behaviour of reinforcements [18]. Bilisik et al. performed experiments to analyse the bending behaviour of single and multi-layered stitched E-Glass fabric structures for composites [19].

The aim of this thesis is not to study intra-ply shear behaviour and intra-ply bending of composites that takes place during the thermoforming of prepreg laminates. The principal aim of this study is to investigate and characterize the inter-ply slippage mechanism between prepreg plies during forming of the composites.

## 2.2 Inter-ply Slippage

Forming of stack of prepregs needs all the plies to deform according to the shape of the tool without causing wrinkles in the final product. Inter-ply slippage, also known as ply/ply slippage, is the phenomenon that governs the transfer of loads between prepreg plies during an automated forming operation [4,20]. Figure 2.4 shows the deformation of a prepreg laminate under the normal pressure. Figure 2.4(b) shows the no buckling deformation of prepreg laminate with interply slip. Figure 2.4(c) shows the deformation of laminate with no interply slip. Wrinkles are seen at the bending of laminate due to lack of slippage between adjacent prepreg plies [8]. The plies nearest to the bend experience a compressive stress as the flat laminate changes shape, and this may cause out-of-plane buckling and the plies farthest to the bend cause the wrinkling by not being able to get stretched to the increased arc length they are supposed to travel [21].

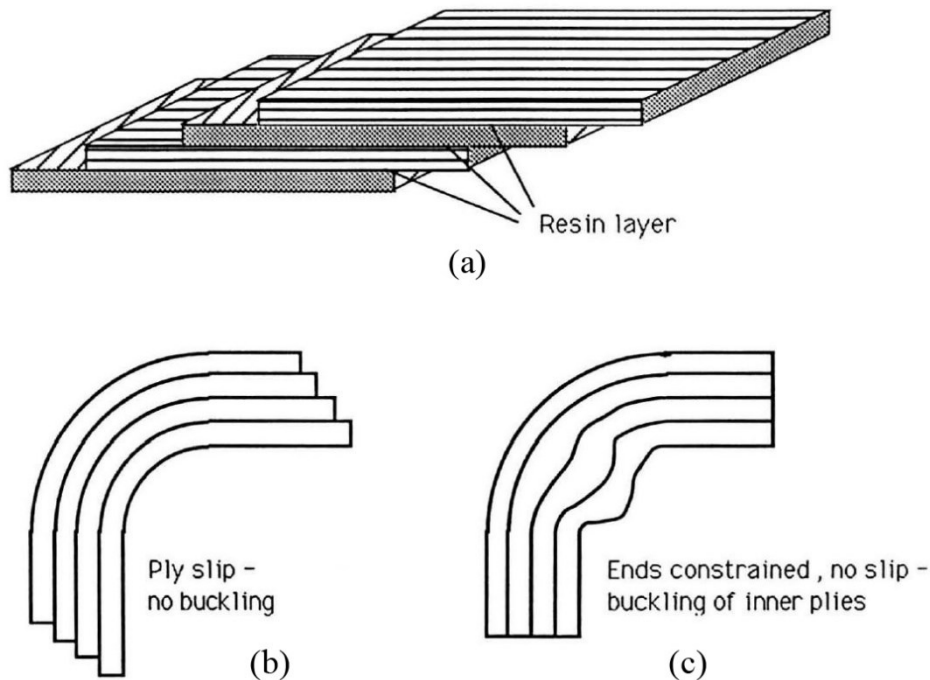


**Figure 2.4 Deformation of prepreg laminate under pressure [21]**

Additionally, previous research work done by Vanclooster et al. [8,22] and Konstantine et al. [23] describes that friction between tool and prepreg ply plays an important role in the quality of the final composite product. Very high inter-ply friction may result in tearing off the prepreg material or may cause wrinkling in the final product [22]. During forming of prepreg laminate with composite layers at different fiber orientations to each other, compression forces are produced in one prepreg layer due to intra-ply shear may get transferred to the adjacent layer, causing compression along the direction of the fiber and producing wrinkles in the product [10].

It is assumed that inter-ply slippage effect happens in the resin layer that exists between the plies. As we know, friction phenomena are governed by different friction mechanisms and according to tribology, these friction mechanisms can be divided into three categories. First category is when there is no fluid between the contact surfaces and this type of friction is usually known as Coulomb friction. Second category is when there is fluid lubricating film between the two contact surfaces and this type of friction is known as Hydrodynamic friction. In third case, the fluid lubricating film does not covers the whole contact surface area and two dry surfaces touch each other at some points, and this type of friction is mixed friction [24].

Coulomb friction is governed according to the equation 2.1 in which  $f$  is the frictional force,  $\mu$  is the coefficient of friction and  $N$  is the normal force to the friction interface.

$$f = \mu N \quad (2.1)$$

For hydrodynamic friction, as given by equation 2.2, shear stress is governed by rate of movement of one surface over other, fluid viscosity and thickness of the fluid film [25], where  $\tau$  is the shear stress,  $\eta$  is the viscosity of fluid,  $d$  is the thickness of fluid film and  $v$  is the velocity of one surface over other.

$$\tau = \frac{\eta}{d} v \quad (2.2)$$

According to Wilks [12], the governing phenomenon for shear stress at the interface is given by equation 2.3 where  $\dot{\gamma}$  is the shear strain rate and  $P$  is the normal pressure.

$$\tau = \eta \dot{\gamma} + \mu P \quad (2.3)$$

For fabrics, fibers are not so inextensible due to the crimped nature of the fabric prepreg and this permits straightening of the fibers while deforming over a bend and once the fibers become

inextensible inter-ply slip begins [21]. In other words, the crimped nature of the tows of the fibers means that there is more probability of buckling in the prepreg plies which undergo compressive stress.

### **2.3 Inter-ply Friction test methodology**

For the measurement of ply/tool and ply/ply friction, there is no standard ASTM test methodology. A number of testing techniques are available for determining the friction. The simplest way to measure inter-ply friction is by using inclined plane method [4]. According to this technique, a block of tooling material is placed on the sheet of prepreg material fixed on a rigid plate. This rigid plate is inclined until the block starts to slide. By measuring the tangent of the angle of inclined plane, coefficient of friction can be calculated [26]. Previous researchers have used various custom designed test rigs for measuring inter-ply friction [5,8,20,24,25,27–33]. Murtagh et al. used friction sled method in which composite specimen was sandwiched between two sheets of steel shim [27]. Scherer and Friedrich used pull-out test method in which individual ply was pulled out of the stack of plies [28]. A modified form of pull-out test, known as pull-through test, was used by Wilks which have an advantage of constant contact area under pressure from starting to end of the test [12]. The platens were heated with the help of cartridge heaters inserted into them and the whole apparatus was placed inside an environmental chamber to obtain constant uniform temperature. Gorczyca et al. [32] used a similar kind of pull-through test apparatus to measure inter-ply friction but the only difference was that he did not use environmental chamber. Gorczyca et al. [32] tried to produce the similar condition as they are in actual forming process and used different materials and different processing conditions that have been previously used by researchers.

Displacement versus load graphs at constant displacement rate show a general trend regardless of the material used, which is peak value of force in the start of test and rapidly decreasing to a constant low value of force [5,31]. In this way, two coefficients of friction can be associated with each set of friction test representing peak and steady state resistance. This type of trend is not seen in some exceptional cases when displacement rate is very low or temperature is very high, that initial peak in the graph decreases or totally disappears. Various processing conditions that effect the force of friction between tool and the prepreg plies were investigated, which include processing temperature, pull out velocity, normal pressure, fiber orientation, type of release agent and cooling conditions [5,27,31]. Some processing conditions are found to be more influential than others.

Murtagh et al. [27] concluded that release agents have much effect on friction coefficient. The most commonly used test apparatus are pull-out test rig and pull-through test rig [5].

### 2.3.1 Pull-out rig

Murtagh [21] developed a pull out test rig to investigate the tool/ply friction by conducting a set of experiments. Figure 2.5 shows the schematic of pull-out test rig. In this technique, a steel shim is pulled from between two prepreg plies clamped from the three sides. The two heated platens provide the normal load which are operated by a universal testing machine. After reaching to the desired temperature, steel shim was pulled out by the lead screw operated by a DC permanent magnet motor. To measure the frictional force, a load cell was installed between the lead screw and the steel shim. A linear variable differential transformer was used to measure the displacement of the steel shim which was mounted horizontally. Harrison et al. [5] conducted the pull out tests at different processing conditions which consist temperature of 180, 200 and 220 °C, 80 kPa to 2.8 MPa of normal pressures and pulling speeds of 0.5, 0.8 and 1.2 mm/sec. In each test all three speeds were conducted. Pulling speed was increased to the next level once the frictional force reached a steady state.

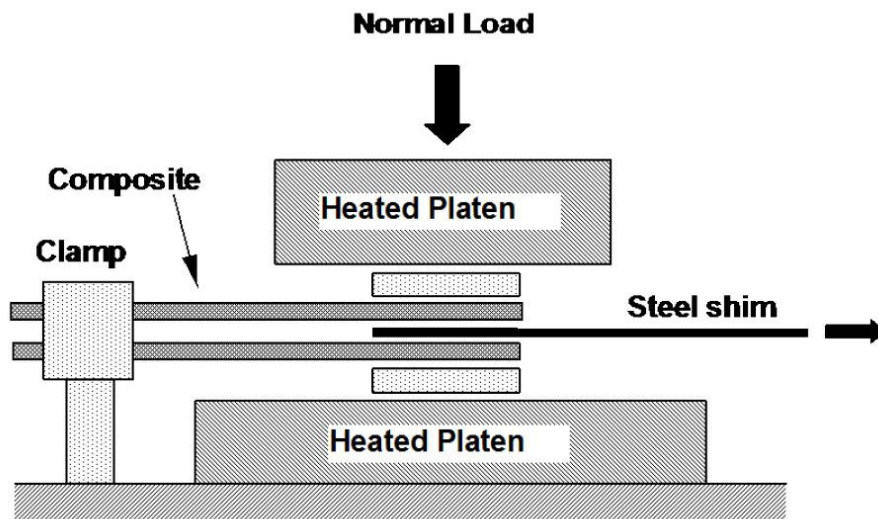


Figure 2.5 Schematic of Pull-out test rig [5]

The force of friction was recorded to be less for the prepregs samples oriented at 90° to the direction of movement than the prepreg samples oriented at 0° [27]. The application of release

agent resulted in the reduction of coefficient of friction and by using different release agents force of friction changed.

### 2.3.2 Pull-through rig

A modified design of pull-out test rig was used by Wilks [12] for tool/ply friction measurements. Figure 2.6 shows the front and side view of the pull-through test rig. Harrison et al. [5] used the similar pull-through rig which consists of a primary steel frame approximately 300 x 200 mm in size and two steel platens for applying normal pressure constitute the top portion of the rig. A secondary steel frame for clamping the sample from the perimeter region is connected to the load cell at the top. The sample size is same as that of the outer perimeter of the secondary steel frame and this frame pulls the composite sample in between the steel platens which provide normal pressure to both front and back side of the sample. The cartridge heaters inserted in each platen, to achieve the desired temperature, were controlled by feedback system by the temperature controller.

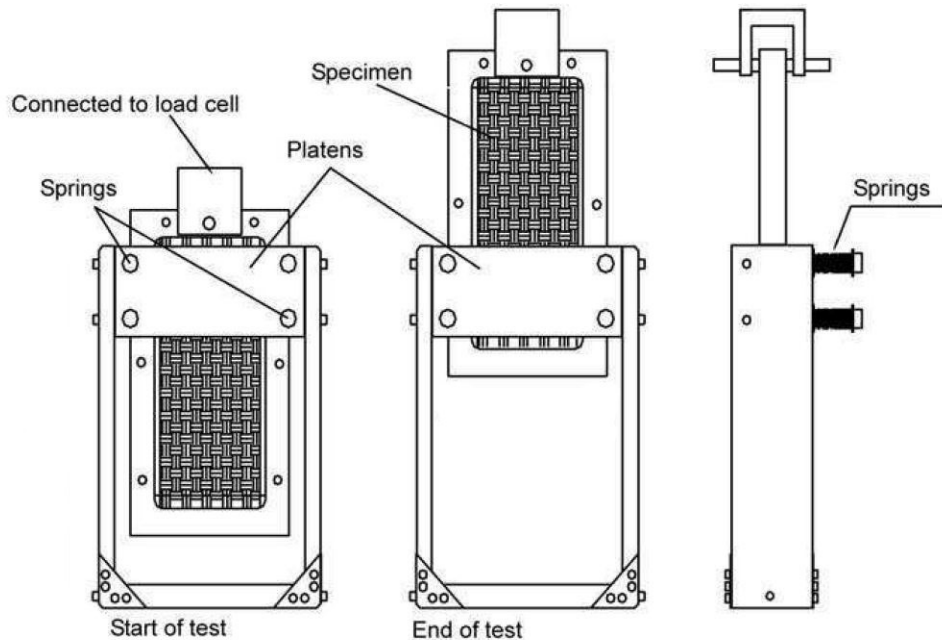


**Figure 2.6 Schematic of Pull-through test rig for ply/tool friction measurement [4]**

Four springs provide the normal pressure to the platens and are calibrated according to their spring constants. The whole apparatus was placed in the environmental chamber to achieve constant and uniform temperature. With the increase in normal pressure frictional force increases. At a constant

normal pressure, force of friction increases with the increase in pulling rate and reduces with the rise in temperature [4].

## **2.4 Out-of-Autoclave curing**

The out-of-autoclave curing technology is a method of curing composite materials in which no autoclave is used. In this technology only temperature and vacuum is used without using the external pressure (just atmospheric pressure). This technique is very advantageous for the manufacturing of large composite parts which cannot fit inside the autoclave and also it can reduce the final cost of the product as there is no need to buy autoclave. The out-of-autoclave curing is the integral parts of aerospace industry but present needs require more satisfactory and cheap processing without effecting the quality of the final product [34]. Many efforts had been made to manufacture the composite parts of same quality but at a less cost [35,36]. The out-of-autoclave prepreg materials are designed for processing without the use of autoclave but in the past years these prepreps had suffered many drawbacks due to the presence of high void contents in the cured products [37,38]. The presence of high void contents have big impact on the mechanical properties of the composite parts [39]. The formation of voids in the final parts can be caused by the presence of moisture in the prepreps or due to the entrapped air bubbles. These defects can be avoided by removing moisture, entrapped air and other volatiles before the curing process. The viscosity of out-of-autoclave prepreps is a very important parameter because it must allow entrapped air and moisture to get out with the application of vacuum only [38,39].

## **2.5 Stribeck Curve**

The Stribeck curve, which is also known as Stribeck-Hersey curve, is the plot of friction as the function of viscosity, speed and normal pressure. The vertical axis of the curve shows the coefficient of friction and the horizontal axis shows the Hersey Number which is product of three parameters [40]. This curve was developed by Prof. Richard Stribeck in early 20<sup>th</sup> century. Figure 2.7 shows the theoretical Stribeck curve.

The Hersey number,  $H = \eta v/P$ , is a magical number which can describe the condition of lubrication film concisely. Another reason why Hersey number is important is because it is dimensionless number and most of the magical numbers in engineering and sciences are dimensionless [40]. The previous researchers tried to plot the coefficient of friction against speed, temperature, load, viscosity and the rate of the fluid but there was a difficulty to show all this data

in a single form. The “Pi-Theorem” proposed by Edgar Buckingham [41] gave the answer. Pi-Theorem states that any physical equation expressing a relation among  $n$  physical variables, then it can be put in the form of a set of  $i=n-k$  dimensionless parameters derived from the variables in the original equation, where  $k$  is the minimum number of fundamental units involved for measuring  $n$  variables [40]. By plotting the coefficient of friction against the product of viscosity and speed divided by load, all the results involving friction can be drawn on a single graph. In Hersey number,  $H = \eta v/P$ ,  $\eta$  is the viscosity of the fluid,  $v$  is the speed of one surface over other and  $P$  is the pressure per unit length.

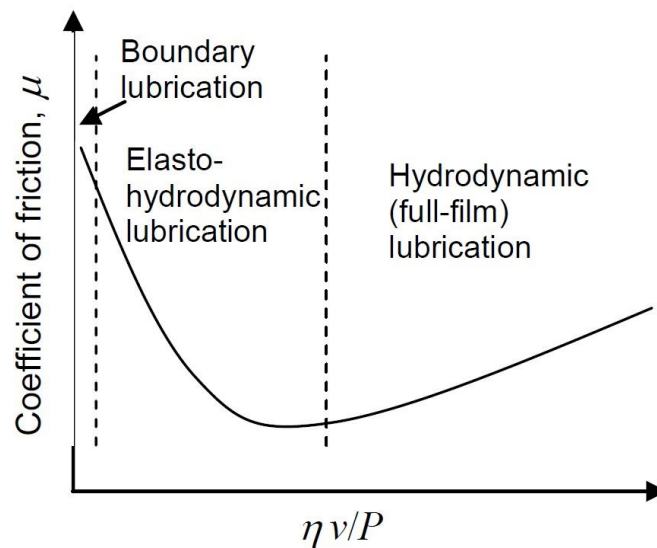


**Figure 2.7 Stribeck Curve [30]**

In 2002, Chow [29] proposed the use of Stribeck curve to explain the experimental results of inter-ply friction tests. As we go from left to right on the horizontal axis, influence of increase in the speed, increase in the viscosity and decrease in load can be noticed. The origin of the Stribeck curve represents the static friction. The theoretical Stribeck curve, as shown in Figure 2.7, consists of three regions related to Boundary lubrication, Elasto-hydrodynamic lubrication and Hydrodynamic lubrication. In boundary lubrication, which represents the case of low viscosity, low speed and high normal load, there is a contact between opposing asperities and the fluid layer is very thin. As the relative speed between two contact surfaces increases or viscosity of the fluid increases or the normal load decreases the thickness of the fluid film between contact surfaces increases. In elasto-hydrodynamic region there is a sharp decrease in the coefficient of friction

which is the result of increase in separation between contact surfaces. After the friction coefficient reaches a minimum value, there is transition to Hydrodynamic lubrication. In hydrodynamic lubrication region of Stribeck curve there is an increase in the friction coefficient which is caused by fluid drag. Hersey [40] originally used normal pressure per unit length in the plot of Stribeck curve but many researchers have used normal force [32,42] and normal pressure [5,43,44] instead. In this study normal pressure is used in calculation of Hersey number. Harrison et al. [5] proposed a friction model based on Stribeck curve. The steady increase in friction coefficient with the increase in Hersey number helped in developing a linear relationship between coefficient of friction and Hersey number.

# Chapter 3 : Materials and Test Apparatus

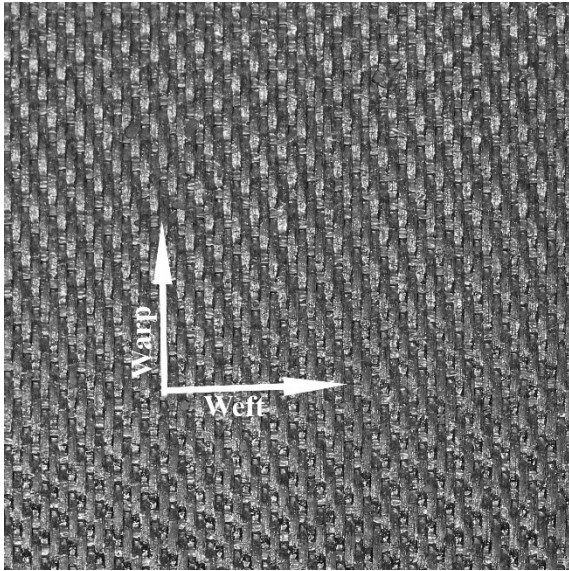
This chapter describes the out-of-autoclave material used in this study in detail. Also, the shape, size and fabrication method of the prepreg samples is explained. The design and manufacturing of friction test rig is described in this chapter. Later, the techniques to check temperature distribution and pressure uniformity are discussed.

## 3.1 Material Selection

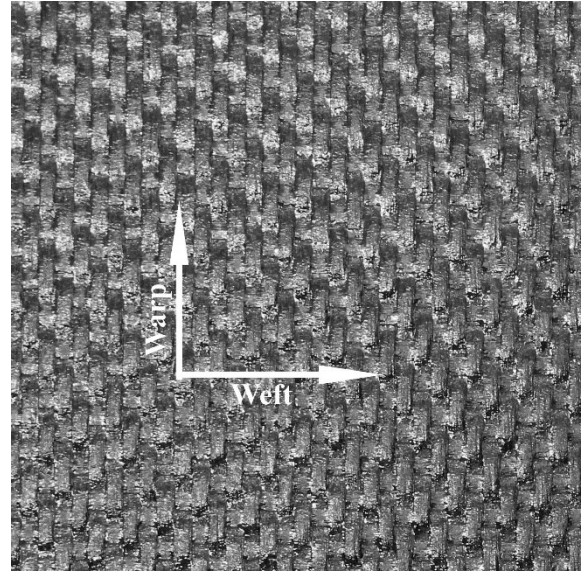
The composite material selected for this research was Cytec engineered material. This prepreg material uses CYCOM 5320-1 resin system. It is an out-of-autoclave curing prepreg material. Cycom 5320-1 is a newly developed out-of-autoclave material for automated manufacturing in aerospace industry [3]. Due to the low temperature curing ability of this material, it can be used for prototyping where low cost and vacuum-bag-only curing is needed [45]. This composite material is suitable to be used in the primary structure of the aircrafts as it has the mechanical properties equivalent to the autoclave cured epoxy systems. The resin system of this material makes the cured composite parts to have very low void contents. Three different forms of this composite material were used in this study which are 8-Harness satin, 5-Harness satin and unidirectional (UD) carbon/epoxy prepreg materials. Table 3.1 shows the properties of the three different forms of Cycom 5320-1 carbon/epoxy system.

**Table 3.1 Material properties of the composite materials used in this study**

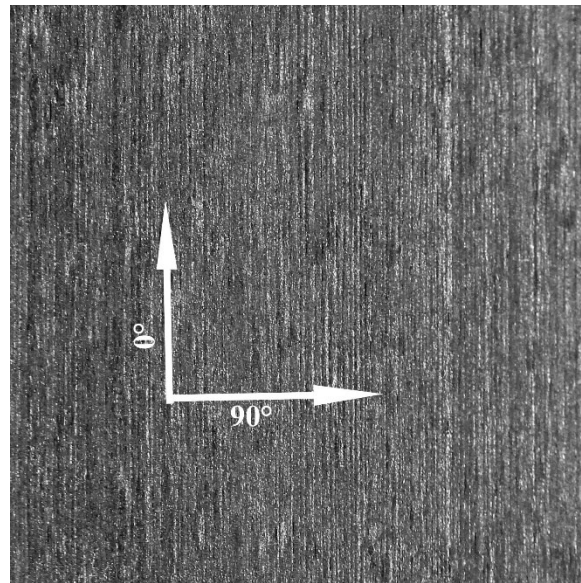
<b>Materials</b>	8-Harness (8HS)	5-Harness (5HS)	Unidirectional (UD)
<b>Manufacturer</b>	Cytec Engineering Materials Inc.	Cytec Engineering Materials Inc.	Cytec Engineering Materials Inc.
<b>Resin</b>	CYCOM 5320-1	CYCOM 5320-1	CYCOM 5320-1
<b>Fabric</b>	T650-3K 8HS	T650-6K 5HS	T650-UD
<b>Resin Content (wt %)</b>	36	36	36
<b>Areal Density (g/m<sup>2</sup>)</b>	569.10	574.90	218.60
<b>Thickness (mm)</b>	0.55	0.60	0.18



(a)



(b)



(c)

**Figure 3.1 Pictures of OOA prepreps as seen under microscope (a) 8-Harness (8HS), (b) 5-Harness (5HS), (c) Unidirectional (UD)**

### 3.1.1 CYCOM 5320-1 Resin System

CYCOM 5320-1 is a toughened carbon/epoxy prepreg system designed for out-of-autoclave manufacturing of primary structural components of aerospace applications. Reduction in the cost of tooling and out-of-autoclave curing is made possible due to its low temperature curing capability. Shelf life of this resin system is 1 year if stored at -12 °C. Wet glass transition temperature of this epoxy resin system is 163 °C. After 177 °C freestanding postcure, it offers mechanical properties equal to other autoclave cured toughened epoxy prepreg systems. Material for this study was provided in three forms, i.e. 8HS, 5HS and UD, in wide tape rolls from Cytec Engineering Materials Inc.

## 3.2 Rheological characterization of the prepreg

The rheological tests performed on the prepreps indicate that viscosity of the resin decreases at initial stage with the increase in temperature. Results indicate that in the initial stages, viscosity of resin at 120°C to be much smaller than that at 100°C, 90°C and 70°C. While later viscosity is found to increase drastically with the increase in temperature [9]. This is explained by the transition of resin from gelled glass regime to vitrification regime as time proceeds.

The variation of the gel time with the isothermal temperature is encapsulated in Table 3.2. It can be observed that the gel time decreases as the temperature increases. This observation confirms the findings of Liangfeng [46] that the time for the transition of the resin from a liquid to rubbery state increases with the rise in isothermal temperature. In addition,  $T_{\text{onset}}$  marks the time taken for the onset of the chemical reaction and Table 3.2 shows that the onset time is less than the gel time. Even though, gel time ( $T_{\text{gel}}$ ) marks the onset of cure reaction, while forming operation it is much safer to stay with the  $T_{\text{onset}}$  regime to avoid curing during the forming operation.

**Table 3.2 Gel time at different temperatures [9]**

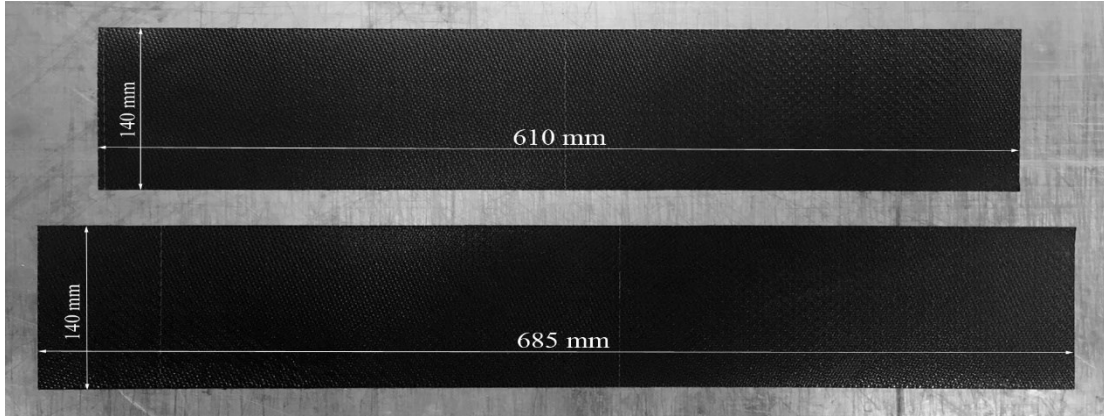
<b>Temperature (°C)</b>	<b>70</b>	<b>90</b>	<b>100</b>	<b>120</b>
<b>T<sub>gel</sub> (min)</b>	1302	453	243	74.9
<b>T<sub>onset</sub> (min)</b>	523	282	176	64
<b>T<sub>extrapolated</sub> (min)</b>	752	373	204	71

### **3.3 Sample Preparation**

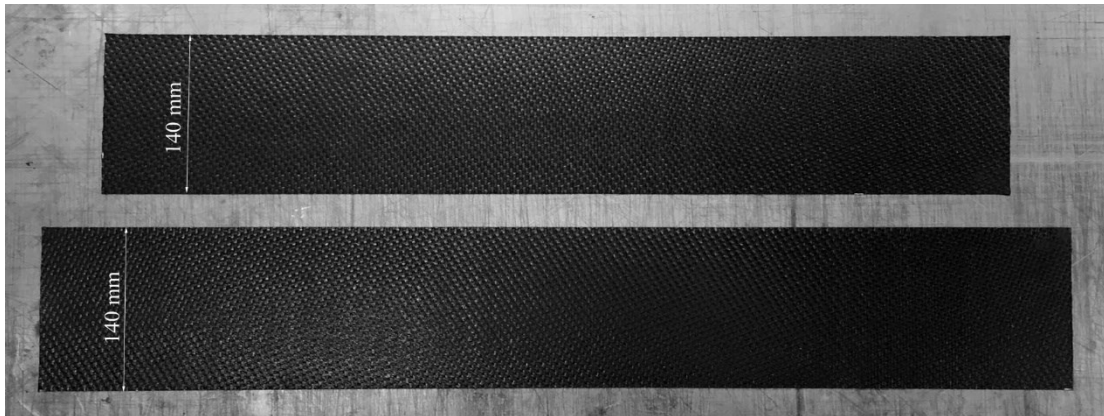
This section describes the steps involved in the preparation of OOA prepreg samples for friction tests.

- a. The wide tape roll of prepreg was taken out of the freezer. The prepregs could not be cut when frozen as they are very hard. It was kept at room temperature for about an hour. After remaining at ambient temperature, the prepregs become soft enough to cut.
- b. Two prepreg plies are needed to perform a friction test. The outer prepreg ply is longer than the inner prepreg ply as it passes through the spar at the bottom of the test rig. The outer ply must be 685 mm (27 inch) long and 140 mm (5.5 inch) wide. The dimensions of inner prepreg ply must be 610 mm (24 inch) of length and 140 mm (5.5 inch) of width. The sizes of the prepreg specimens were chosen according to the dimensions of the test rig.
- c. The prepreg tape was cut according to the lengths of the test specimens i.e. 685 mm and 610 mm. After that these composite prepreg sheets were cut into the wide stripes with 140 mm width. For storing the cut samples in the freezer for future a plastic bag was used that was sealed to prevent the samples from moisture.

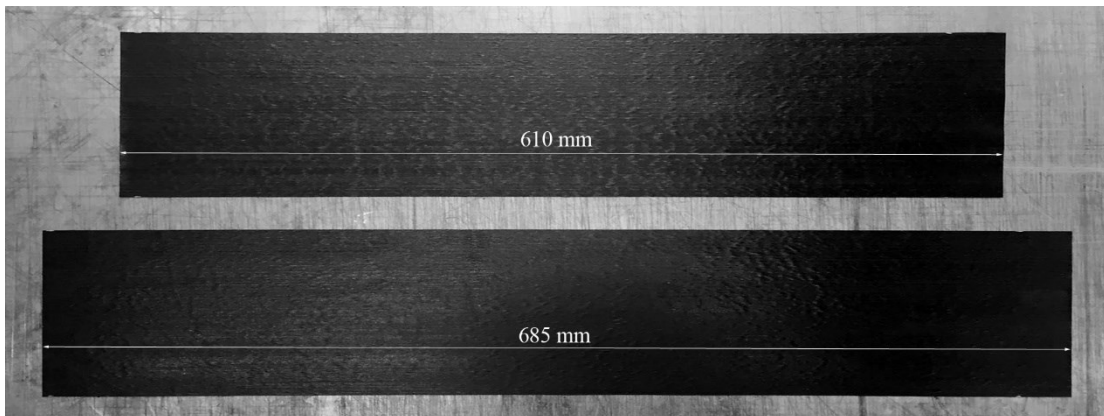
The images of the cut samples from the prepreg rolls are shown in figure 3.2 with 8-Harness material in figure (a), 5-Harness material in figure (b) and unidirectional material in figure (c).



(a)



(b)



(c)

**Figure 3.2 Final samples for friction test (a) 8-Harness prepreg, (b) 5-Harness prepreg and (c) Unidirectional prepreg**

### 3.4 Design of Friction Test Rig

To perform the interply friction tests, a test rig was designed and manufactured as shown in figure 3.3. Test rig consists of a steel middle plate and two steel platens for applying normal pressure to prepreg plies. Six cartridge heaters and a thermocouple were inserted in the middle plate. Three cartridge heaters and a thermocouple were inserted in each platen. Temperature was controlled by using three controllers through feedback system. Four springs were used to apply normal pressure to prepreg plies. Springs were calibrated according to their force-displacement curves. Inner prepreg ply was clamped on the middle plate with the help of clamping plates. C-clamps were used to help clamping plates hold the prepreg material firmly. The middle plate was held in between two platens.

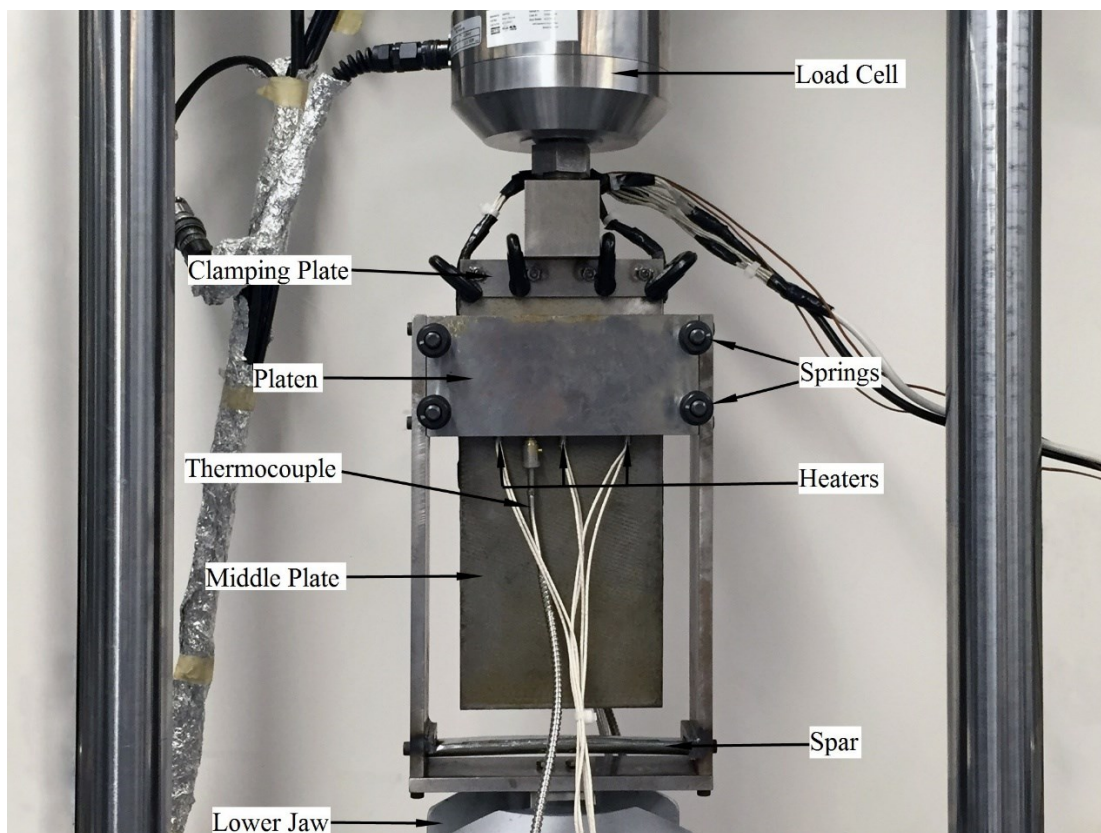


**Figure 3.3 Friction Test Rig**

Outer prepreg ply was mounted over a wide spar at the bottom of test rig and was clamped between two platens on the inner ply. The contact area between two prepreg plies is 140 x 76 mm (area = 10640 mm<sup>2</sup>). Test rig was installed on a tensile testing machine which can perform tests at different

pulling rates. The middle plate effectively pulls the clamped prepreg sample between the two steel platens which apply pressure to the front and back surfaces of the prepreg ply. A load cell attached to the top of middle plate was used to measure the frictional resistance between two prepreg plies.

### 3.4.1 Schematic of Test Rig

The test rig used for this study, as described above, is the modified form of the test apparatus used by Wilks [12]. The main advantage of using a pull-through test rig is that the area of contact between the prepreg plies remains constant throughout the whole test. The test apparatus used by some previous researchers [24,27,31] were not capable to provide the friction interface of constant area as the prepreg plies move with respect to each other. The schematic of the cross-section of the friction test rig is shown in figure 3.4.

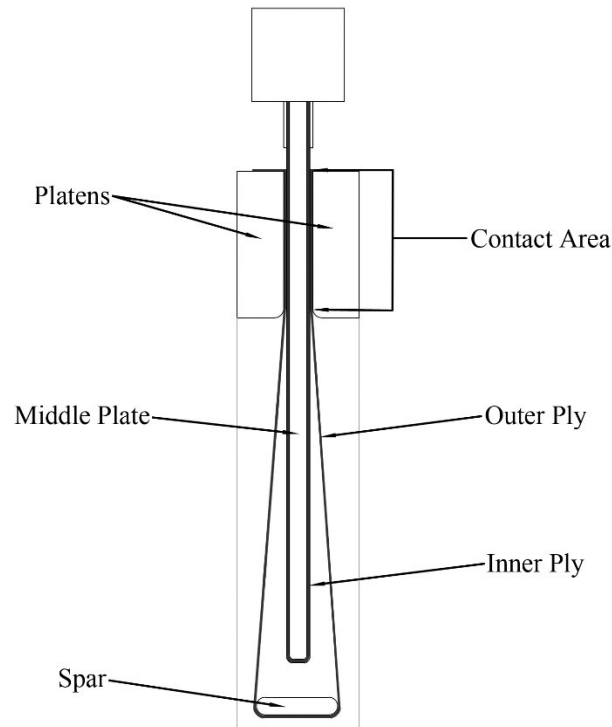


**Figure 3.4 Schematic of the cross-section of Test Rig**

The lower edge of each platen is milled to prevent snagging of the prepreg ply as it is pulled through the platens. The spar at the lower end of the test rig provides the stoppage to the outer ply when the inner ply is drawn upwards. Also, wide shape of the spar prevents the two plies from touching each other outside the area between platens.

### 3.4.2 Temperature Control

To perform friction tests at higher temperatures, heating facility is needed that could be able to reach the desired temperature in short time and maintain it throughout the experiments. Cartridge heaters, inserted inside the middle plate and the platens, were used for this purpose. The middle plate contains 6 heaters inserted in it from both sides and there are 3 cartridge heaters in each platen. The K-type thermocouples were used to measure the temperature and control the heaters. The middle plate and the two platens contains one thermocouple in each of them. The Benchtop temperature controller by OMEGA controls the temperature through feedback system as shown in figure 3.5.



**Figure 3.5 Benchtop temperature controller by Omega**

Three temperature controllers maintain the desired temperature in the test rig and the sample. The controller used in this study works on the PID principle which is Proportional, Integral and Derivative. The thermocouples send the information to the PID controller and the controller then tries to minimize the difference in the desired and measured temperatures. The desired temperature, or the set point, is the temperature which is selected according to the experimental conditions. The proportional part of the PID controller assists in controlling the temperature by lowering the power supplied to the heater as the temperature approaches the desired set point. The

proportional action of the controller is necessary as it prevents the temperature from rising above the set point and maintains a stable temperature [3]. The PID controller turns the power output on or off for the short intervals of time in order to control the temperature. If the temperature is too low, the output will be turned on for a longer interval and if the temperature is too high from the set point, the output will be off for a longer interval. The schematic of the temperature control process is shown in the figure 3.6.

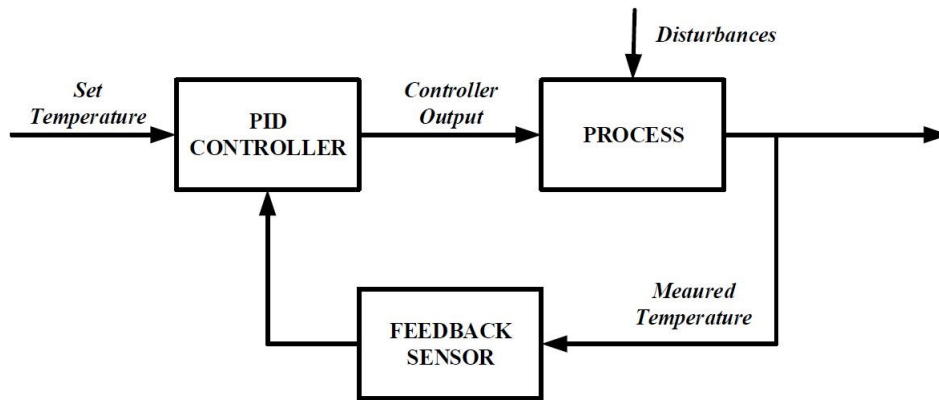
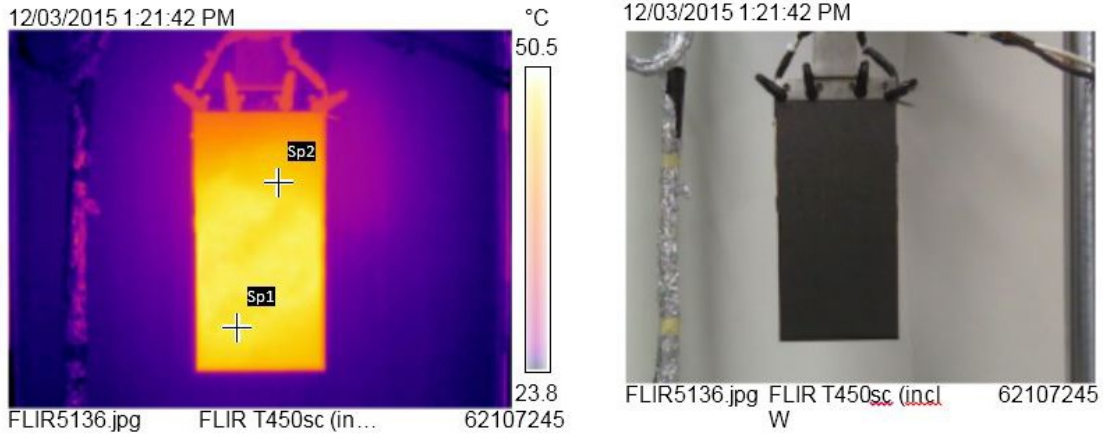


**Figure 3.6 Working of PID Controller [3]**

The other two actions, integral and derivative, also help to stabilize the temperature in short interval of time. All the three terms, proportional, integral and derivative are individually adjusted using the “auto-tune” function in the controller. The set point is adjusted in the PID controller and the output of the controller is given to the process which is the test rig in this study. The input to the controller is provided as feedback by the thermocouples and the calculations, by PID controller, are done according to the feedback.

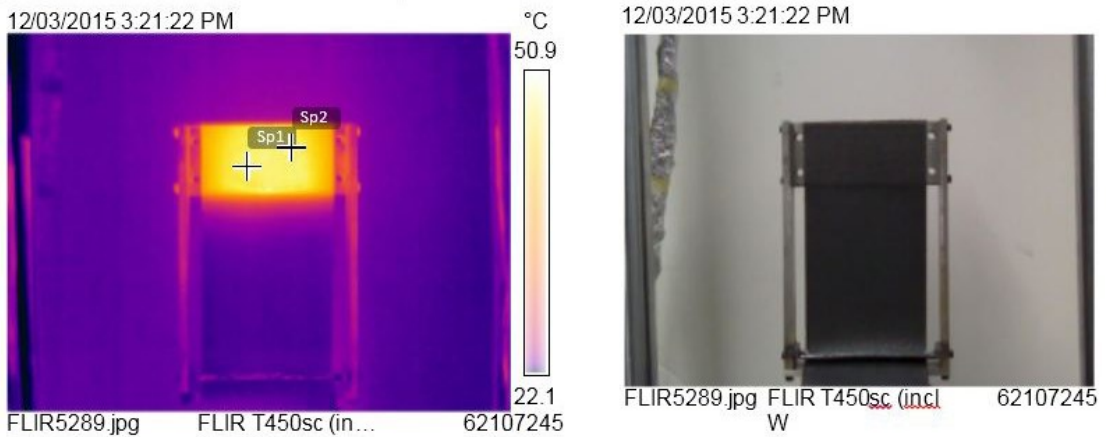
### **3.4.3 Temperature Distribution**

In order to monitor the temperature distribution across the middle plate and the platens, a FLIR T420 infrared camera was used. Figure 3.7 shows the temperature distribution across the prepreg surface obtained by the FLIR infrared camera. The tables in the figure show the temperature differences at the two points, sp1 and sp2, on the prepreg samples.



Measurements	°C
Sp1	49.9
Sp2	50.3

(a)



Measurements	°C
Sp1	50.2
Sp2	49.4

(b)

Figure 3.7 Infrared images showing temperature gradient of (a) Middle Plate, (b) Platen

### 3.4.4 Pressure Control

The application of normal pressure is very important in friction tests as normal pressure is one of the principal factors influencing the forming operation. The test apparatus used in this research consists of four spring-screw sets that provide necessary normal pressure to the platens. For the calibration of the spring-screw sets, compression tests were performed on the springs using MTS machine. The load cell attached on the upper head of the MTS machine recorded the compression force applied on the spring to compress it to a specific displacement. Figure 3.8 shows the images of start and end of the compression test.



(a)

(b)

**Figure 3.8 Measurement of the Spring Constant (a) Start and (b) End of the test**

The tests were performed on all the four springs. The recorded data was, then, converted into force displacement graph, as shown in figure 3.9. The spring constant,  $k$ , was calculated using the following formula:

$$k = \frac{F_2 - F_1}{d_2 - d_1}$$

where  $F_2$  and  $F_1$  are compression forces at two specific points and  $d_2$  and  $d_1$  are displacements at those points. The value of spring constant calculated from the force-displacement graph is

$$\begin{aligned} k &= 16.97 \text{ N/mm} \\ &= 430.94 \text{ N/inch} \end{aligned}$$

The spring constants for all the springs appeared as equal.

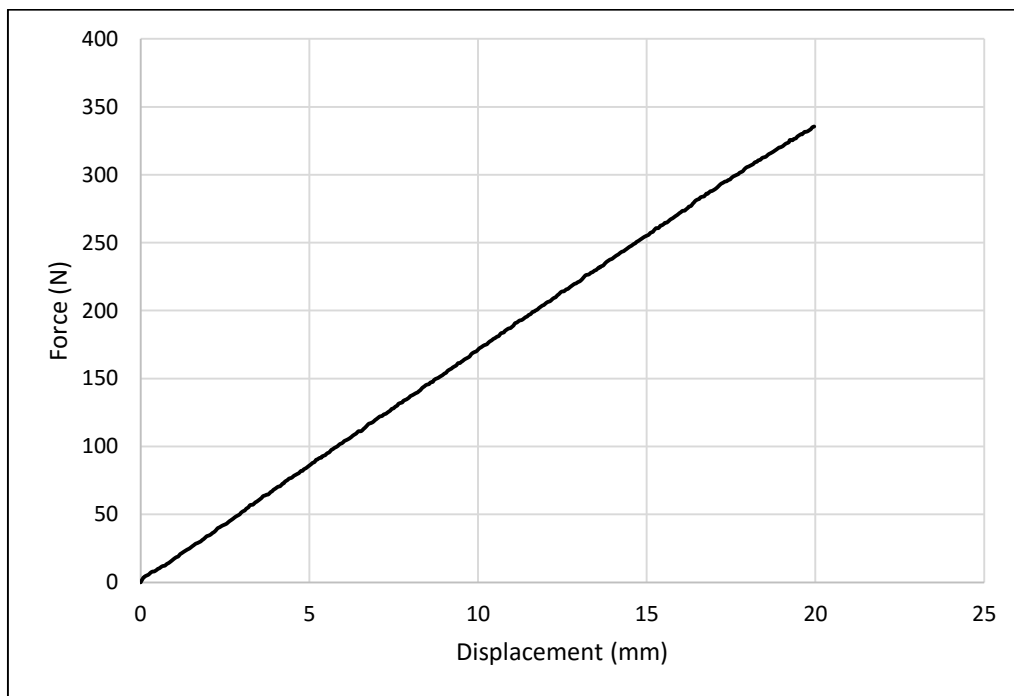


**Figure 3.9 Force-Displacement graph for calculation of spring constant**

The screws and nuts, with 16 threads per inch, were used in the test rig to hold the platens and the springs. According to the Hooke's Law,

$$F = -kx$$

where  $F$  is the restoring force by spring,  $k$  is rate or spring constant and  $x$  is the displacement vector

As we know that spring constant is equal to 430.94 N/inch, which means that the spring will apply a restoring force of 430.94 N if compressed by 1 inch. The nuts move 1 inch in the axial direction by giving them 16 rotations.

$$\text{Area under pressure} = 140 \times 76 \text{ mm} = 10640 \text{ mm}^2 = 0.01064 \text{ m}^2$$

For getting the pressure of 1 atm (= 101,325 N/m<sup>2</sup>), force required is,

$$F = 101,325 \times 0.01064 = 1078.6 \text{ N}$$

As four springs are used in the test rig, the required force from 1 spring (for 1 atm normal pressure) is,

$$= \frac{1078.6}{4} = 269.65 \text{ N}$$

A restoring force of 430.94 N is received by the compression of 1 inch or 16 rotations

or 1 N by 16/430.94 rotations

(P = 1 atm) 269.65 N by 10.01 rotations

(P = 0.8 atm) 215.72 N by 8.01 rotations

(P = 0.5 atm) 134.83 N by 5 rotations

Using the above relations between normal pressure and the rotations of the nuts, desired pressure could be applied to the platens.

### **3.5 Summary**

The out-of-autoclave composite material was selected for this research. The OOA composites have advantages over the other composite materials in terms of the less initial cost as no autoclave is needed and less processing time. The friction test rig was designed and manufactured based on the information available from the previous researches. The test rig is capable of simulating the actual processing conditions for forming operation such as desired processing temperature, normal pressure and pulling velocity.

# Chapter 4 : Experiments, Results and Discussions

This chapter explains the inter-ply slippage mechanism in 8-harness, 5-harness and unidirectional prepreg composite materials and the influence of processing parameters like temperature, pulling rate, normal pressure and fiber orientation. Experiments were performed using friction test rig at different operating conditions in order to analyse the influence of each operating condition.

## 4.1 Experimentation and Results

A pair of two samples was used in each test, i.e. inner and outer ply. Samples from 8-harness and 5-harness material were cut rectangular in shape. The inner prepreg ply was clamped on the middle plate with the help of clamping plates. Four C-clamps were used to apply pressure on the ends of the ply to hold it firmly. The outer prepreg ply was placed over the inner ply between the two platens. The outer ply was mounted over a wide spar at the bottom of the test rig to ensure that it would not move when inner ply is pulled upwards. Two steel platens apply normal pressure on the friction interface and four spring-screw sets, which were calibrated according to their load-displacement curves, provide the necessary force to the platens.

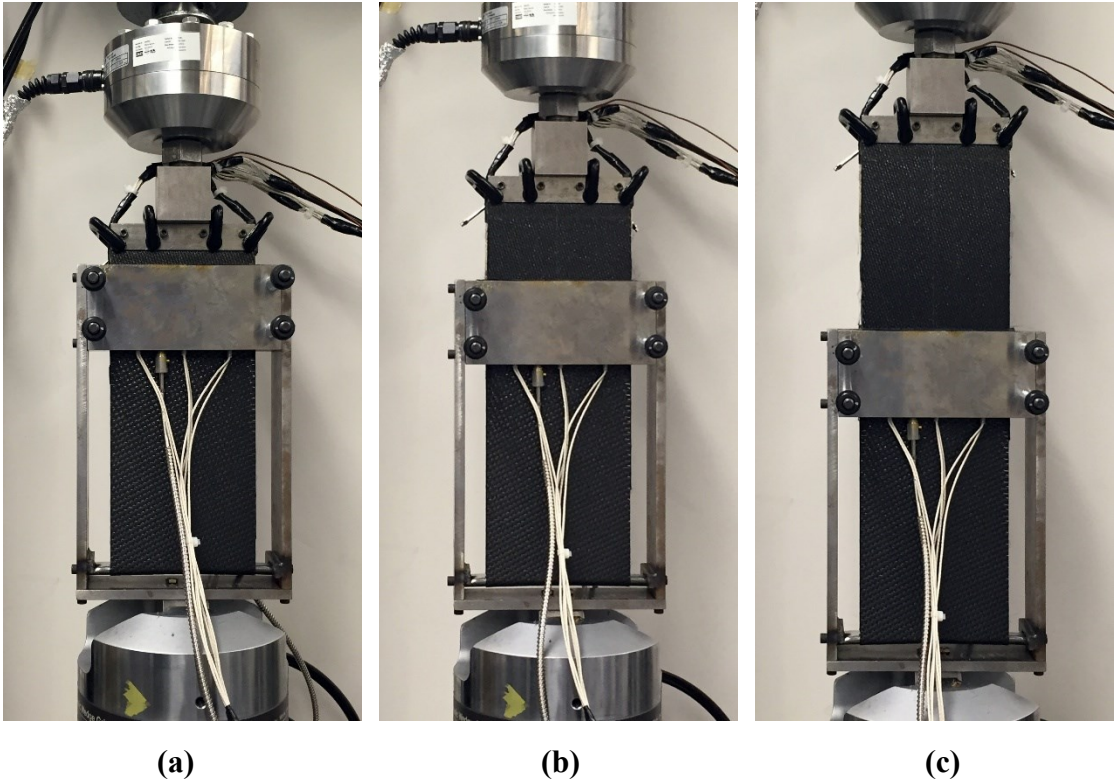
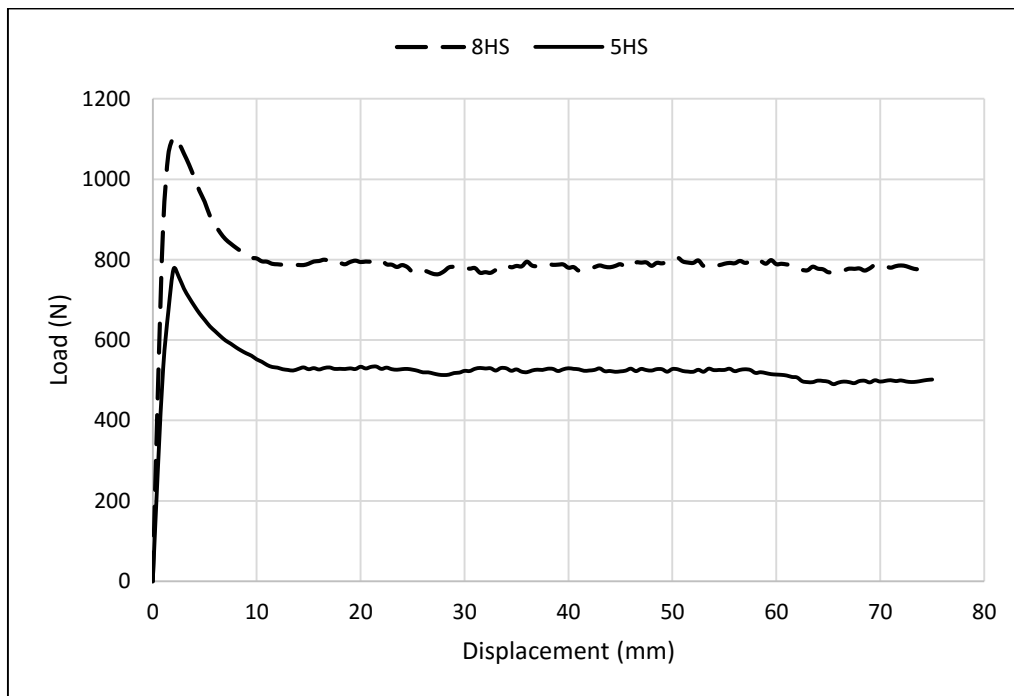


Figure 4.1 (a) Start, (b) Mid and (c) End of the test

The desired temperature for experiments was achieved by using cartridge heaters which were inserted in the middle plate as well as the two steel platens. The force required to overcome the friction between the plies was recorded by a load cell installed on the top of the rig. The data from the load cell was collected by the computer attached to it. The results explained here are based on load-displacement graphs that were obtained from tensile testing machine. In each test, plies were moved to the displacement of 75mm. Figure 4.2 shows the load-displacement curves for 8-harness and 5-harness prepreg materials at the temperature of 50 °C, pulling rate of 0.5 mm/sec and normal pressure of 0.5 atm.



**Figure 4.2 Load-Displacement graphs at 50 °C, 0.5 mm/sec and 0.5 atm**

It is observed that frictional load reaches a maximum value at the starting of the slippage and it gradually decreases to a steady state. The graphs show stick-slip peaks which is similar to the characteristics of dry Coulomb friction [24]. The state of stick is the viscous nature of one prepreg ply sliding over another ply instead of quasi-static state. After the peak state, the composite plies slip which is due to weakening of the viscous behaviour and the force state comes to the equilibrium. At higher temperatures and slower pulling rates the trend of load-displacement curve

changes slightly. The peak in the beginning of the graph decreases and in some exceptional cases it disappears.

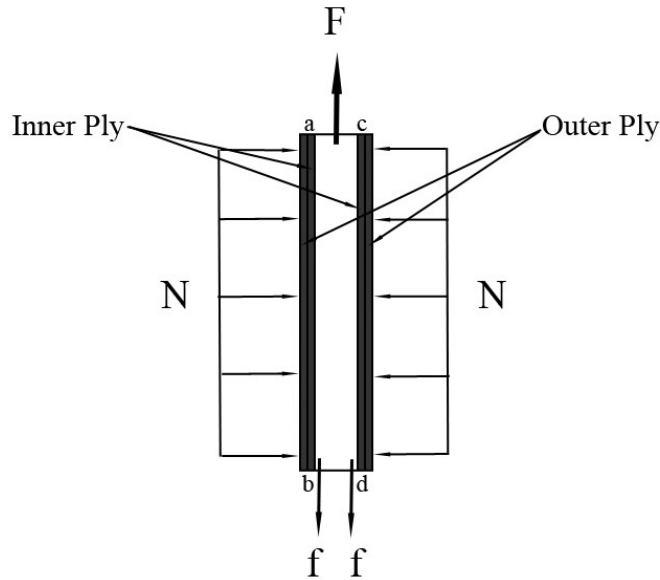


**Figure 4.3 Testing Region**

The slippage occurs at two interfaces, a-b and c-d, between inner and outer plies as shown in figure 4.3. The relationship between tensile load  $F$  recorded by load cell and frictional force  $f$  is given by equation 4.1.

$$F = 2f \quad (4.1)$$

Combining equation 2.1 and 4.1, we get

$$\mu = f/N = F/2N \quad (4.2)$$

The coefficient of friction is the ratio of force of friction to the normal force at the interface. Equation 4.2 was used to calculate the coefficient of friction at different test conditions. As the load-displacement graphs show peak and steady state value of friction, coefficient of friction for both these values were calculated. Figure 4.4 shows the comparison between maximum value coefficient of friction and steady state coefficient of friction for 8-harness and 5-harness prepreg materials at 50 °C, 0.5 mm/sec and 0.5 atm. Steady state friction coefficient appeared less than the peak value friction coefficient. For 8-harness prepreps, coefficient of friction decreases from 1.02 to 0.72 as the frictional force reaches the steady state. Similarly, for 5-harness material, friction

coefficient decreases from 0.72 to 0.49 as friction state changes from peak to steady value. Both friction coefficients, peak and steady state, have their importance in the prediction of forming operation before the actual process happens. A simulation model of inter-ply slippage process could be developed based on the coefficients of friction shown in figure 4.4.

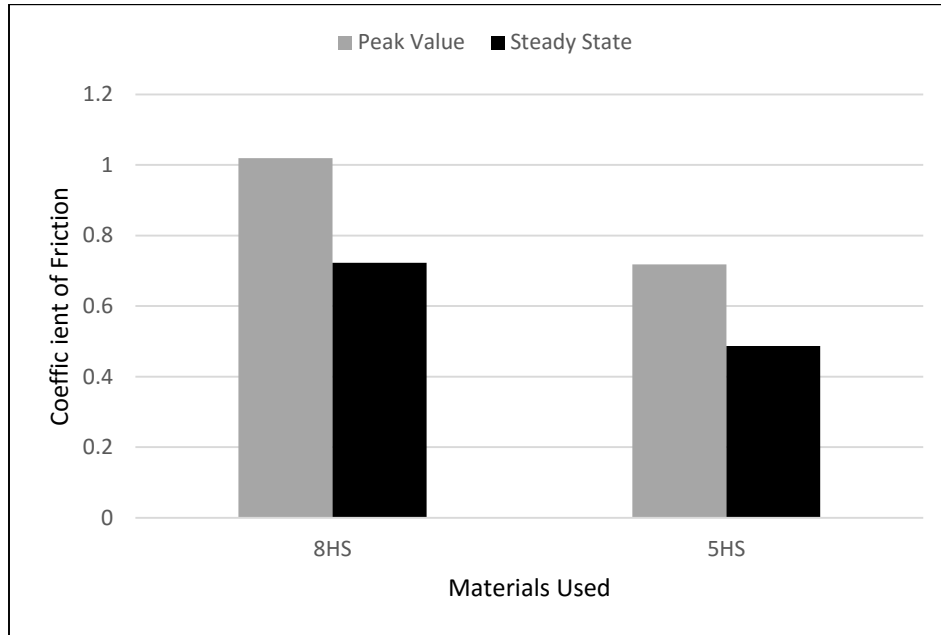


**Figure 4.4 Comparison between coefficients of friction for 8HS and 5HS at 50 °C, 0.5 mm/sec and 0.5 atm**

## 4.2 Test Conditions

To study the effect of each process parameter, tests were performed by varying process parameters. Three of the four process parameters (temperature, pressure, rate and fiber orientation) were kept constant and one parameter was varied to study its effect on interply friction. Table 4.1 shows the test conditions used in this study.

**Table 4.1 Test Conditions**

<b>Temperature (°C)</b>	50, 70, 90
<b>Rate (mm/sec)</b>	0.2, 0.5, 1, 2
<b>Pressure (atm)</b>	0.5, 0.8, 1
<b>Fiber (fabric) Orientation</b>	0°, 15°, 30°, 45°

The values of processing conditions were chosen according to the actual forming process. As CYCOM 5320-1 is an out-of-autoclave thermoset composite, its curing temperature is around 110°C. So, the highest temperature chosen for testing was 90°C and for minimum value 50°C, resin viscosity is too high for the interply slippage to take place easily below this temperature. Pulling rates were chosen in the range of 0.2 – 2 mm/sec taking into account the actual forming process. The normal pressure is applied by vacuum during forming, so the maximum value chosen was 1 atmosphere. Fiber orientation is necessary for the mechanical properties of the composite materials. Fiber angles were selected according to the review of previous studies and the generally used layouts of prepreg laminates.

### 4.3 Influence of Temperature

In order to facilitate the forming operation, these processes usually take place at high temperatures. To investigate the influence of operating temperature, tests were performed at a constant pulling rate of 0.5 mm/sec, a constant normal pressure of 0.5 atmosphere and fiber orientation at 0° to the pulling direction at different temperatures. Both 8-harness and 5-harness carbon/epoxy prepreg composites were analysed in the tests. Results are based on load-displacement graphs that were obtained from tensile testing machine at different conditions of test parameters. Figure 4.5 and 4.6 shows load-displacement graphs for 8HS and 5HS at 50, 70 and 90 °C to analyse the effect of processing temperature on inter-ply friction. The graphs show that frictional load measured by load cell reduces as the temperature increases from 50 °C to 90 °C. Similar results were observed by some previous researchers [24,31]. This is in agreement with the fact that the viscosity of resin decreases with the increase in temperature and resin changes from rubbery state to liquid state. According to the equation 2.2, shear stress is directly proportional to the viscosity of fluid.

$$\tau = \frac{\eta}{d} v \quad (2.2)$$

Therefore, force of friction is reduced at higher temperatures. The rheological tests show that with the rise in temperature resin viscosity reduces at initial stages while later it increases drastically [9]. The later rise in viscosity is due the increase in degree of cure of the resin. In this study we are interested only in the initial stage as actual forming operation takes place during this period. As stated earlier, load-displacement graphs for both 8HS and 5HS prepreps show high peak in the frictional load at the start of test and steady state afterwards.

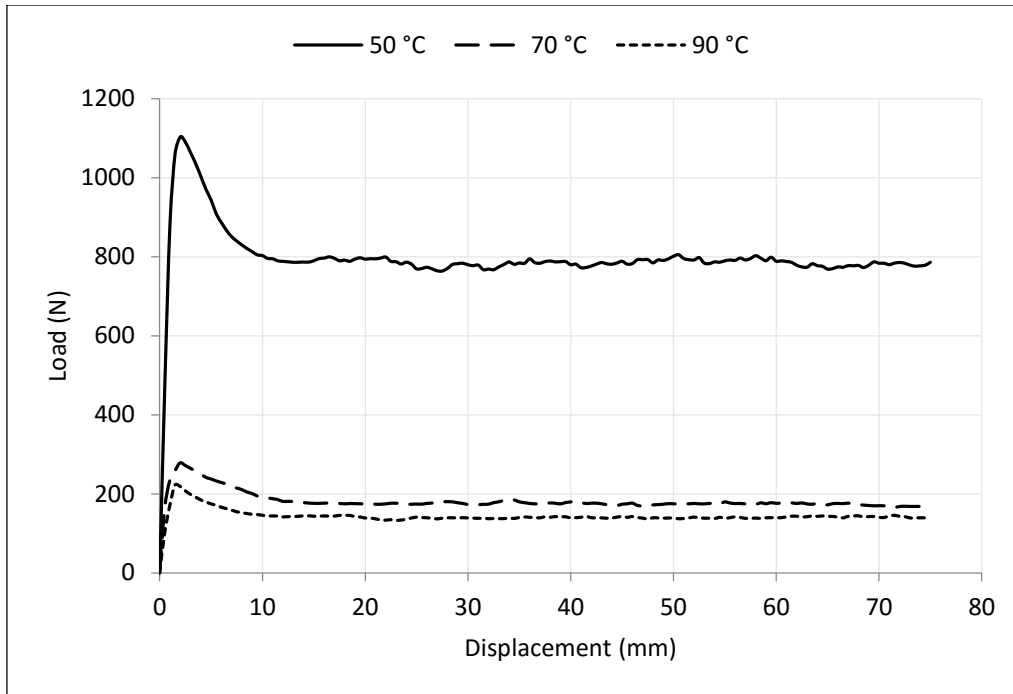


**Figure 4.5 Influence of temperature on Inter-Ply friction at 0.5 mm/sec, 0.5 atm and 0° fiber orientation for 8-harness carbon/epoxy prepregs [47]**

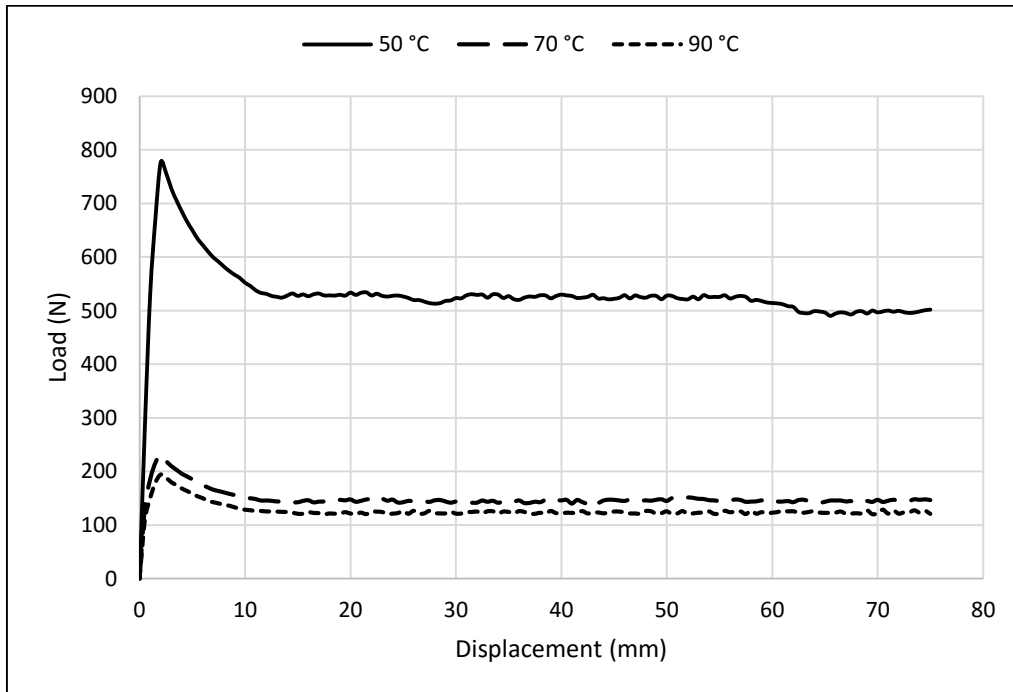


**Figure 4.6 Influence of temperature on Inter-Ply friction at 0.5 mm/sec, 0.5 atm and 0° fiber orientation for 5-harness carbon/epoxy prepregs [48]**

Friction coefficients are very important in the modelling of the inter-ply friction mechanism. Equation 4.2 was used to calculate the coefficient of friction at different temperatures. As shown in figures 4.5 and 4.6, the load-displacement graphs show the initial rise in friction and then gradually decrease to a steady state, coefficient of friction for both these values were calculated. Figures 4.7 and 4.8 show the comparison between coefficient of friction at maximum value and steady state coefficient of friction at 50, 70 and 90 °C. Maximum value friction coefficient decreases from 1.02 to 0.2 for 8-harness preregs and from 0.72 to 0.18 for 5-harness preregs as the temperature rises from 50 °C to 90 °C.

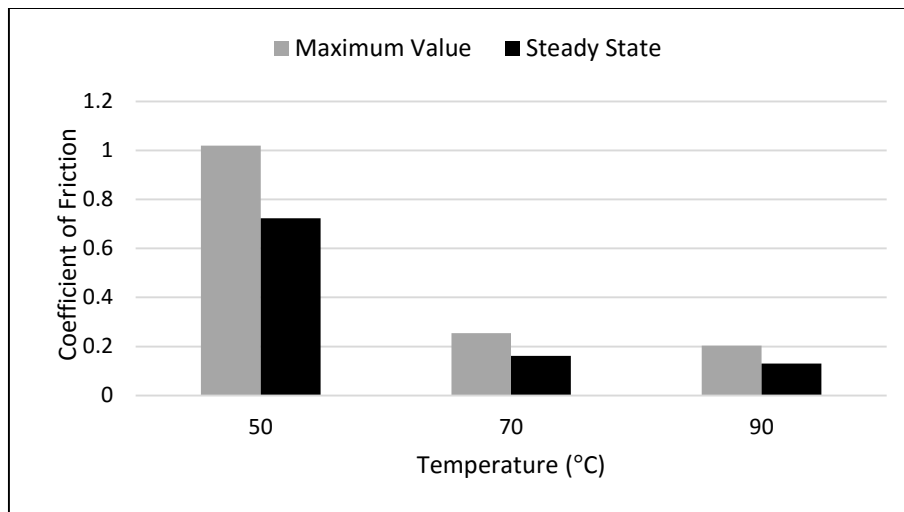


**Figure 4.7 Comparison of coefficients of friction at elevated temperatures for 8HS preregs**

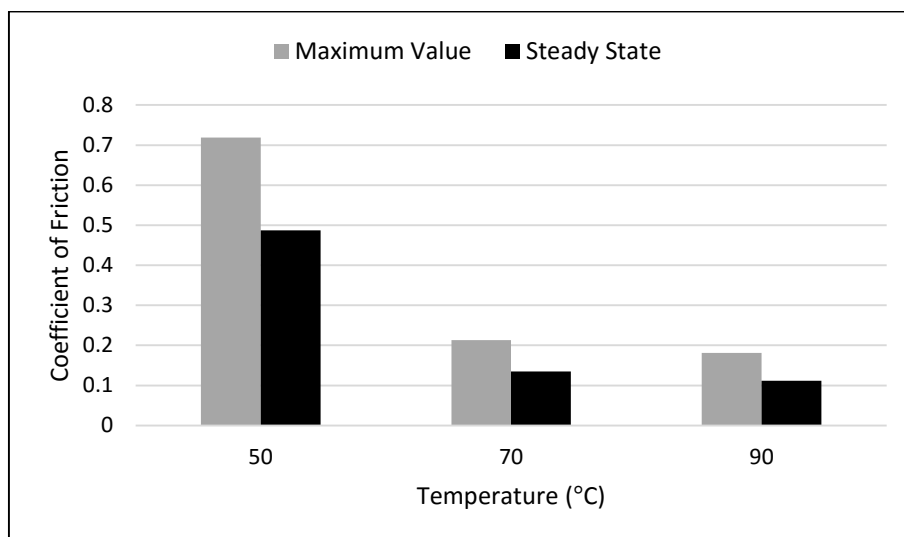


**Figure 4.8 Comparison of coefficients of friction at elevated temperatures for 5HS preregs**

#### 4.4 Influence of Pulling Rate

Pulling rate during experiments represents the slippage speed of one prepreg ply over other. Tests were performed at a constant temperature of 50 °C and a constant normal pressure of 0.5 atmosphere at different pulling rates. The tensile testing machine provided the different pulling rates. Fiber orientation was 0° in these experiments. The materials used for these tests were 8-Harness satin and 5-Harness satin carbon/epoxy preregs. Results were recorded from tensile testing machine at various conditions of test parameters. Table 4.2 lists the maximum frictional resistances for 8HS and 5HS. Figure 4.9 and 4.10 shows load-displacement graphs at 0.2, 0.5, 1 and 2 mm/sec to investigate the influence of pulling rate on inter-ply friction. It could be noticed that these graphs have similar stick-slip peaks of dry-coulomb as they were in the graphs for elevated temperatures. The graphs show that frictional load increases as pulling velocity increases from 0.2 mm/sec to 2 mm/sec. This is in agreement with the fact that the shear stress between prepreg plies is directly proportional to the velocity of one ply with respect to other. Equation 2.2 shows that when resin film thickness and viscosity are constant, shear stress increases as the velocity increases.

**Table 4.2 Maximum frictional loads for 8HS and 5HS at different rates**

Pulling Rate (mm/sec)	Maximum Frictional Load	
	8-Harness (N)	5-Harness (N)
0.2	752	585
0.5	1101	775
1	2008	1304
2	3011	1802

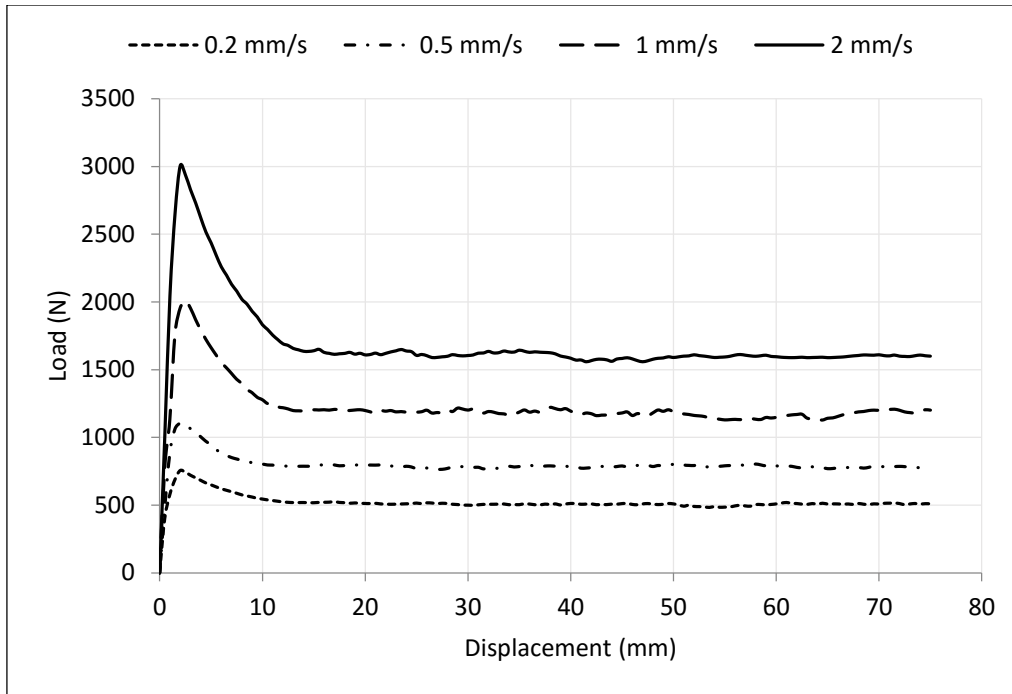


**Figure 4.9 Influence of pulling rate on inter-ply friction at 50 °C, 0.5 atm and 0° fiber orientation for 8-harness carbon/epoxy prepregs**

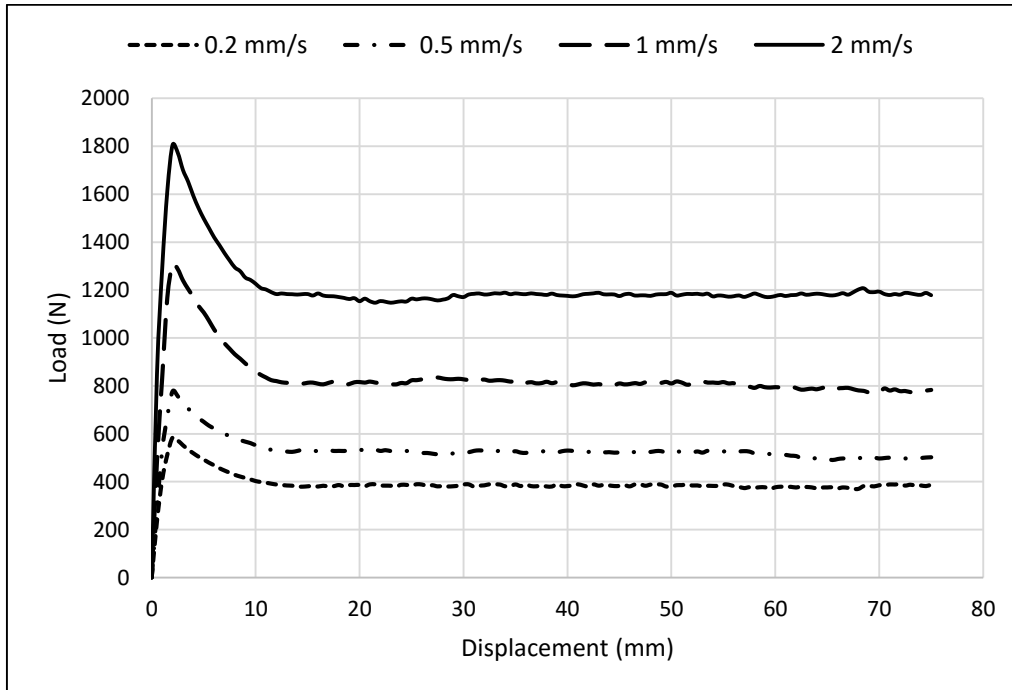


**Figure 4.10 Influence of pulling rate on inter-ply friction at 50 °C, 0.5 atm and 0° fiber orientation for 5-harness carbon/epoxy prepregs**

To calculate the coefficient of friction at different pulling rates, equation 4.2 was used. As load-displacement graphs show peak and steady states of friction, coefficient of friction for both these values were calculated. Figures 4.11 and 4.12 show the comparison between maximum value coefficient of friction and steady state coefficient of friction at 0.2, 0.5, 1 and 2 mm/sec. Maximum value friction coefficient increases from 0.69 to 2.78 for 8-harness composites and from 0.54 to 1.67 for 5-harness composites as the pulling rate increases from 0.2 mm/sec to 2 mm/sec.

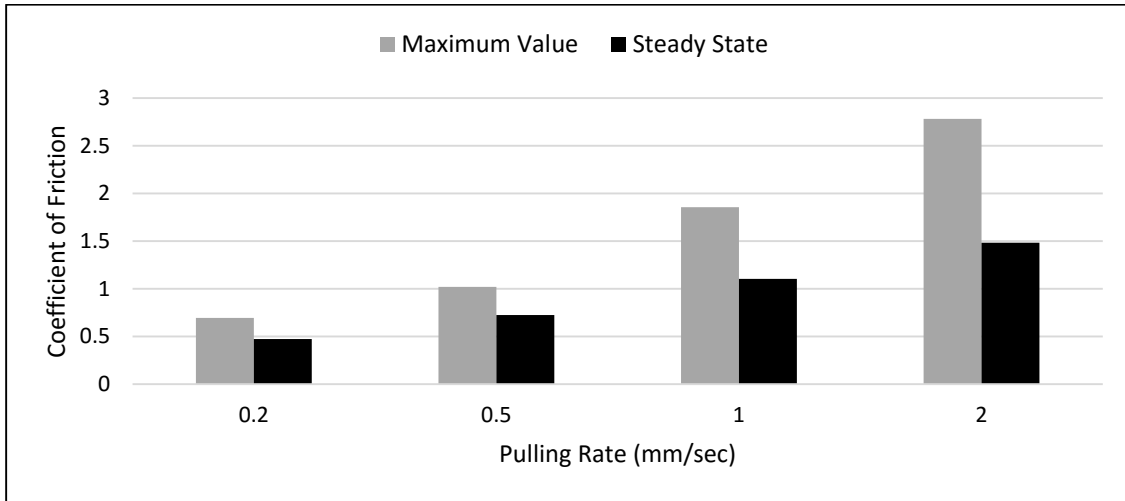


**Figure 4.11 Comparison of coefficients of friction at different pulling rates for 8HS preregs**

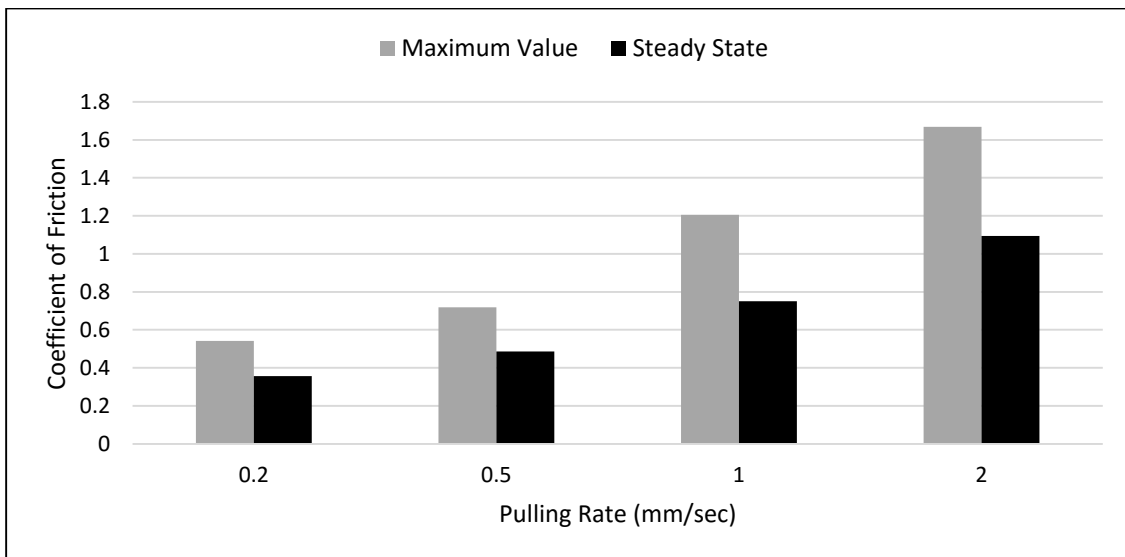


**Figure 4.12 Comparison of coefficients of friction at different pulling rates for 5HS preregs**

## 4.5 Influence of Normal Pressure

Normal pressure in the thermoforming operations is essential to consolidate the prepreg plies with each other. To study the influence of normal pressure on Inter-Ply friction, tests were performed at a constant pulling rate of 0.5 mm/sec and a constant processing temperature of 50 °C at different pressures on 8-harness satin and 5-harness satin carbon/epoxy prepregs. Plies were oriented at 0° to the direction of movement. Figures 4.13 and 4.14 show load-displacement graphs at 0.5, 0.8 and 1 atmosphere. The results show that frictional load increases as the pressure increases from 0.5 to 1 atm.

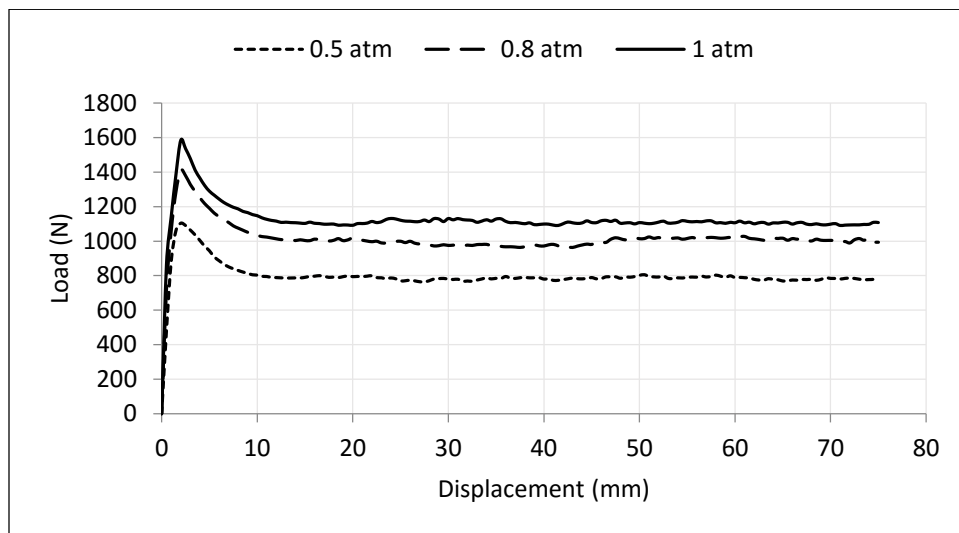


Figure 4.13 Influence of pressure on inter-ply friction at 50 °C, 0.5 mm/sec for 8HS

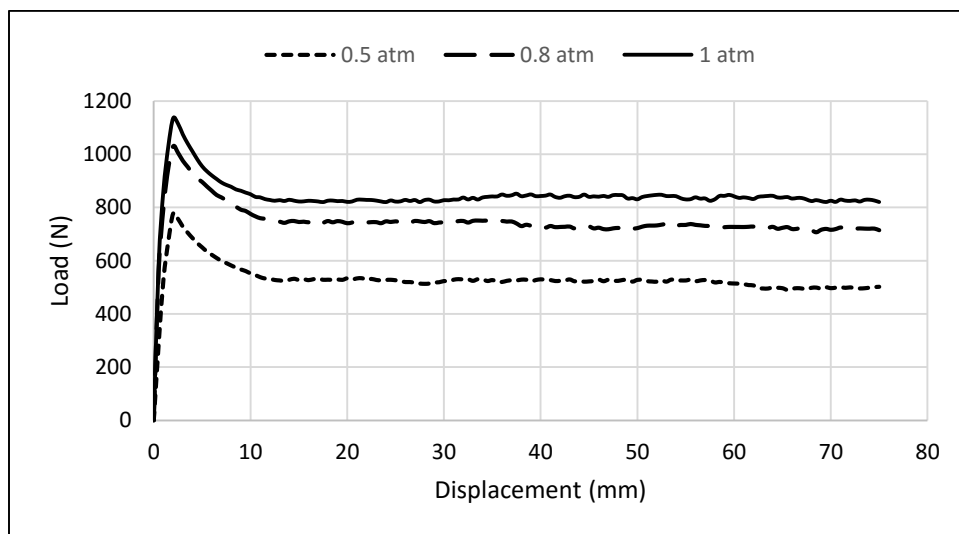
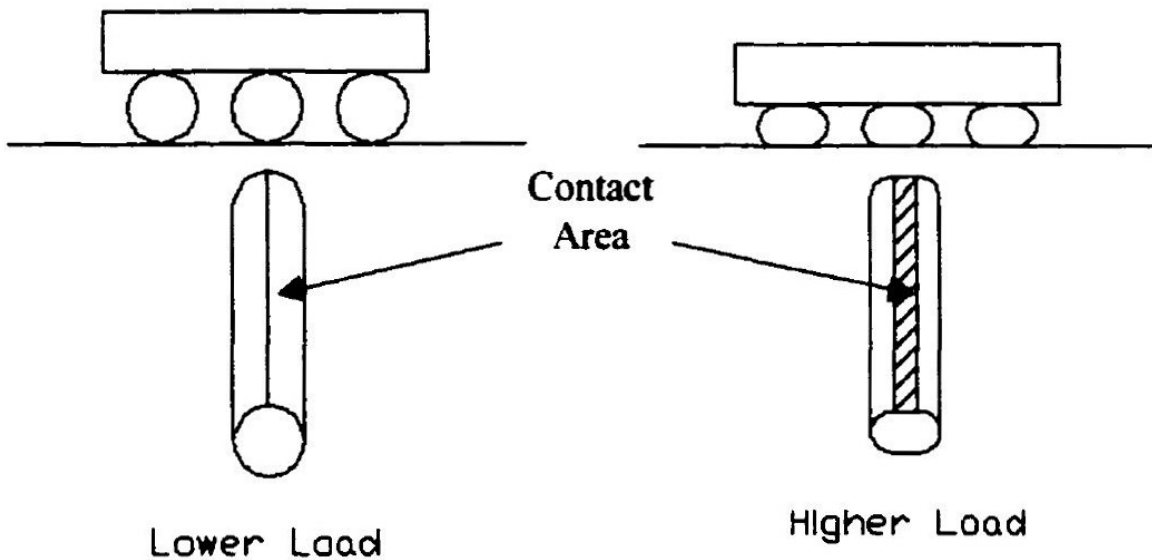


Figure 4.14 Influence of pressure on inter-ply friction at 50 °C, 0.5 mm/sec for 5HS

The results could be explained by the deformation of the fiber geometry under different loading magnitudes. Chow [29] explains that the increase in actual contact area is the change in fiber yarn geometry. The fibers are assumed to have circular cross-section before the application of normal pressure. The width of the contact area between single yarn and the pressure plate increases as it gets compressed. With the increase in contact area, the force of friction increases accordingly. Figure 4.15 shows the deformation of fiber geometry under the influence of normal pressure.



**Figure 4.15 Fiber deformations under different loading magnitude [29]**

The coefficients of friction were calculated using equation 4.2 for both maximum and steady state values at different normal pressures. Figures 4.16 and 4.17 show the comparison between maximum value coefficient of friction and steady state coefficient of friction at 0.5, 0.8 and 1 atm. It is observed from the graphs, friction coefficients decrease as the normal pressure increases. These results are consistent with some previous works [25,31–33].

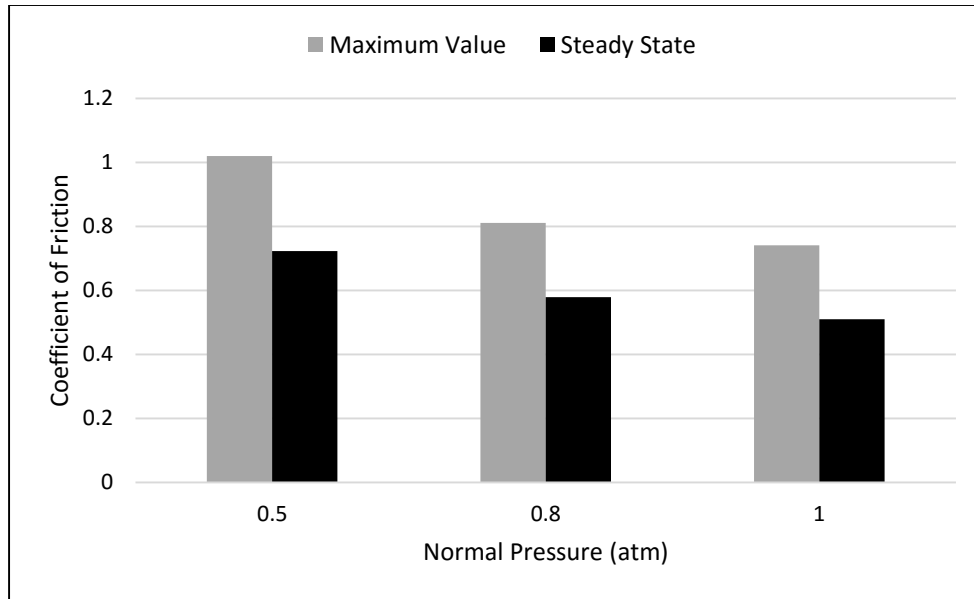


**Figure 4.16 Comparison of coefficients of friction at different normal pressures for 8HS**

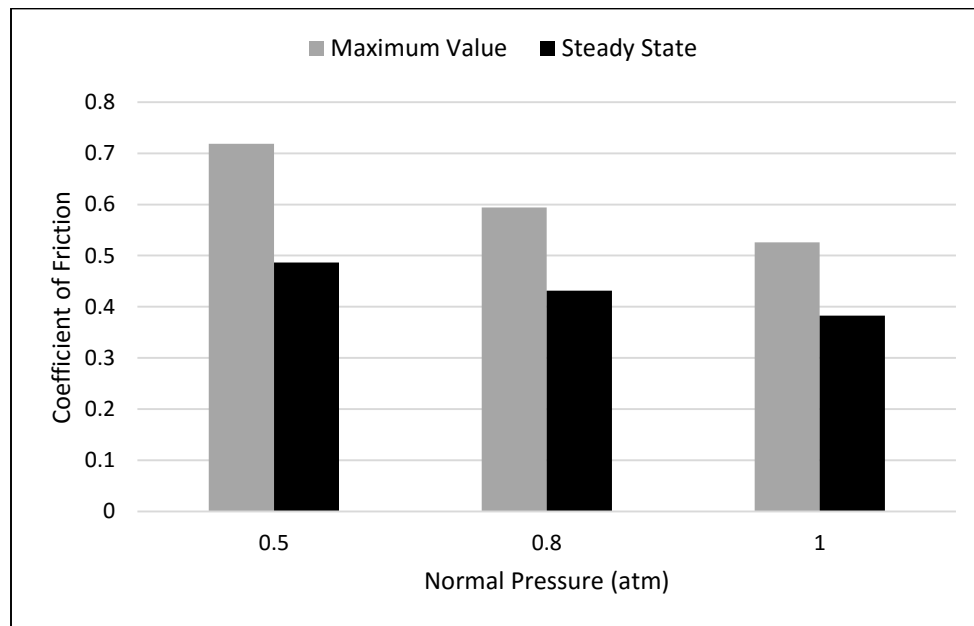


**Figure 4.17 Comparison of coefficients of friction at different normal pressures for 5HS**

Maximum value friction coefficient decreases from 1.02 to 0.74 for 8-harness composites and from 0.72 to 0.53 for 5-harness composites as the pressure increases from 0.5 atmosphere to 1 atmosphere. An increase of 100% in normal pressure gives a 45% increase in frictional load for 5HS. The reason for decrease in coefficients of friction with increasing normal pressure is that as coefficient of friction is the ratio of force of friction to the normal force and increase of normal

force gives percentagewise less increase in force of friction. Relationship of frictional load, normal pressure and coefficient for both 8-harness and 5-harness carbon/epoxy prepregs are shown in figures 4.18 and 4.19.

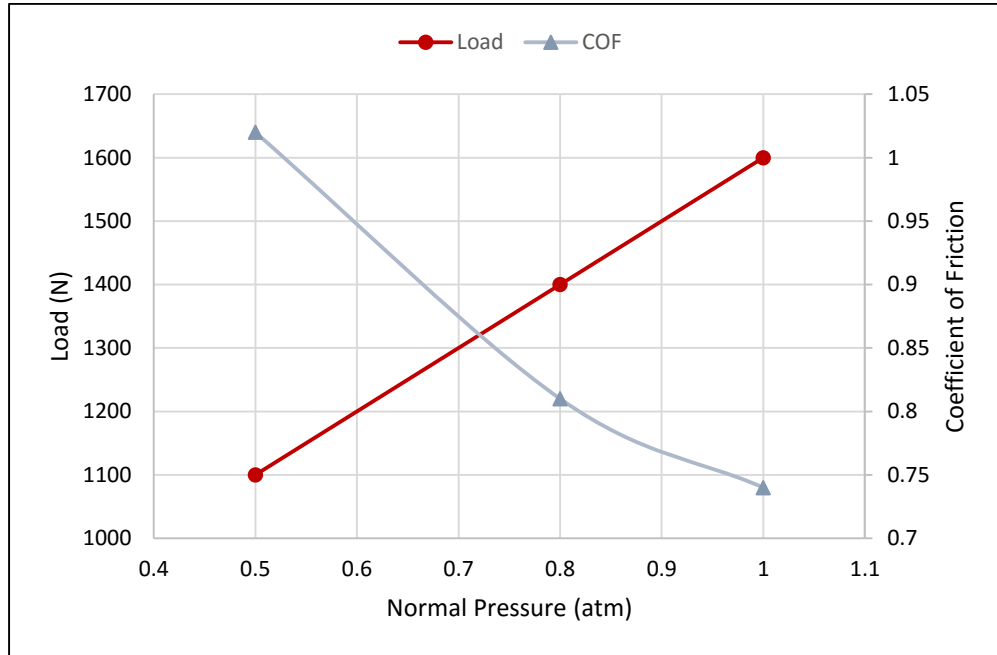


**Figure 4.18 Relationship between Load, Normal Pressure and Friction Coefficient for 8HS**

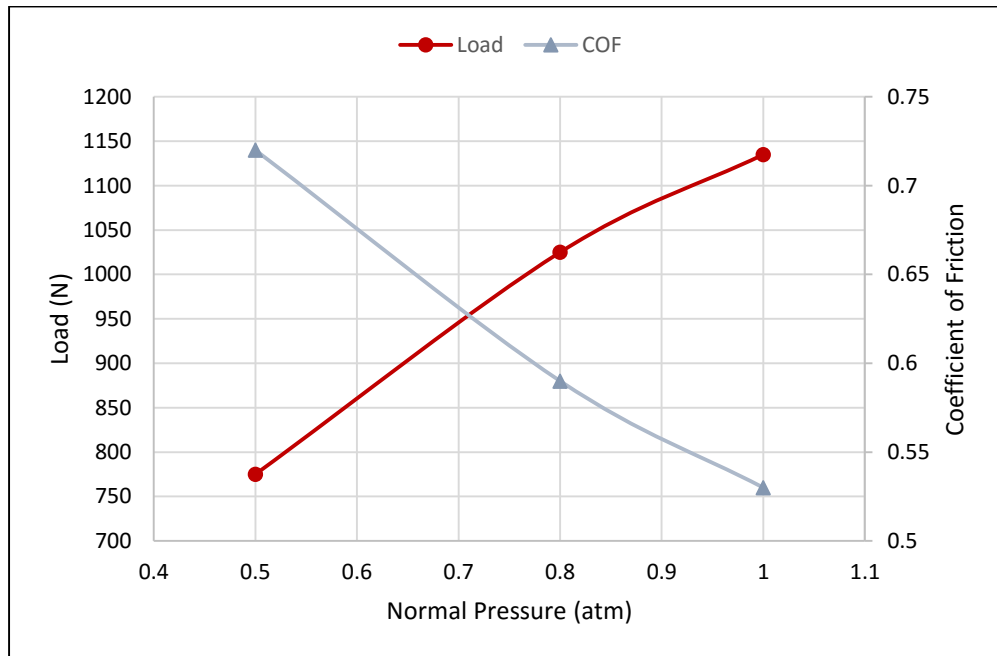


**Figure 4.19 Relationship between Load, Normal Pressure and Friction Coefficient for 5HS**

## 4.6 Influence of Fiber Orientation

For a stack of laminate, the orientation of the fibers in each prepreg ply is very important to obtain desired mechanical properties. During forming operations, fiber orientation could affect the occurrence of wrinkles and other defects in the final product.

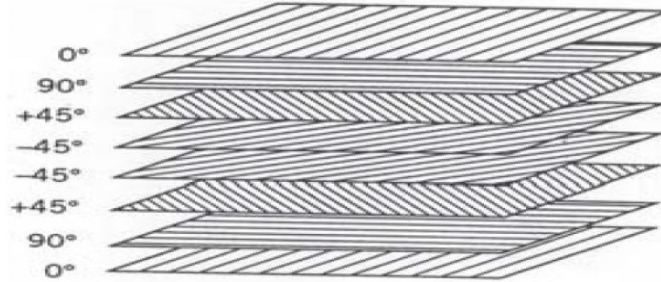


**Figure 4.20 Fiber Orientation in a prepreg laminate [7]**

The classical laminate theory gives the relationship between shear stresses and resultant shear strains. The stiffness matrices A, B and D provide the relation between orientations of fibers and the mechanical strengths of the composite material. Equation 4.3 shows the combined matrix relation for classical laminate theory.

$$\begin{Bmatrix} N_x \\ N_y \\ N_{xy} \\ M_x \\ M_y \\ M_{xy} \end{Bmatrix} = \begin{bmatrix} A_{11} & A_{12} & A_{16} & B_{11} & B_{12} & B_{16} \\ A_{12} & A_{22} & A_{26} & B_{12} & B_{22} & B_{26} \\ A_{16} & A_{26} & A_{66} & B_{16} & B_{26} & B_{66} \\ B_{11} & B_{12} & B_{16} & D_{11} & D_{12} & D_{16} \\ B_{12} & B_{22} & B_{26} & D_{12} & D_{22} & D_{26} \\ B_{16} & B_{26} & B_{66} & D_{16} & D_{26} & D_{66} \end{bmatrix} \begin{Bmatrix} \varepsilon_x^0 \\ \varepsilon_y^0 \\ \gamma_{xy}^0 \\ \kappa_x^0 \\ \kappa_y^0 \\ \kappa_{xy}^0 \end{Bmatrix} \quad (4.3)$$

To analyse the influence of fiber orientation, friction tests were performed at a constant normal pressure of 0.5 atmosphere, a constant temperature of 50 °C and a varying pulling rate of 0.2 mm/sec, 0.5 mm/sec, 1 mm/sec and 2 mm/sec. The orientation of the fibers to the pulling direction was changed to study its influence on inter-ply friction. Both 8-harness and 5-harness carbon/epoxy prepreg composites were analysed in the tests. Results are based on load vs. pulling rate graphs that were obtained from tensile testing machine at different conditions of test parameters. Figures 4.21 and 4.22 show load vs. pulling rate graphs for 8HS and 5HS at 0°, 15°, 30° and 45° fiber angle to the direction of ply movement to analyse its effect on inter-ply friction.

The graphs show that frictional resistance decreases as fiber angle changes from  $0^\circ$  to some angle to the pulling direction.

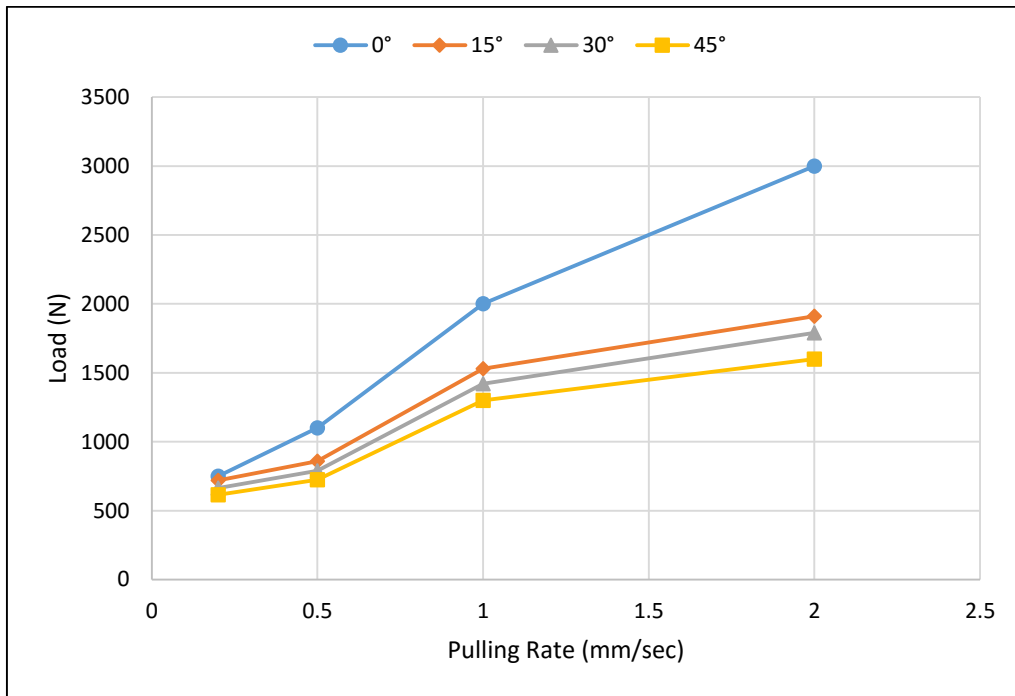


**Figure 4.21** Plot of load versus pulling rate for 8HS at different fiber orientations

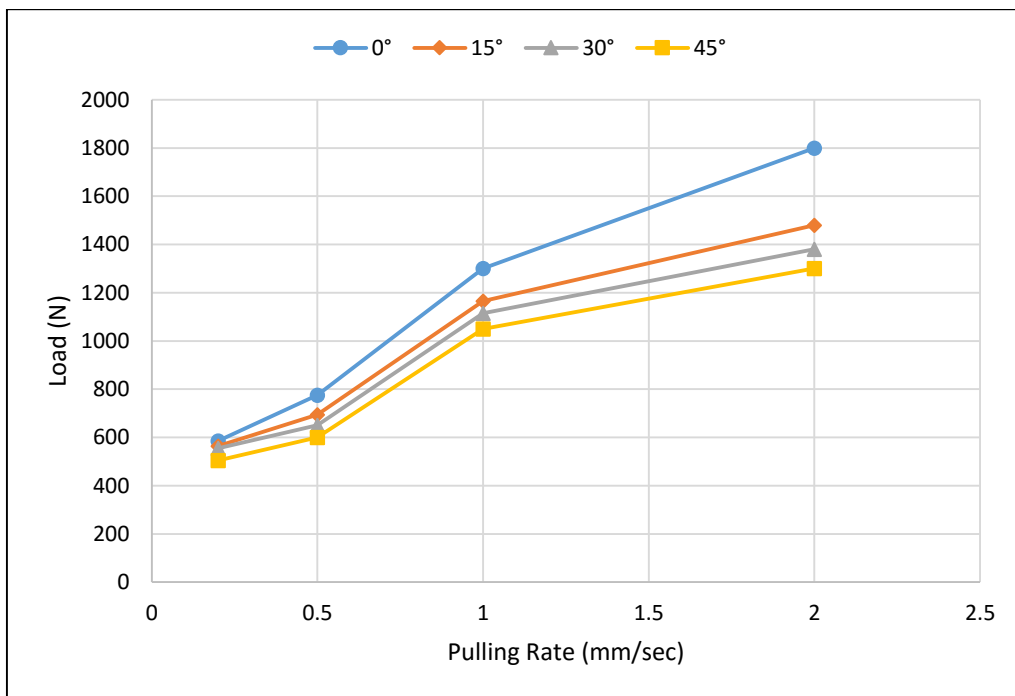


**Figure 4.22** Plot of load versus pulling rate for 5HS at different fiber orientations

The force of friction appeared almost same for the fiber angle  $15^\circ$ ,  $30^\circ$  and  $45^\circ$ . But if it is analysed closely, force of friction decreases as the angle changes from  $15^\circ$  to  $30^\circ$  to  $45^\circ$ . Some previous researchers have also observed the change in friction with the change in fiber orientation [27,28,46]. Murtagh et al. [27] proposed that this effect is due the higher apparent viscosity in the direction of fibers as compared to the transverse direction. The flow of prepreg resin is easier across the fibers than the flow along the fiber direction. According to Chow [29], as the angle of warp yarn increases, the force of friction decreases and reached the minimum value as the warp fiber angle reaches  $45^\circ$ . In the case of  $0^\circ$ , the composite plies are constantly sliding along the yarns, which are oriented in the same direction of sliding and therefore results in the higher force of friction. At a higher warp yarn angle, the rotation of fibers eased the sliding and decreased the frictional resistance. Figure 4.23 shows the rotation versus sliding of the fiber oriented perpendicular and parallel to the direction of sliding.

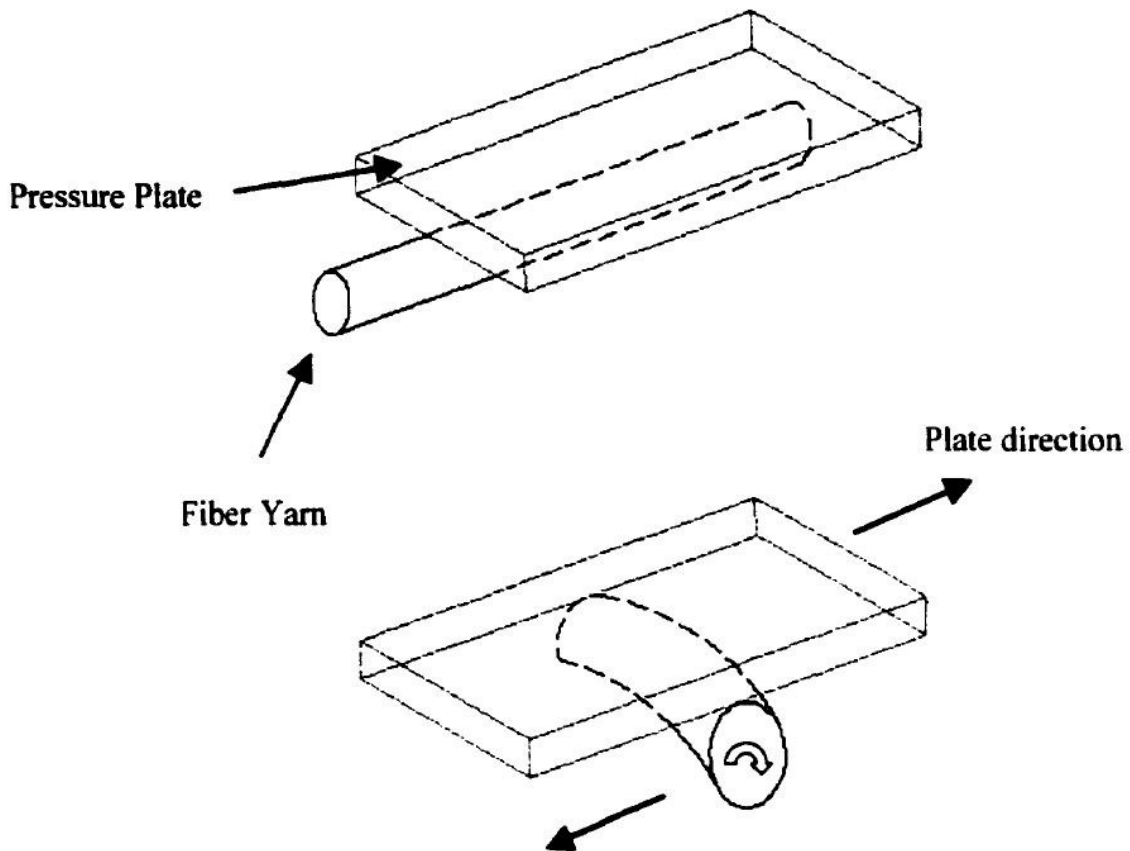


**Figure 4.23 Fiber Yarn rotation and deformation [29]**

The coefficient of friction was calculated for both peak value and steady state for 8-harness and 5-harness carbon/epoxy prepregs at different fiber angles. Figures 4.24 and 4.25 show the comparison between peak value coefficient of friction and steady state coefficient of friction for 8HS and 5HS at 50°C, 0.5 mm/sec and 0.5 atm. As observed in the previous experiments, steady state friction coefficient appeared less than the peak value friction coefficient. Peak value friction coefficient decreases from 1.02 to 0.67 for 8HS and from 0.72 to 0.56 for 5HS as fiber angle changes from 0° to 45°.

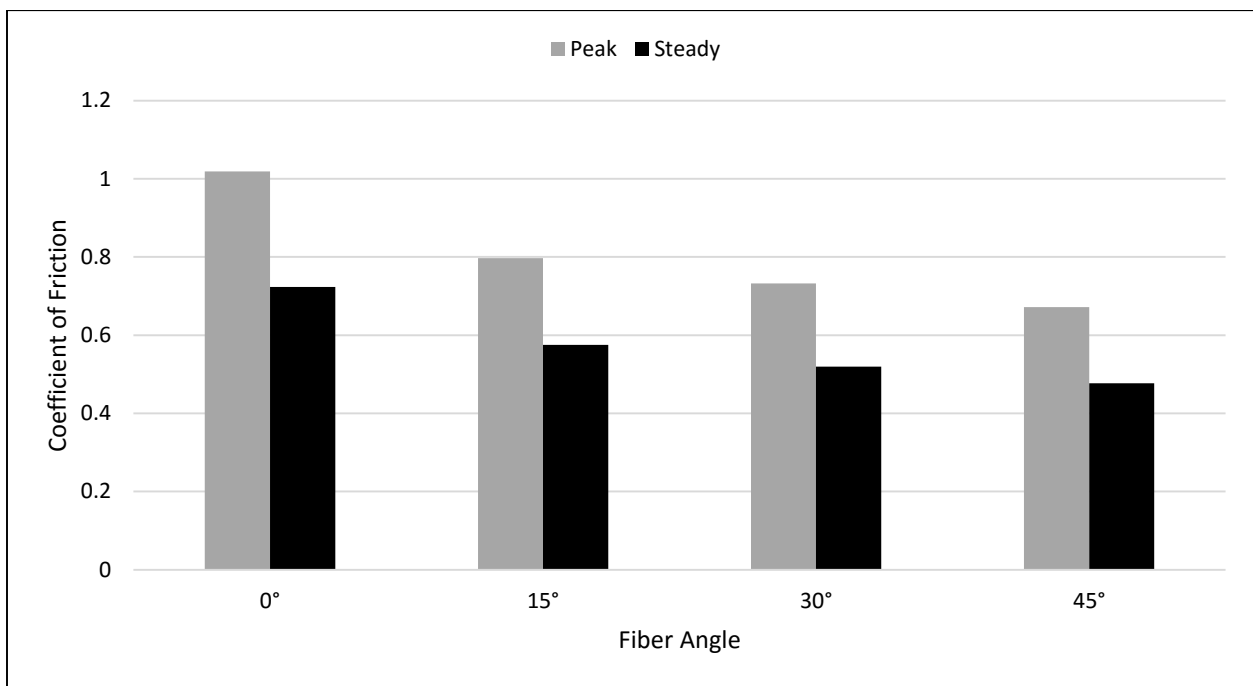


**Figure 4.24 Influence of fiber orientation on friction coefficients for 8HS at 50°C, 0.5 mm/sec and 0.5 atm**

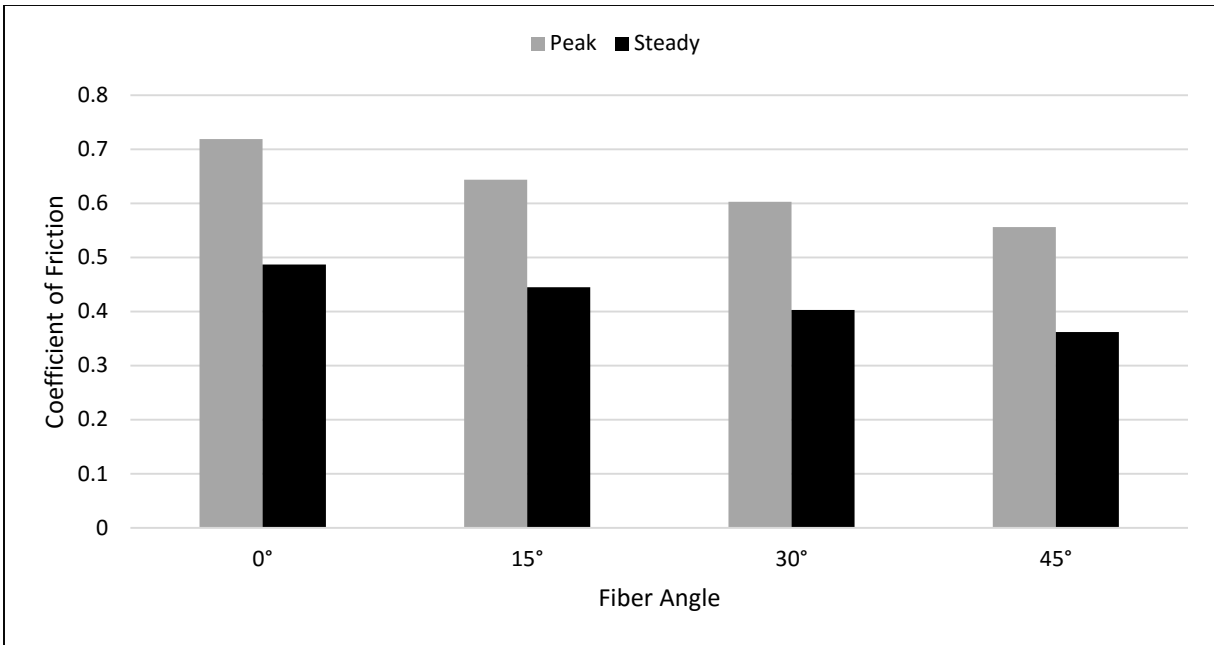


**Figure 4.25 Influence of fiber orientation on friction coefficients for 5HS at 50°C, 0.5 mm/sec and 0.5 atm**

#### **4.7 Microscopic Analysis**

Microscopic analysis was performed in order to visualize the micro-structures of the cured composite laminates. An optical microscope was used to accomplish a detailed analysis. The composite laminates were prepared from 8-harness and 5-harness carbon/epoxy prepregs. The specimen for microscopic observations were cut with the size of 10 cm x 10 cm each. Four specimen were stacked on each other for one laminate. The laminates were then cured in the oven at 125 °C for 3 hours. A full vacuum, equivalent to 1 atmosphere normal pressure, was applied during the curing operation. The fiber orientation was kept at 0° for each layer. After that, specimen of size 2.0 cm x 1.5 cm was cut from the cured laminate. The specimen was placed inside a mold and a mixture of resin and hardener was poured into the mold. The mold was left at room temperature for 24 hours and then heated in the oven at 110 °C for 1 hour. In order to make the surface of the specimen smooth, it was grinded and polished using Mecatech 234 polishing machine as shown in figure 4.26. A constant speed of 300 RPM and the force of 20 N at maintained while performing grinding operation. The grinding papers with different grades (180 $\mu$ , 300 $\mu$ , 600 $\mu$ ) were used, in the order of courser to finer, for making the specimen surface viewable under

microscope. The samples were polished by diamond polishing solution ( $9\mu$ ,  $3\mu$ ) to make them free from any kind of scratches.



**Figure 4.26 Mecatech 234 polishing machine**

Chang et al. [50] performed the microscopic investigation of tow geometry of 5HS dry satin weave fabric. Figure 4.27 shows various tow geometry parameters schematically such as, tow spacing ( $\Delta X$ ,  $\Delta Y$ ), tow width ( $W$ ), tow thickness ( $t$ ), amplitude ( $A$ ) and wavelength ( $\lambda$ ).

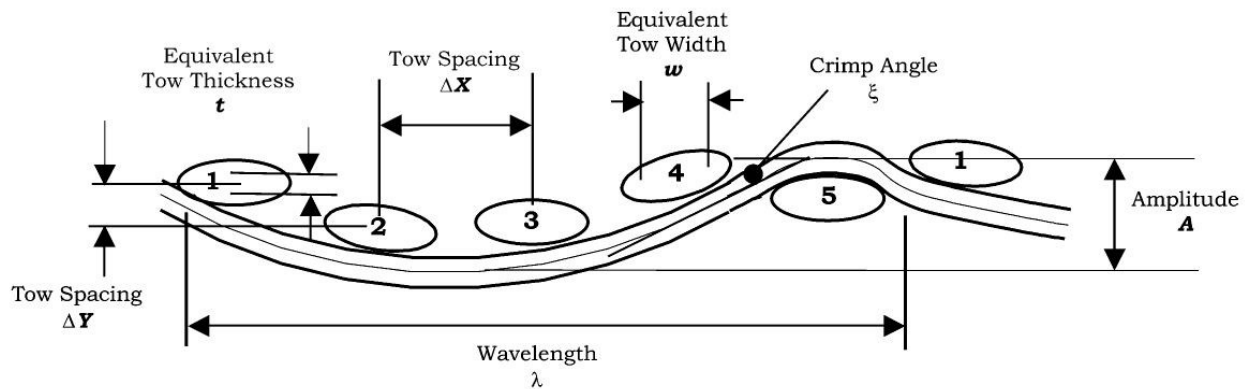


**Figure 4.27 Tow geometry parameters [50]**

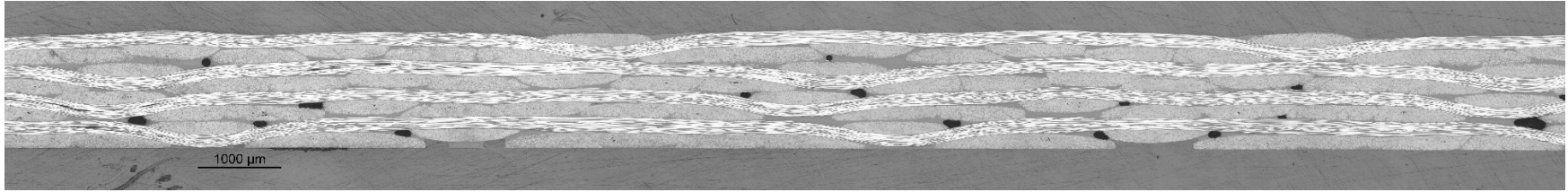


**Figure 4.28 Microscopic view of 8-Harness carbon/epoxy composite laminate**

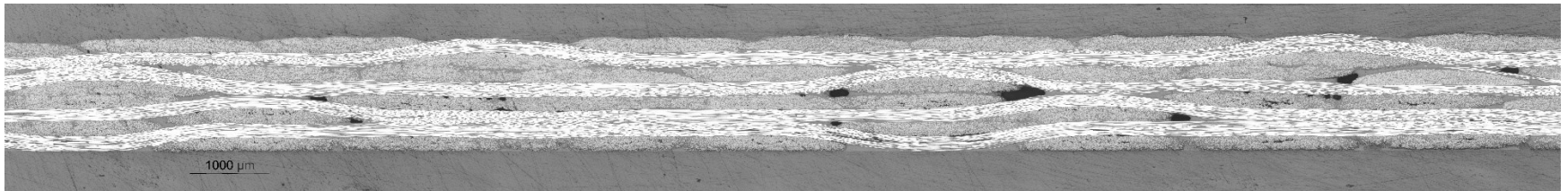


**Figure 4.29 Microscopic view of 5-Harness carbon/epoxy composite laminate**

Figures 4.28 and 4.29 show the microscopic views of 8-harness and 5-harness carbon/epoxy prepregs at 5x magnification. The dark black spots seen in the figures are the voids present in the cured laminate. The software analysis technique was used to calculate fiber volume fraction, void contents and laminate thickness. Table 4.3 shows the observations obtained from the microscope. Fiber volume fraction for 8-harness composite is observed more than 5-harness composite. Void contents for 8HS is 0.993 % and for 5HS is 0.925%. Less voids in 5HS may be because of more resin content in it as compared to 8HS. The laminate thickness for 8HS is 1381.06  $\mu\text{m}$  and for 5HS is 1402.88  $\mu\text{m}$ .

**Table 4.3 Microscopic observations of 8HS and 5HS laminates**

<b>Materials</b>	<b>8-Harness (8HS)</b>	<b>5-Harness (5HS)</b>
<b>Fiber Volume Fraction</b>	0.624	0.579
<b>Voids Content (%)</b>	0.993	0.925
<b>Laminate Thickness (<math>\mu\text{m}</math>)</b>	1381.06	1402.88

#### **4.8 Unidirectional Prepreg Analysis**

Unidirectional prepreg composites have considerable contribution in the manufacturing of automobile and aerospace parts. But, not much research has been done on the formability characteristics of UD laminates. In order to analyse the behaviour of unidirectional composites, this section describes the influences of different processing parameters on the inter-ply shear behaviour of UD. Tests were performed at a constant pulling rate of 0.5 mm/sec and a constant normal pressure of 0.5 atmosphere on unidirectional carbon/epoxy prepreg composites. Fiber orientation was kept  $0^\circ$  to the direction of motion for these tests. The results are based on load-displacement graphs that were obtained from tensile testing machine at different values of processing conditions. Figure 4.30 shows that frictional resistance recorded by load cell decreases as the temperature increases from 50  $^\circ\text{C}$  to 90  $^\circ\text{C}$ . The results for UD prepregs are similar to the previous results for 8HS and 5HS. As described earlier, reduction in force of friction with the increase in temperature can be explained by the reduction in resin viscosity with the rise in

temperature. Similar stick-slip curves were seen for 8-harness and 5-harness as they are for unidirectional composites.

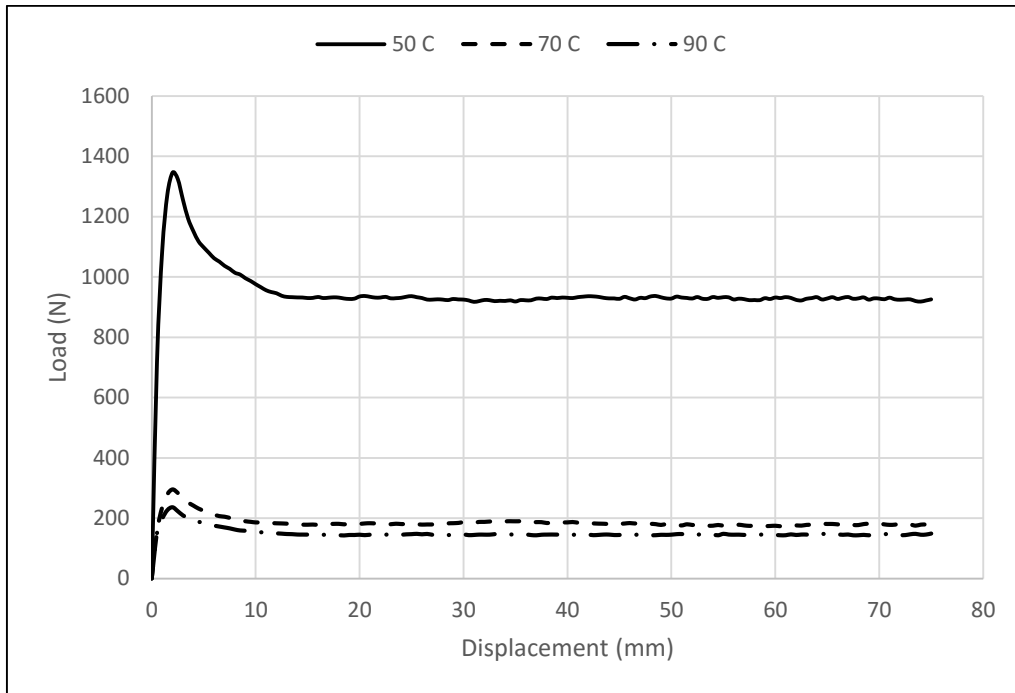


**Figure 4.30 Influence of temperature on inter-ply friction between UD preregs at 0.5 mm/sec, 0.5 atm and 0° fiber orientation**

To calculate the coefficients of friction, equation 4.2 was used. Figure 4.31 shows the comparison of peak value coefficients of friction for 8-harness satin, 5-harness satin and unidirectional carbon/epoxy preregs at different temperatures, 0.5 mm/sec pulling speed, 0.5 atmosphere normal pressure and 0° fiber orientation. Similar trend in the behaviour of friction coefficients for UD was observed as it was observed for 8HS and 5HS. Peak value of friction coefficients decreases from 1.25 to 0.22 for unidirectional preregs as the temperature rises from 50 °C to 90 °C. For UD, coefficients of friction came out as the higher from the 8-harness and 5-harness. It could be explained from the phenomenon of penetration of fibers from one prepreg layer to other. As there are fibers in one direction only in UD, so fiber penetration will be more as compared to fabrics in which fibers in the transverse direction resist interference of one fiber layer into other.

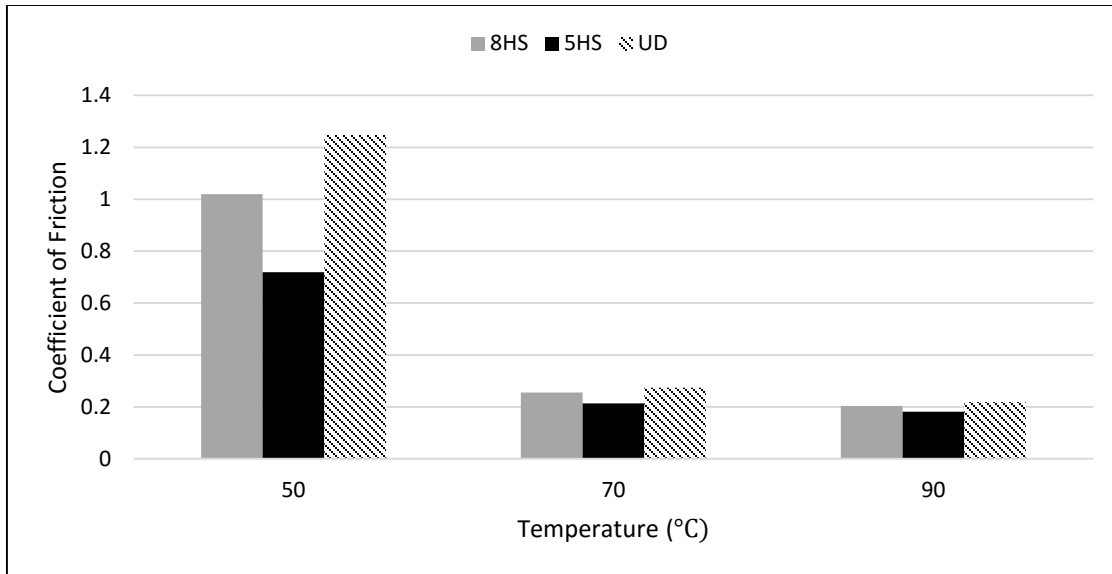


**Figure 4.31 Influence of temperature on coefficients of friction for 8HS, 5HS and UD at 0.5 mm/sec, 0.5 atm and 0° fiber orientation**

In order to study the effect of pulling rate on UD, tests were performed at a constant temperature of 50 °C and a constant normal pressure of 0.5 atmosphere at different pulling rates on unidirectional carbon/epoxy prepregs. Fiber angle of 0° was used in the experiments. Figure 4.32 shows load vs. pulling rate graphs at 0.2, 0.5, 1 and 2 mm/sec to investigate the influence of pulling rate on inter-ply friction. The graphs show the similar trend in UD as it was for 8HS and 5HS. The frictional load increases as pulling velocity increases from 0.2 mm/sec to 2 mm/sec. This is in agreement with the fact that the shear stress between prepreg plies is directly proportional to the velocity of one ply with respect to other as shown in equation 2.2.

Figure 4.33 shows the influence of pulling rate on coefficients of friction for 8HS, 5HS and UD at 50°C, 0.5 atm and 0° fiber orientation. Only peak value of friction coefficients has been plotted. It was observed that friction coefficients increases with the increase in pulling velocity which is same for frictional load for UD as well. For UD, coefficient of friction increases from 0.88 to 2.99 as the pulling velocity increases from 0.2 mm/sec to 2 mm/sec.

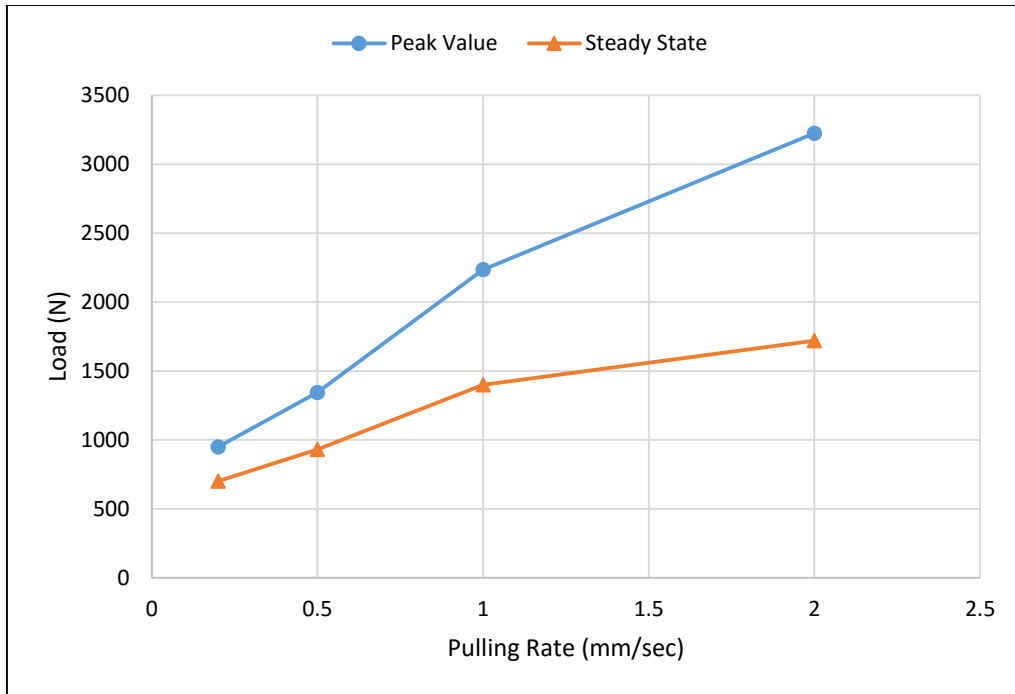


**Figure 4.32 Influence of pulling rate on inter-ply friction of UDs at 50 °C and 0.5 mm/sec**

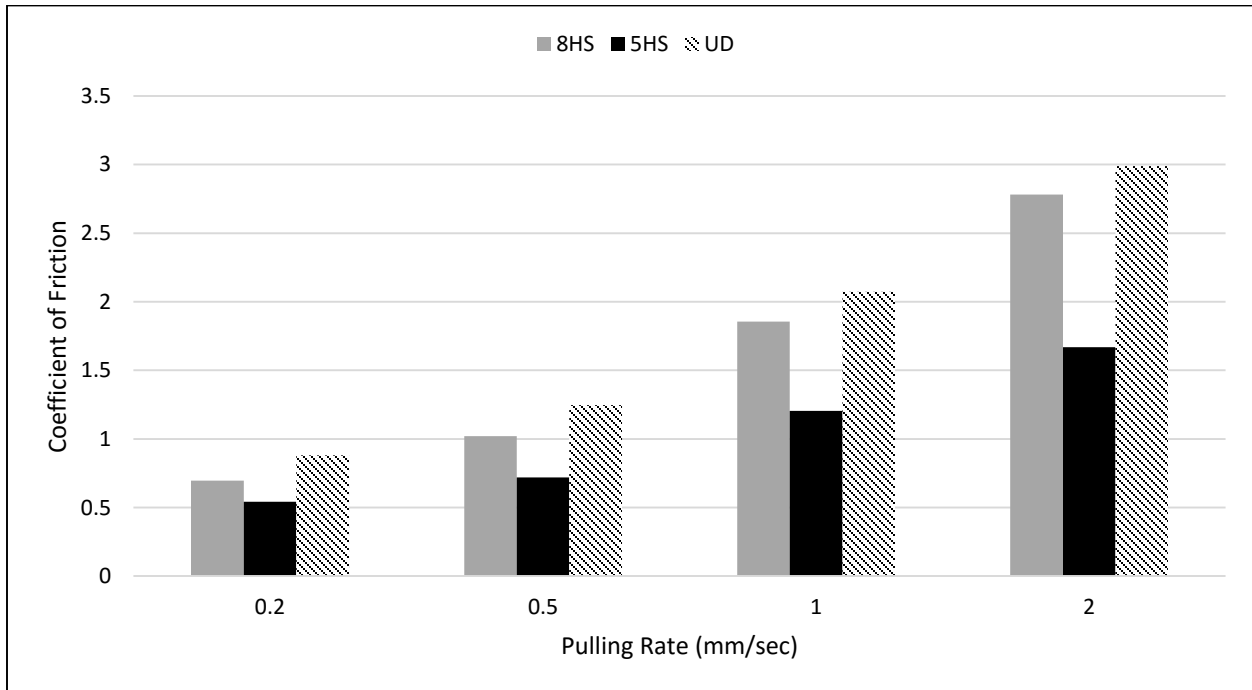


**Figure 4.33 Comparison of friction coefficients for 8HS, 5HS and UDs at different pulling rates, 50°C, 0.5 atm and 0° fiber orientation**

To study the influence of normal pressure on Inter-Ply friction, tests were performed at a constant pulling rate of 0.5 mm/sec and a constant processing temperature of 50 °C at different pressures on unidirectional carbon/epoxy prepregs. Fibers were kept at 0° to the direction of motion while performing these experiments. Figure 4.34 shows load vs. normal pressure graphs at 0.5, 0.8 and 1 atmosphere. Similar to the results for 8HS and 5HS, the graphs show that frictional load increases as the pressure increases from 0.5 to 1 atm.

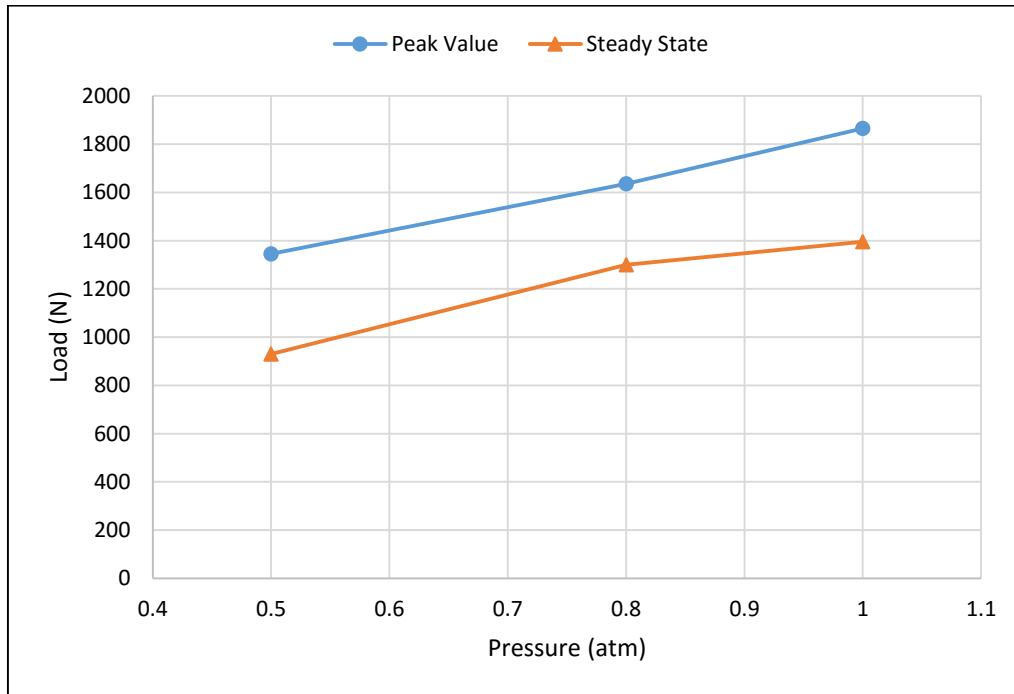


**Figure 4.34 Influence of normal pressure on interply friction for UD<sub>s</sub> at 50 °C, 0.5 mm/sec and 0° fiber orientation**

#### 4.9 Investigation of Tool/Ply Friction

In actual thermoforming process, the slippage occurs between prepreg-prepreg plies as well as tool-ply interface. It is very important that composite plies slide along the tool to avoid the generation of compressive forces in the fibers which are the major cause of the wrinkles and other defects in the composite parts. In hot drape forming, which is the major area of investigation of this thesis, vacuum bag is used above and below the composite laminate. During the deformation

of the laminate, prepreg plies slide along the vacuum bag to attain desired shape. In this dissertation, vacuum bag is considered as the tooling material.

In order to investigate the behaviour of tool/ply friction under different processing parameters, tests were performed using friction test rig. To study the effect of temperature, experiments were done at a constant pulling rate of 0.5 mm/sec and a constant normal pressure of 0.5 atmosphere at different temperatures on 8HS-Vacuum Bag and 5HS-Vacuum Bag. Fiber orientation for these tests was kept at 0° to the direction of movement. Results are based on load vs. temperature graphs as shown in figure 4.35. Similar to the previous results for inter-ply friction, the graphs show that frictional load reduces as the temperature increases from 50 °C to 90 °C. It could be explained by the fact that the viscosity of resin decreases with the increase in temperature and resin changes from rubbery state to liquid state. The graphs also show that peak value of load is more than the steady state value and both friction states reflect the same behaviour with the change in temperature.

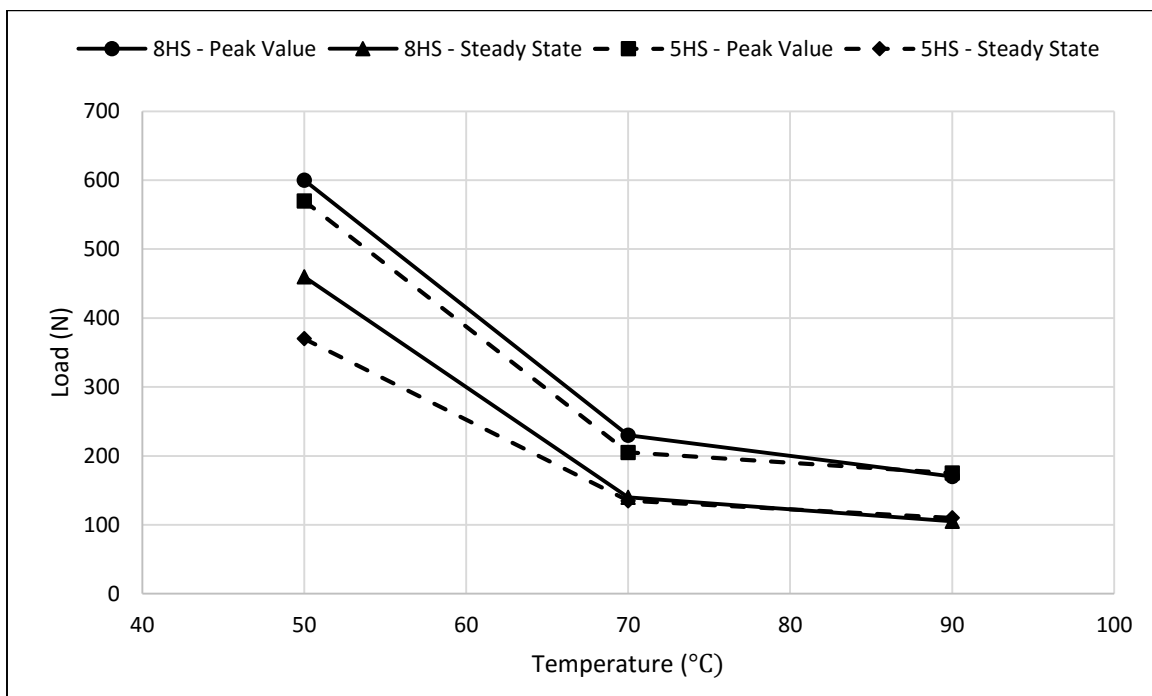


**Figure 4.35 Influence of temperature on tool-ply friction for 8HS and 5HS at 0.5 mm/sec, 0.5 atm and 0° fiber orientation**

To investigate the effect of pulling rate, tests were performed at a constant temperature of 50 °C and a constant normal pressure of 0.5 atmosphere at different pulling rates on 8HS-Vacuum Bag

and 5HS-Vacuum Bag. Figure 4.36 shows load vs. pulling rate graphs at 0.2, 0.5, 1 and 2 mm/sec. The graphs show that frictional load increases as pulling velocity increases from 0.2 mm/sec to 2 mm/sec. Similar trend of increase in frictional load has been seen for both 8-harness and 5-harness composite materials. Equation 2.2 explains these results which states that the shear stress between prepreg plies is directly proportional to the velocity of one ply with respect to other.

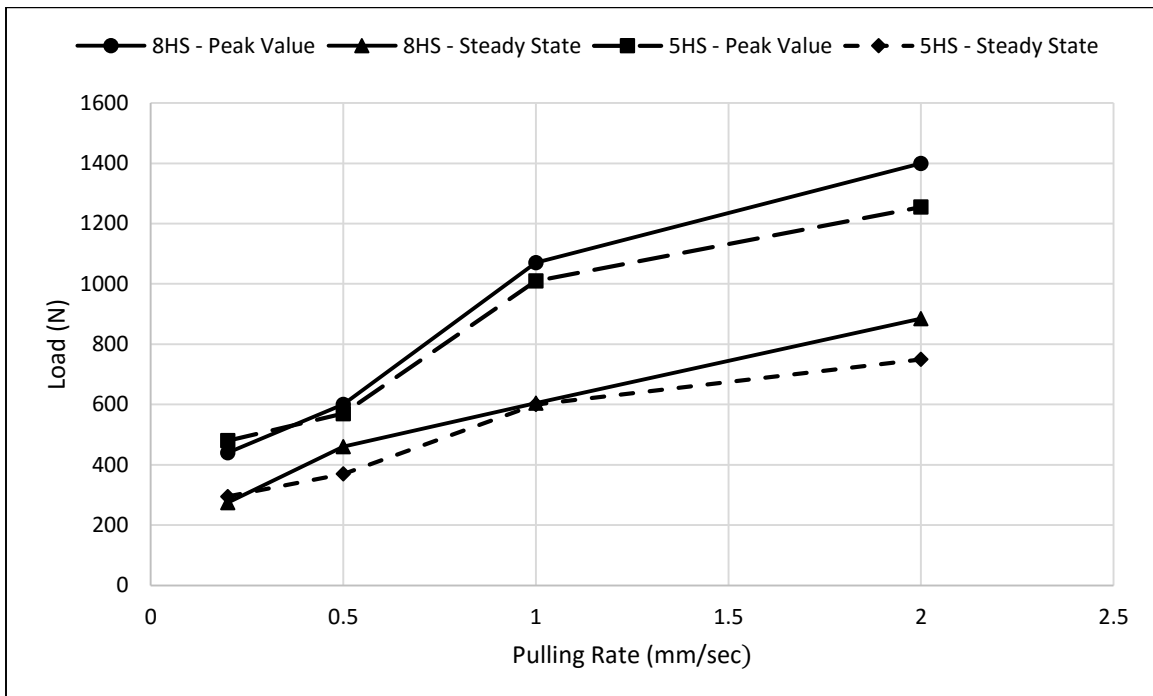


**Figure 4.36 Influence of pulling rate on tool-ply friction for 8HS and 5HS at 50 °C, 0.5 atm and 0° fiber orientation**

Influence of normal pressure on tool/ply friction shows the same trends as seen in previous test results of ply/ply friction. Tests were performed at a constant pulling rate of 0.5 mm/sec and a constant processing temperature of 50 °C at different pressures on 8HS-Vacuum Bag and 5HS-Vacuum Bag. Plies were oriented at 0° to the direction of movement. Figure 4.37 shows load vs. normal pressure graphs at 0.5, 0.8 and 1 atmosphere. The results show that frictional load increases as the pressure increases from 0.5 to 1 atm. The behaviour of 8-harness prepreg material with vacuum bag under different conditions of pressure is similar with the behaviour of 5-harness material with the vacuum bag.

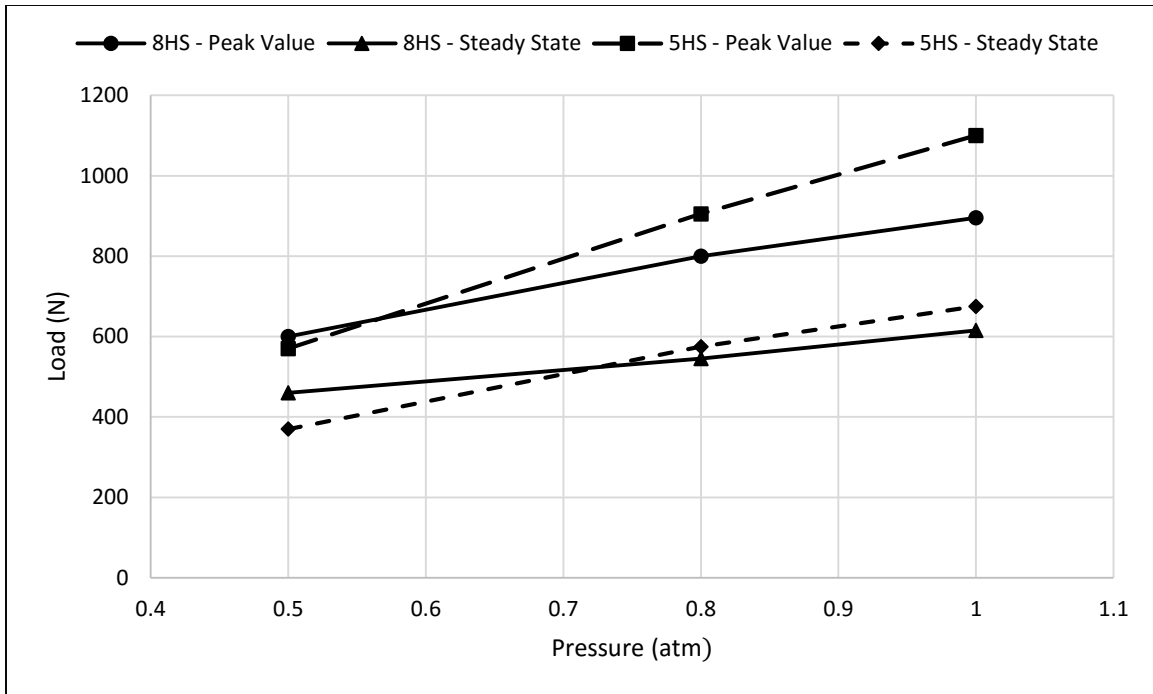


**Figure 4.37 Influence of normal pressure on tool-ply friction for 8HS and 5HS at 50 °C, 0.5 mm/sec and 0° fiber orientation**

#### 4.10 Investigation of 5HS/8HS Friction

A composite laminate may consists of prepreg layers of different fiber structures. The use of different materials within the same laminate could improve its mechanical properties. Experiments were done to investigate the ply/ply friction between 5-Harness and 8-Harness prepreg materials. To study the influence of temperature, tests were performed at a constant pulling rate of 0.5 mm/sec and a constant normal pressure of 0.5 atmosphere at different temperatures on 5HS/8HS carbon/epoxy prepreg materials. Fibers were orientated at 0° to the direction of movement. Results are based on load vs. temperature graphs as shown in figure 4.38. Similar to the previous results for ply/ply friction of same materials, the graphs show that frictional load reduces as the temperature rises from 50 °C to 90 °C. The graphs also show that peak value of load is more that the steady state value and both friction states shows the same behaviour with the change in temperature.

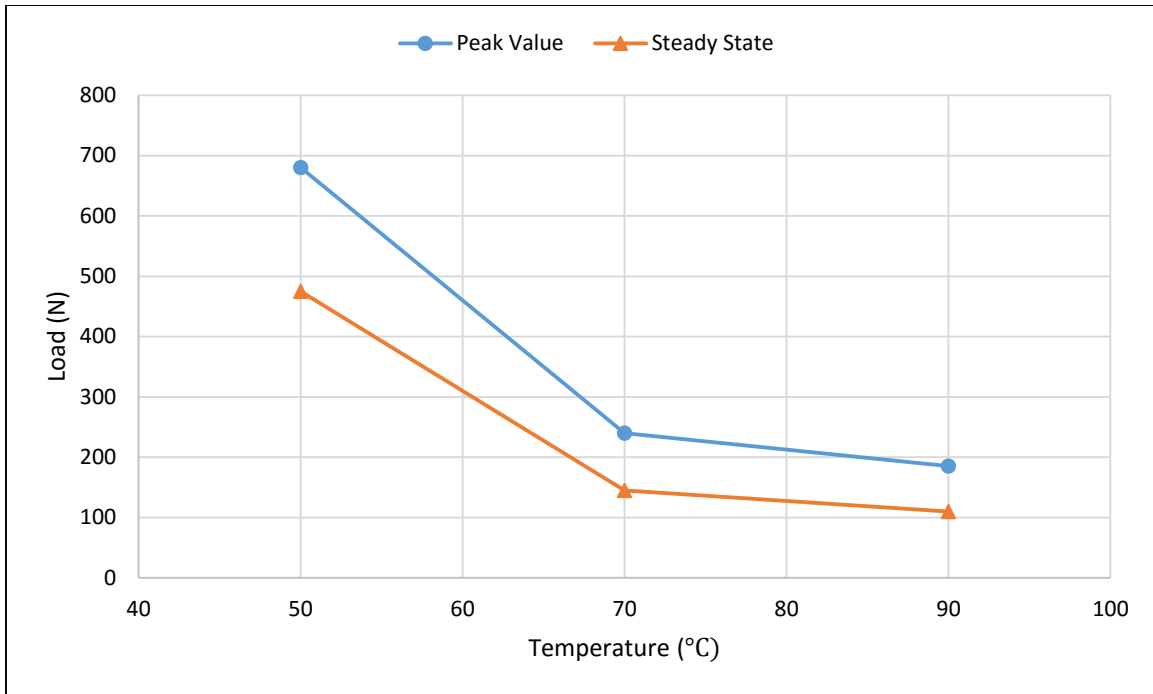


**Figure 4.38 Load vs. Temperature graphs for 5HS/8HS friction at 0.5 mm/sec, 0.5 atm and 0° fiber orientation**

The effect of pulling rate on ply/ply friction between 5HS and 8HS could be explained from the load vs. pulling rate graphs shown in figure 4.39. The graphs show that with the increase in pulling rate from 0.2 mm/sec to 2 mm/sec the frictional load increases. As expected, behaviour of 5HS/8HS is similar with the behaviour of same materials under the changing conditions of pulling rates.

To study the influence of normal pressure on Ply/Ply friction between 5-harness and 8-harness preregs, tests were performed at a constant pulling rate of 0.5 mm/sec and a constant processing temperature of 50 °C at different pressures. Figure 4.40 shows load vs. normal pressure graphs at 0.5, 0.8 and 1 atmosphere. The results show that frictional load increases as the pressure increases from 0.5 to 1 atm. Results are similar with the previous results for ply/ply friction between same materials.

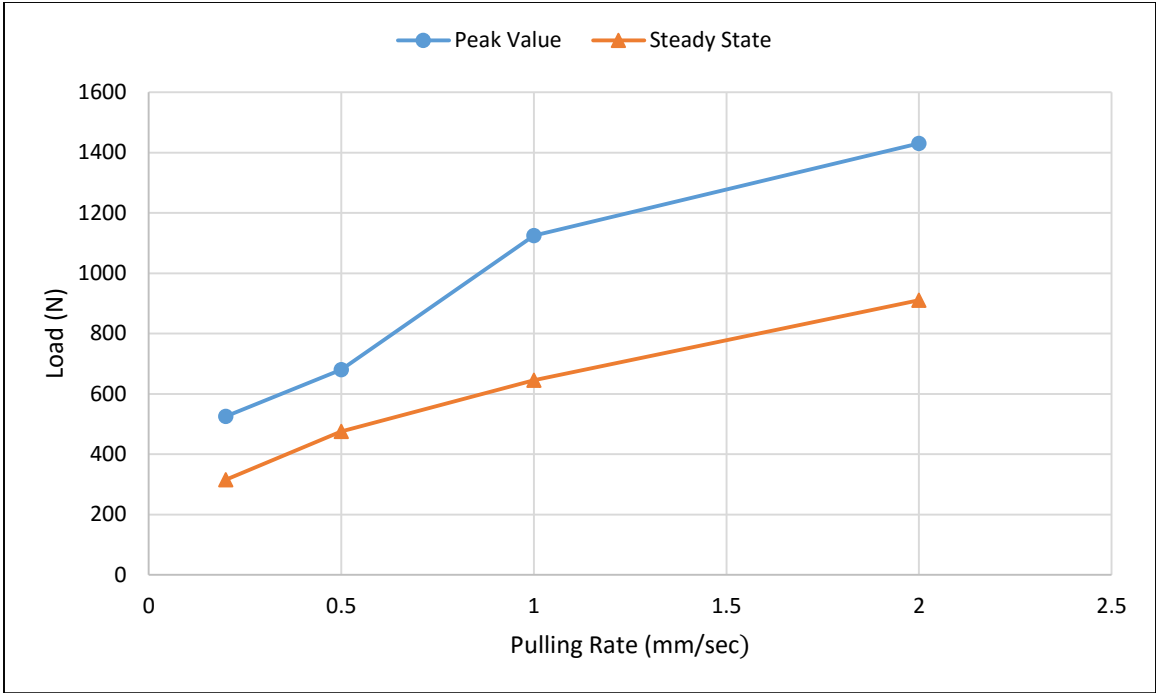


**Figure 4.39 Load vs. Pulling Rate graphs for 5HS/8HS friction at 50 °C, 0.5 atm and 0° fiber orientation**

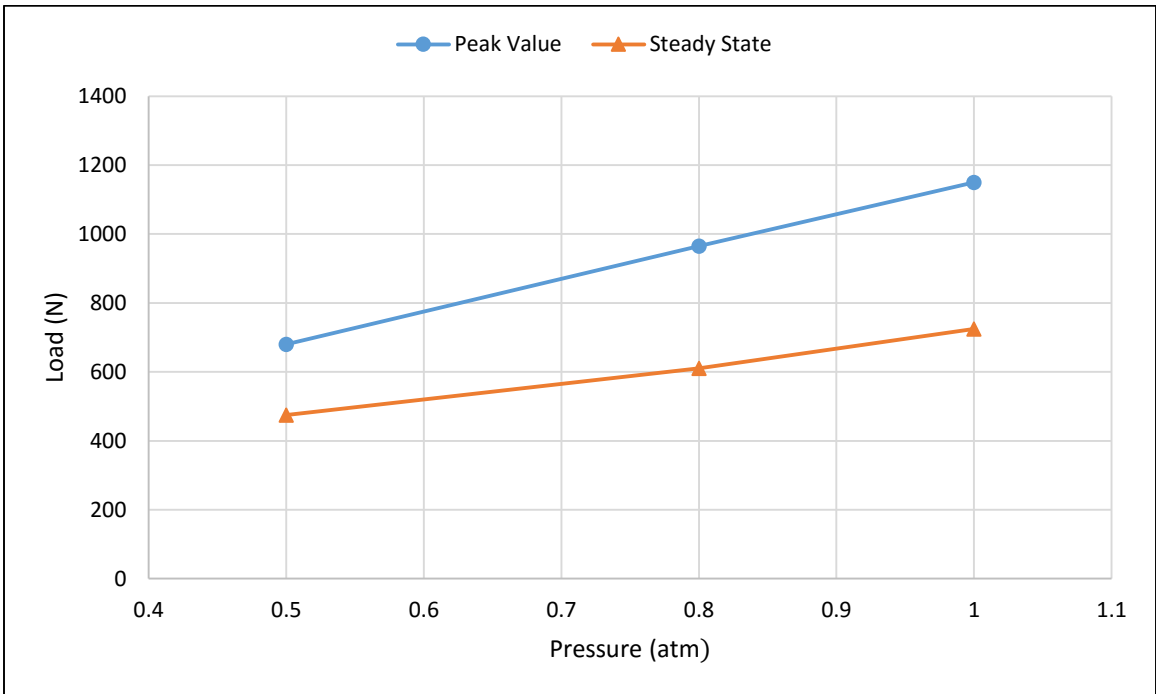


**Figure 4.40 Load vs. Normal Pressure graphs for 5HS/8HS friction at 50 °C, 0.5 mm/sec and 0° fiber orientation**

## 4.11 Summary

To sum up this chapter, the ply-ply and tool-ply friction behavior of out-of-autoclave (OOA) carbon/epoxy prepregs was investigated at different processing conditions using a friction test-rig developed for this study and the results show that temperature, pulling rate and normal pressure have different impacts on inter-ply friction. Increase in temperature and decrease in the pulling rate can enhance slippage between prepreg plies. It was observed that friction mechanism between prepreg plies is mixed friction type i.e., combination of both coulomb and hydrodynamic friction. The presence of stick-slip peaks in load-displacement graphs indicate that it is a coulomb dominated friction while dependence of inter-ply friction on the pulling velocity shows friction is hydrodynamic in nature. Normal pressure has the least influence on inter-ply friction. Decrease in normal pressure is helpful in inter-ply slippage.

The results show that change in fiber orientation has effect on inter-ply friction. As the fiber angle is changed from  $0^\circ$  to  $45^\circ$ , there is a slight decrease in the force of friction. The ply-ply friction for unidirectional prepregs came out as more than the ply-ply friction for both 8HS and 5HS. The tests for tool-ply friction shows that tool-ply shear stress is less than the ply-ply shear stress. The tool-ply friction results show the same behaviour as it is for ply-ply friction under the influence of temperature, pulling rate and normal pressure. The friction behaviour of 5HS with 8HS was investigated and results were similar with the results for inter-ply friction for same materials.

# Chapter 5 : Modelling and Optimization

This chapter explains the use of Hersey number and Stribeck curves to develop a model for inter-ply friction mechanism. The characterization of coefficients of friction was done by the linear equations obtained from the Stribeck curves. Additionally, the optimization techniques such as Taguchi method and analysis of variance are described to find out ideal processing conditions.

## 5.1 Stribeck Analysis

To develop the analytical model for frictional behavior of prepreg plies, Hersey number was calculated for each set of processing parameters. Table 5.1 lists the viscosity of epoxy resin at different temperatures [51].

**Table 5.1 Viscosity Values of Epoxy Resin**

Temperature (°C)	50	70	90
Viscosity (Pa.s)	$2.5 \times 10^3$	$3.0 \times 10^2$	$6.0 \times 10^1$

Hersey number was plotted against the coefficient of friction, for 8HS oriented at 0° to the direction of motion, as shown in Figure 5.1. The coefficients of friction are based on the peak values of frictional resistance obtained from load-displacement graphs. A curve was fitted to the intersecting points of friction coefficient and Hersey number. It is observed from the Stribeck curve that coefficient of friction increases with the increase in Hersey number. The curve shows that inter-ply friction of 8-harness carbon/epoxy prepreg is hydrodynamic in nature as the slope of the curve is positive. A linear relationship, as proposed by Gorczyca [32], is found between Hersey number and coefficient of friction:

$$\mu = 27609.H + 0.264 \quad (5.1)$$

The above linear equation could be used to find out friction coefficient at any particular set of processing conditions. As Hersey number ( $H$ ) is the function of viscosity of resin, normal pressure and pulling rate, so using the viscosity values at any given temperature and using other processing conditions, coefficient of friction could be easily calculated with help of the linear equation 5.1.

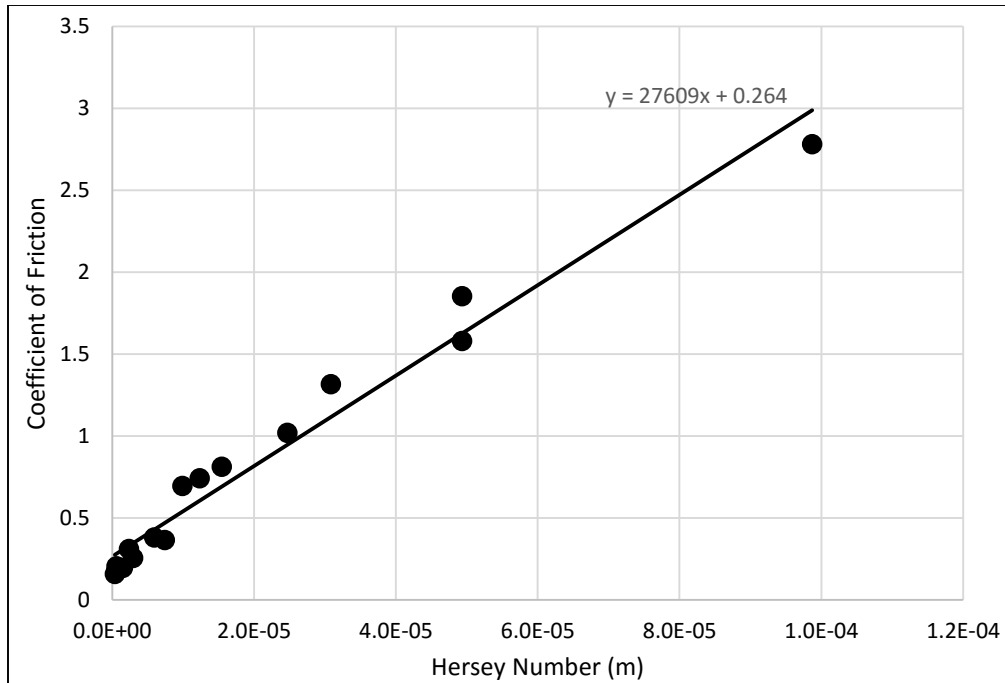


**Figure 5.1 Experimental Stribeck curve for 8-harness satin carbon/epoxy prepreg oriented at 0° to the direction of slippage**

As discussed in the previous chapter, force of friction changes with the change in fiber orientation. So, Stribeck curves must differ for the prepreg plies at some angle to direction of movement. Figures 5.2, 5.3 and 5.4 show the experimental Stribeck curves for 8-harness OOA prepreps at 15°, 30° and 45° respectively. The Stribeck curves for 8HS at 60°, 75° and 90° are given in Appendices. The linear equations obtained at these fiber orientations are shown in table 5.2.

**Table 5.2 Linear equations for 8HS at 15°, 30°, 45°, 60°, 75° and 90° fabric orientation**

Fiber Orientations	Linear Equations
8HS at 15°	$\mu = 17956.H + 0.2912$
8HS at 30°	$\mu = 16867.H + 0.281$
8HS at 45°	$\mu = 15214.H + 0.2636$
8HS at 60°	$\mu = 16852.H + 0.2803$
8HS at 75°	$\mu = 18004.H + 0.29$
8HS at 90°	$\mu = 27272.H + 0.2934$

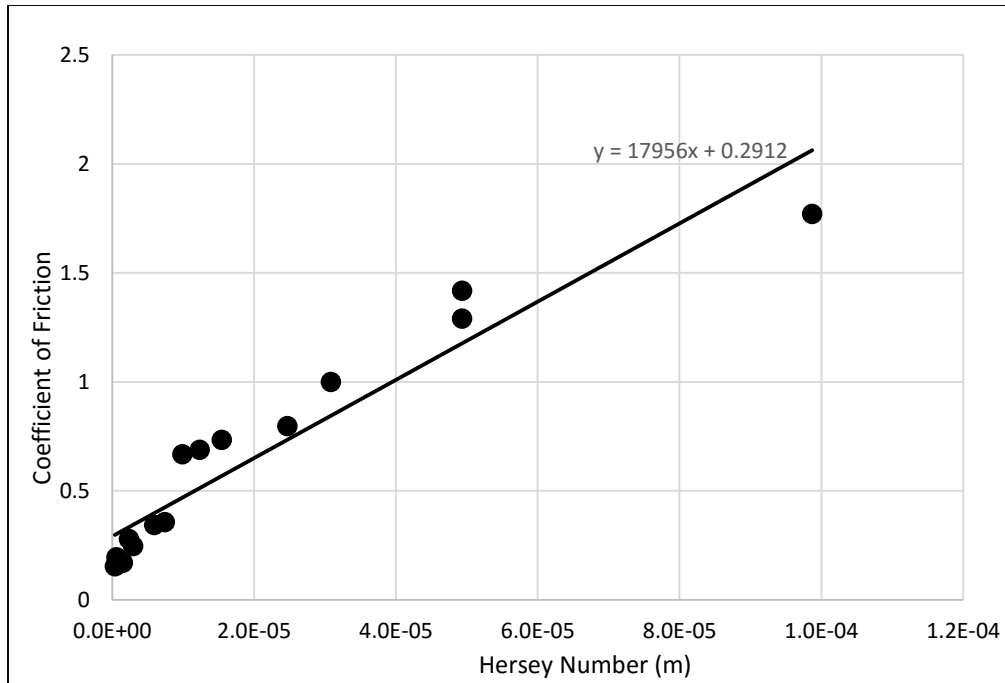


**Figure 5.2 Experimental Stribeck curve for 8-harness satin carbon/epoxy prepreg oriented at 15° to the direction of slippage**

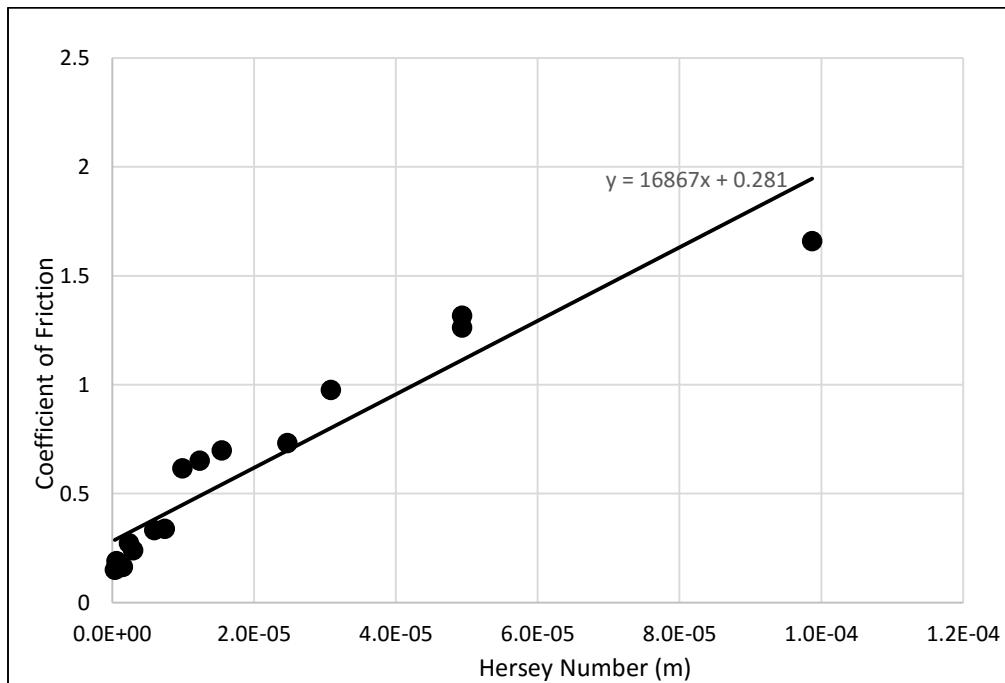


**Figure 5.3 Experimental Stribeck curve for 8-harness satin carbon/epoxy prepreg oriented at 30° to the direction of slippage**

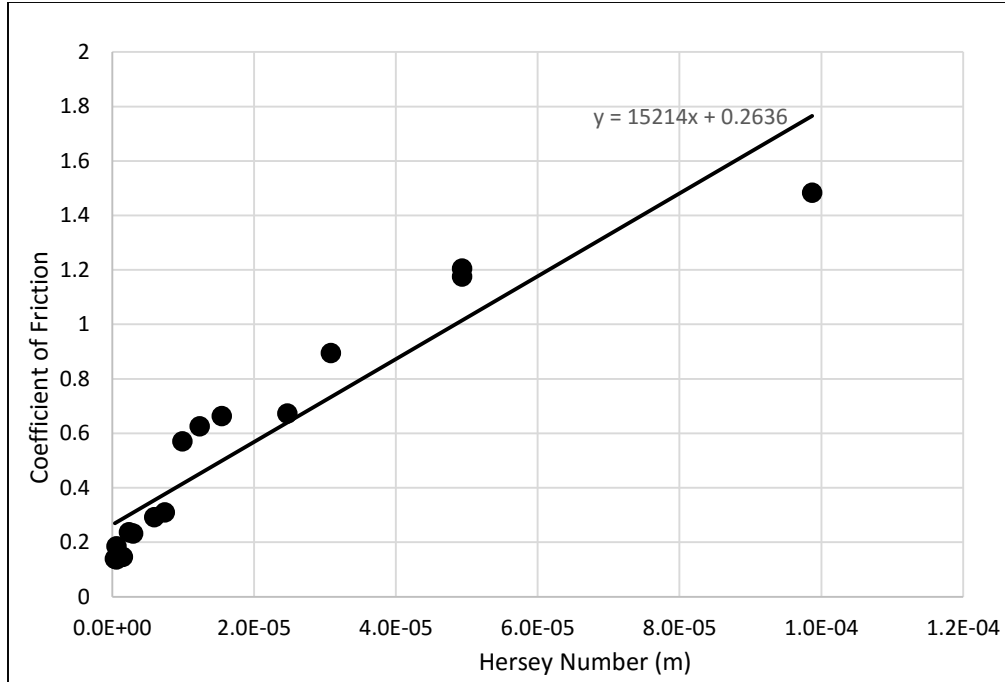


**Figure 5.4 Experimental Stribeck curve for 8-harness satin carbon/epoxy prepreg oriented at 45° to the direction of slippage**

It is noticed that linear equations obtained from the Stribeck curves are in the form

$$\mu = a \cdot H + b$$

where variables  $a$  and  $b$  have different values for each set of fabric orientation. Figures 5.5 and 5.6 show the variables  $a$  and  $b$  plotted against fabric angle  $\theta$ . The lines are fitted through the intersecting points. The equations of these fitted lines are given below:

$$a = 5.9467 \theta^2 - 537.41 \theta + 26757$$

$$b = 1E-05 \theta^2 - 0.0011 \theta + 0.301$$

A general equation was developed which could be used to predict coefficient of friction for any set of processing conditions for 8HS at any fabric orientation, as given by equation 5.2.

$$\mu = (5.9467 \theta^2 - 537.41 \theta + 26757) \cdot H + (1E-05 \theta^2 - 0.0011 \theta + 0.301) \quad (5.2)$$

where  $\theta$  is the fabric orientation angle in degrees.

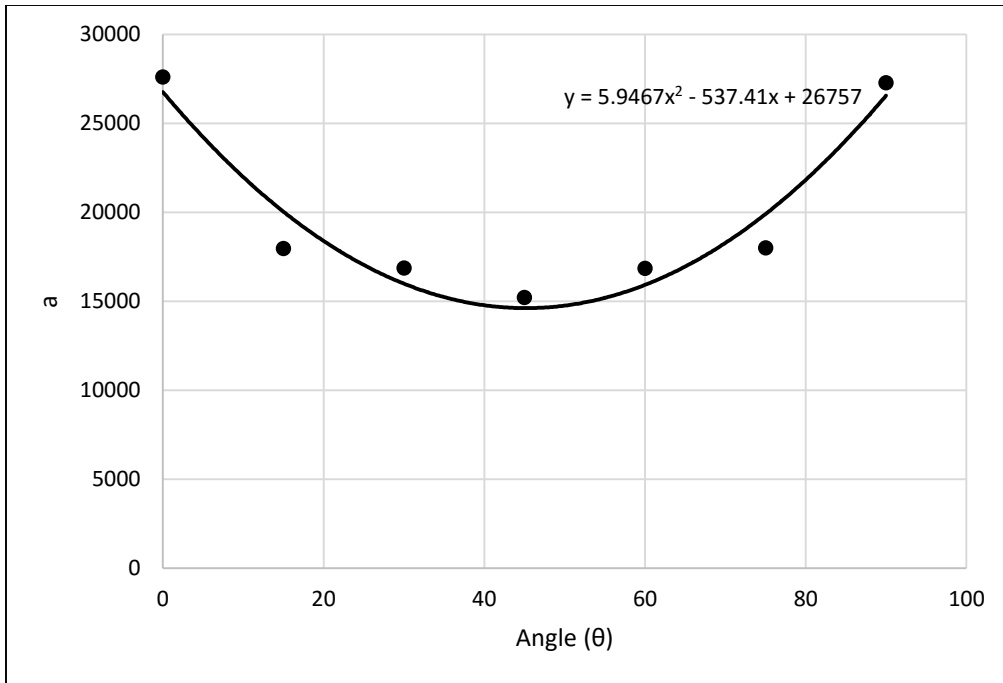


**Figure 5.5 Relationship between “a” and fabric angle “ $\theta$ ” for 8HS**

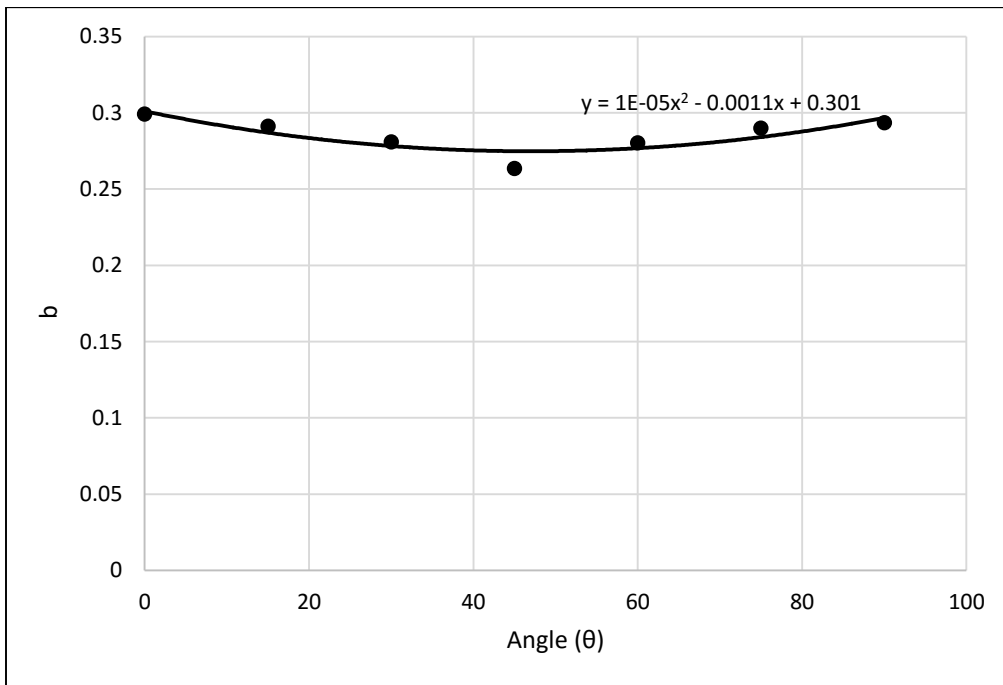


**Figure 5.6 Relationship between “b” and fabric angle “ $\theta$ ” for 8HS**

As explained in the previous chapter, 5-harness OOA preregs have different inter-ply shear properties than 8-harness preregs. So, Hersey number was plotted against Coefficient of Friction for 5HS at 0°, 15°, 30° and 45° fiber orientation as shown in figures 5.7, 5.8, 5.9 and 5.10 respectively. Table 5.3 describes the linear equations for 5HS at different fiber orientations.

**Table 5.3 Linear equations for 5HS at 0°, 15°, 30°, 45°, 60°, 75° and 90° fabric orientation**

Fiber Orientations	Linear Equations
5HS at 0°	$\mu = 16087.H + 0.2312$
5HS at 15°	$\mu = 13361.H + 0.2287$
5HS at 30°	$\mu = 12547.H + 0.2272$
5HS at 45°	$\mu = 11835.H + 0.2189$
5HS at 60°	$\mu = 12521.H + 0.2272$
5HS at 75°	$\mu = 13334.H + 0.2287$
5HS at 90°	$\mu = 16137.H + 0.2292$

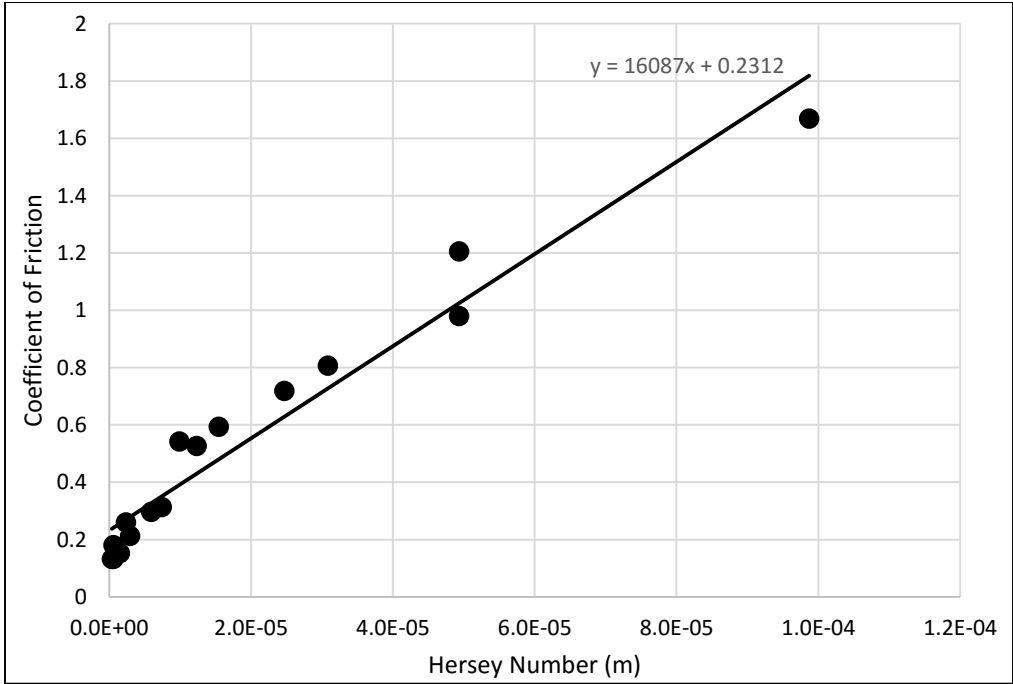


**Figure 5.7 Experimental Stribeck curve for 5-harness satin carbon/epoxy prepreg oriented at 0° to the direction of slippage**

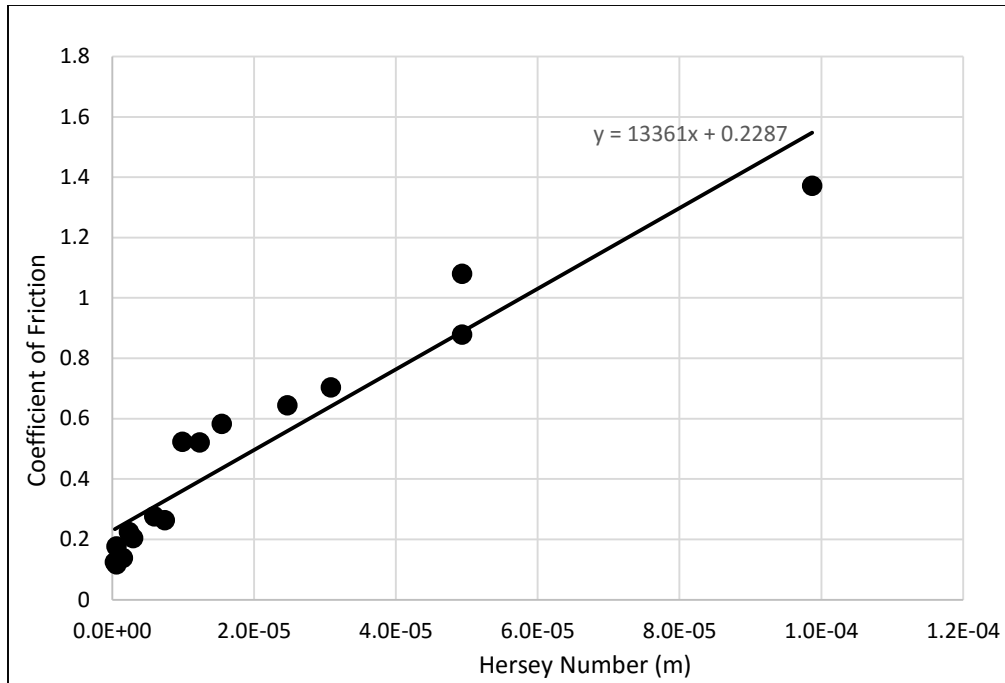


**Figure 5.8 Experimental Stribeck curve for 5-harness satin carbon/epoxy prepreg oriented at 15° to the direction of slippage**

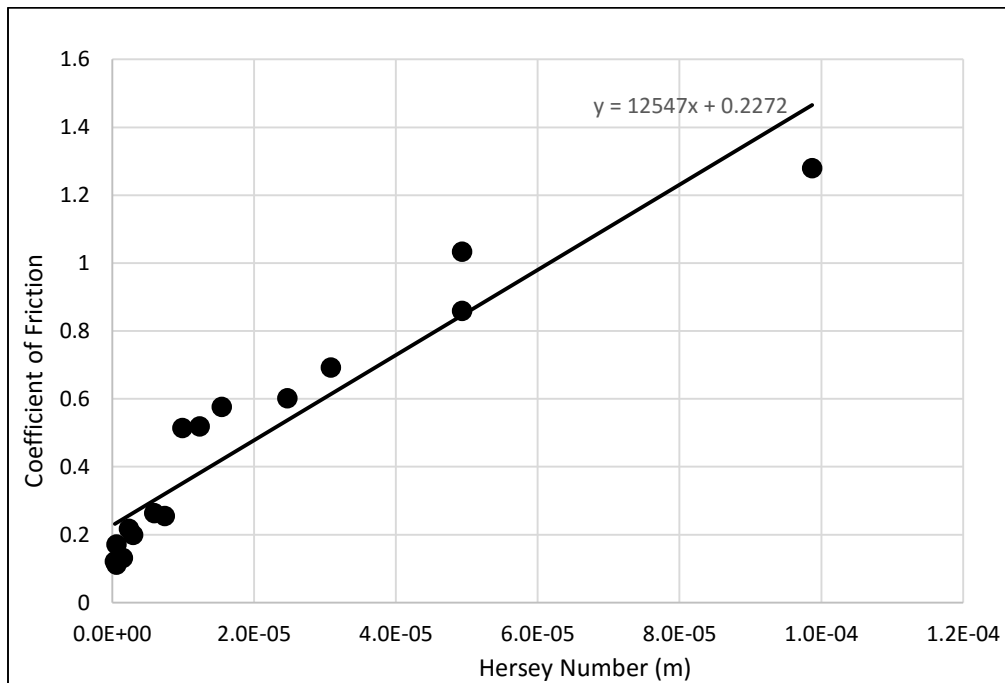


**Figure 5.9 Experimental Stribeck curve for 5-harness satin carbon/epoxy prepreg oriented at 30° to the direction of slippage**

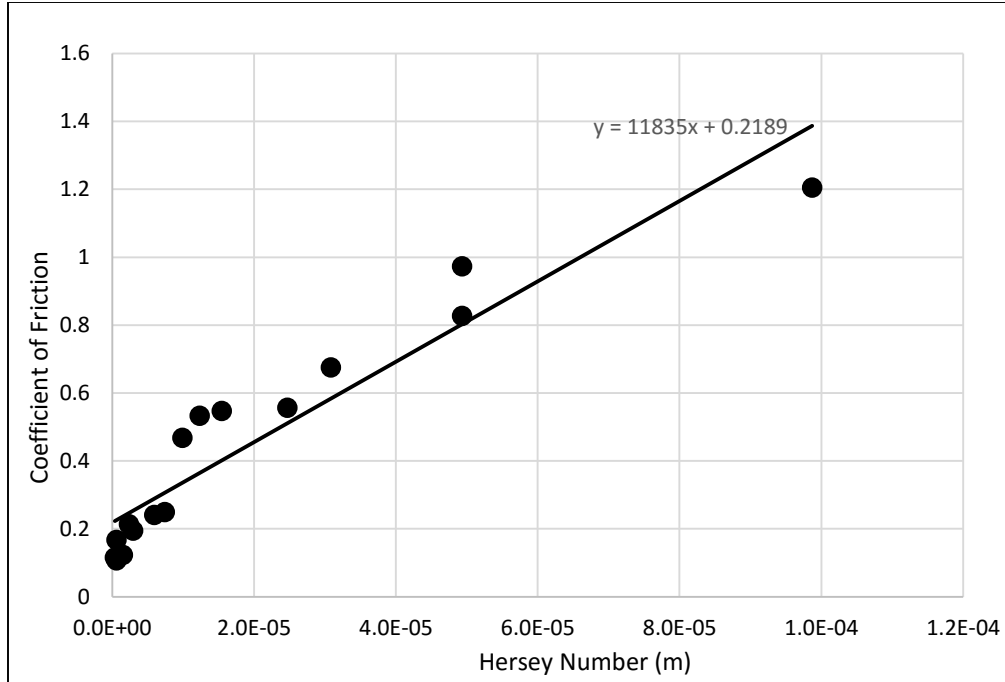


**Figure 5.10 Experimental Stribeck curve for 5-harness satin carbon/epoxy prepreg oriented at 45° to the direction of slippage**

Similar to 8-harness preregs, it is noticed that linear equations obtained from the Stribeck curves for 5HS are in the form

$$\mu = a . H + b$$

where variables a and b have different values for each set of fabric orientation. Figures 5.11 and 5.12 show the variables a and b plotted against fabric angle  $\theta$ . The lines are fitted through the intersecting points. The equations of these fitted lines are given below:

$$a = 2.0411 \theta^2 - 183.53 \theta + 15978$$

$$b = 3E-06 \theta^2 - 0.0003 \theta + 0.2317$$

A general equation was developed which could be used to predict coefficient of friction for any set of processing conditions for 5HS at any fabric orientation, as given by equation 5.3.

$$\mu = (2.0411 \theta^2 - 183.53 \theta + 15978).H + (3E-06 \theta^2 - 0.0003 \theta + 0.2317) \quad (5.3)$$

where  $\theta$  is the fabric orientation angle in degrees.

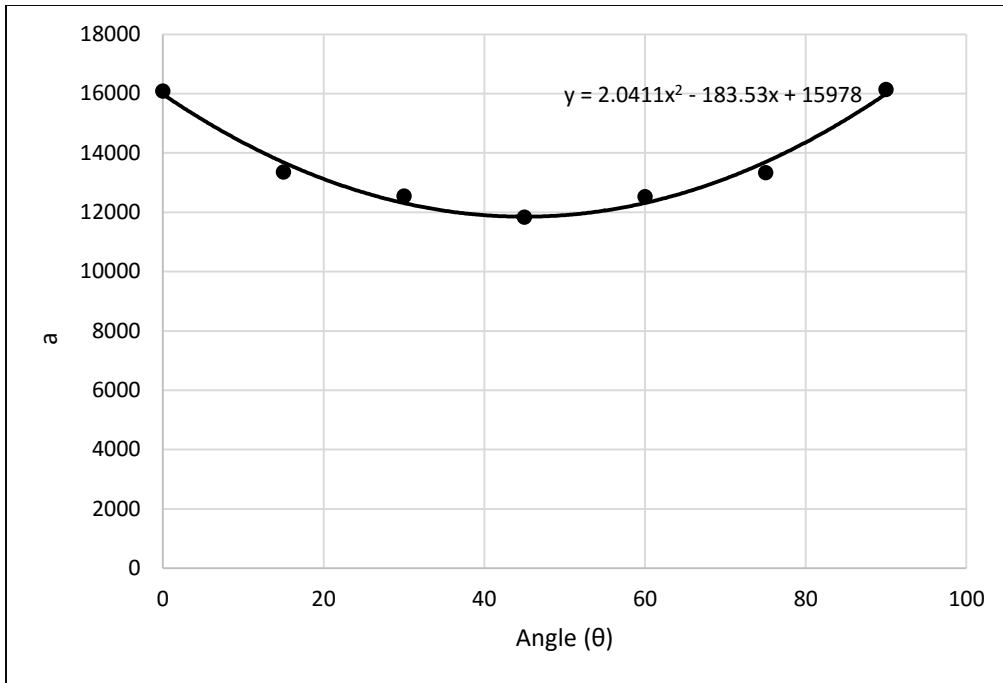


**Figure 5.11 Relationship between “a” and fabric angle “θ” for 5HS**

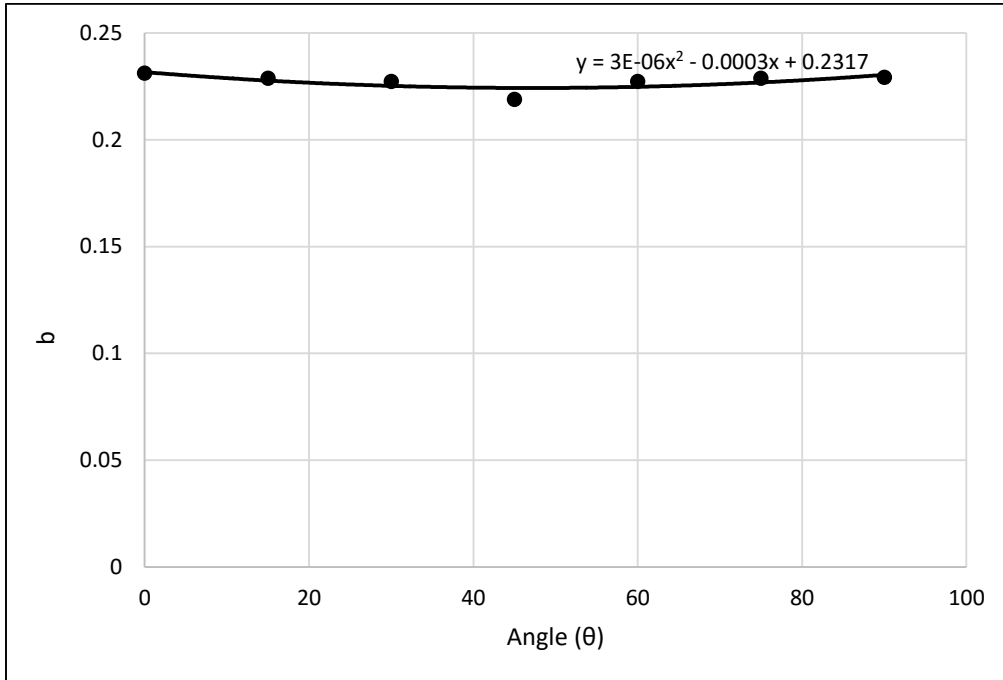


**Figure 5.12 Relationship between “b” and fabric angle “θ” for 5HS**

## 5.2 Modelling of Unidirectional Prepregs

The unidirectional prepregs have a significant role in the manufacturing of composite parts in aerospace and automobile industries. It is very important to create the friction model for UD composites so that inter-ply friction phenomenon could be predicted in advance before performing the actual operation. Figures 5.13 to 5.19 show the Stribeck curve for UD carbon/epoxy prepregs at 0°, 15°, 30°, 45°, 60°, 75° and 90° fiber orientations based on the experiments explained in the previous chapter. The linear relationships between coefficient of friction and Hersey number for UD composites are given in the table 5.4.

**Table 5.4 Linear equations for UD at 0°, 15°, 30°, 45°, 60°, 75° and 90° fiber orientation**

<b>Fiber Orientations</b>	<b>Linear Equations</b>
UD at 0°	$\mu = 29623.H + 0.3233$
UD at 15°	$\mu = 25886.H + 0.2841$
UD at 30°	$\mu = 24835.H + 0.2549$
UD at 45°	$\mu = 23859.H + 0.2314$
UD at 60°	$\mu = 23290.H + 0.2159$
UD at 75°	$\mu = 22797.H + 0.2088$
UD at 90°	$\mu = 21757.H + 0.1966$

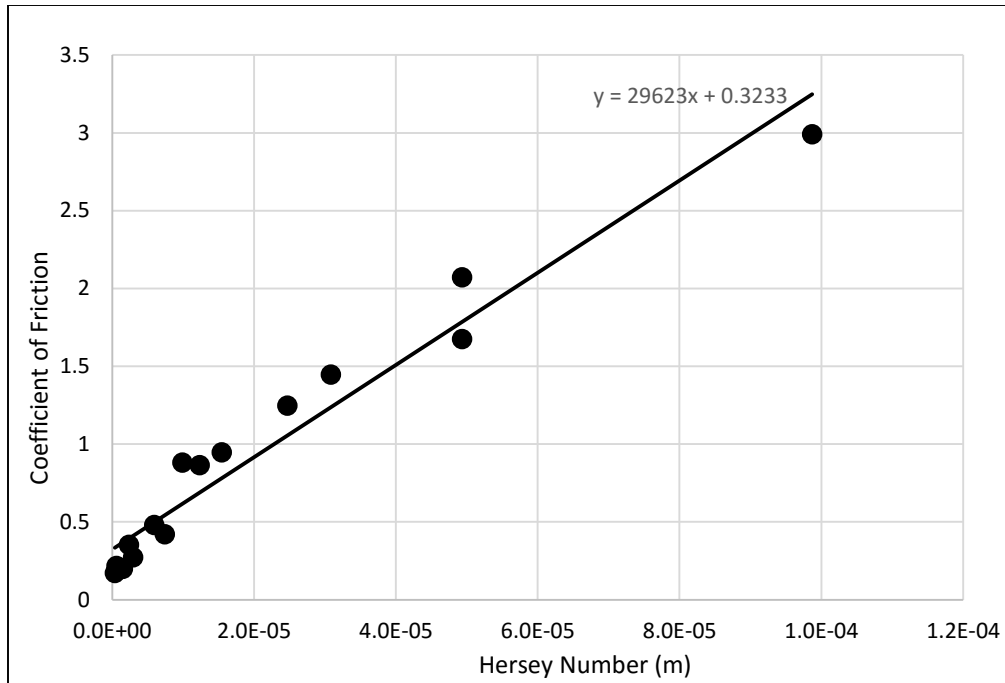


**Figure 5.13 Experimental Stribeck curve for unidirectional carbon/epoxy prepreg oriented at 0° to the direction of slippage**

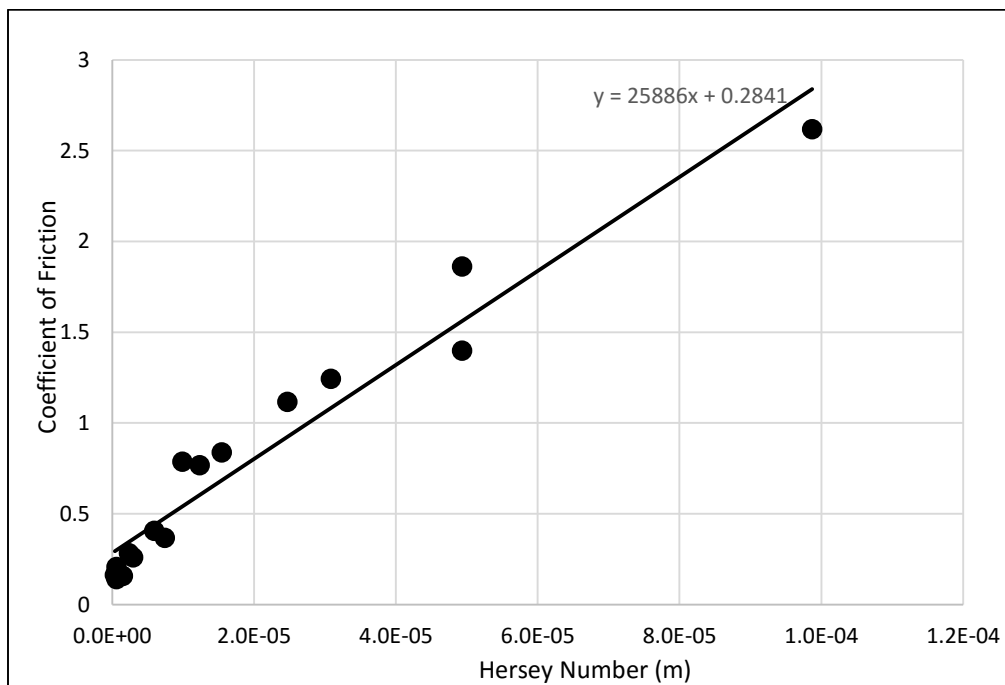


**Figure 5.14 Experimental Stribeck curve for unidirectional carbon/epoxy prepreg oriented at 15° to the direction of slippage**

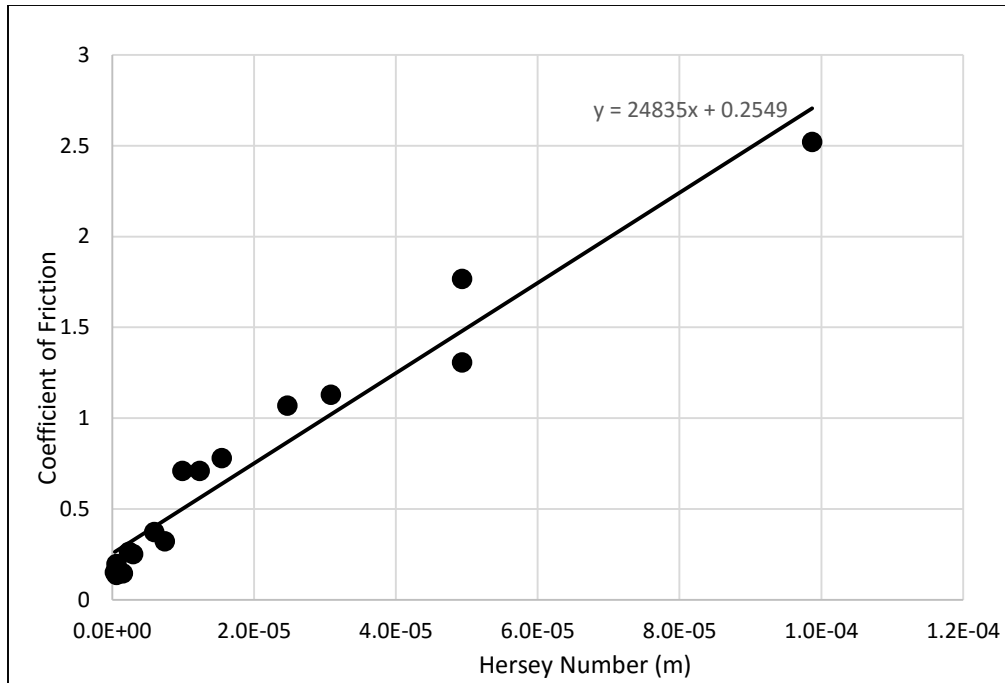


**Figure 5.15 Experimental Stribeck curve for unidirectional carbon/epoxy prepreg oriented at 30° to the direction of slippage**

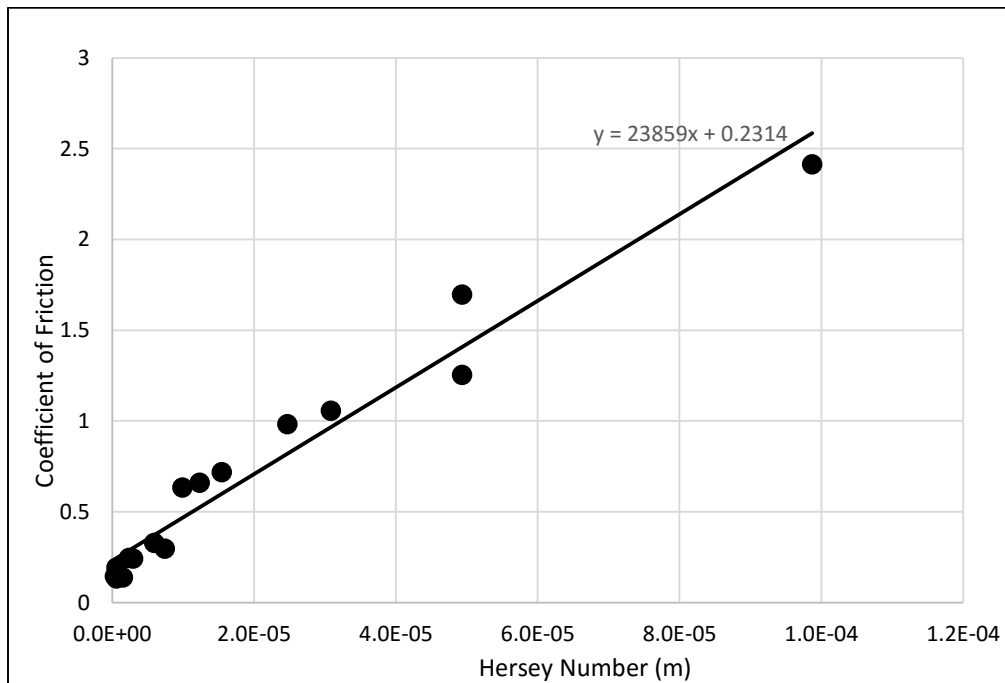


**Figure 5.16 Experimental Stribeck curve for unidirectional carbon/epoxy prepreg oriented at 45° to the direction of slippage**

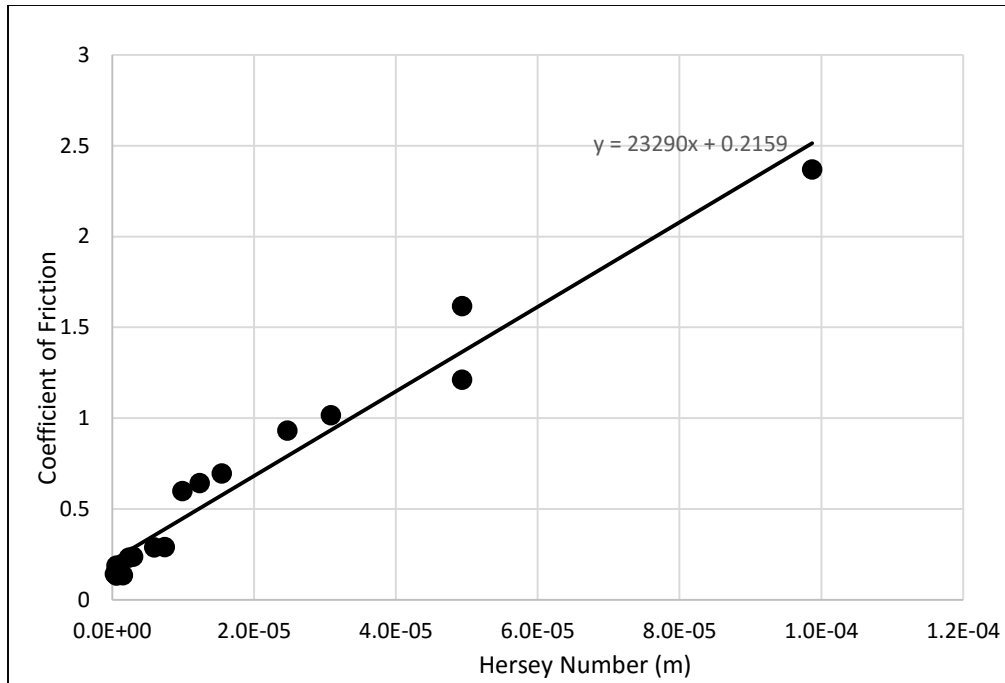


**Figure 5.17 Experimental Stribeck curve for unidirectional carbon/epoxy prepreg oriented at 60° to the direction of slippage**

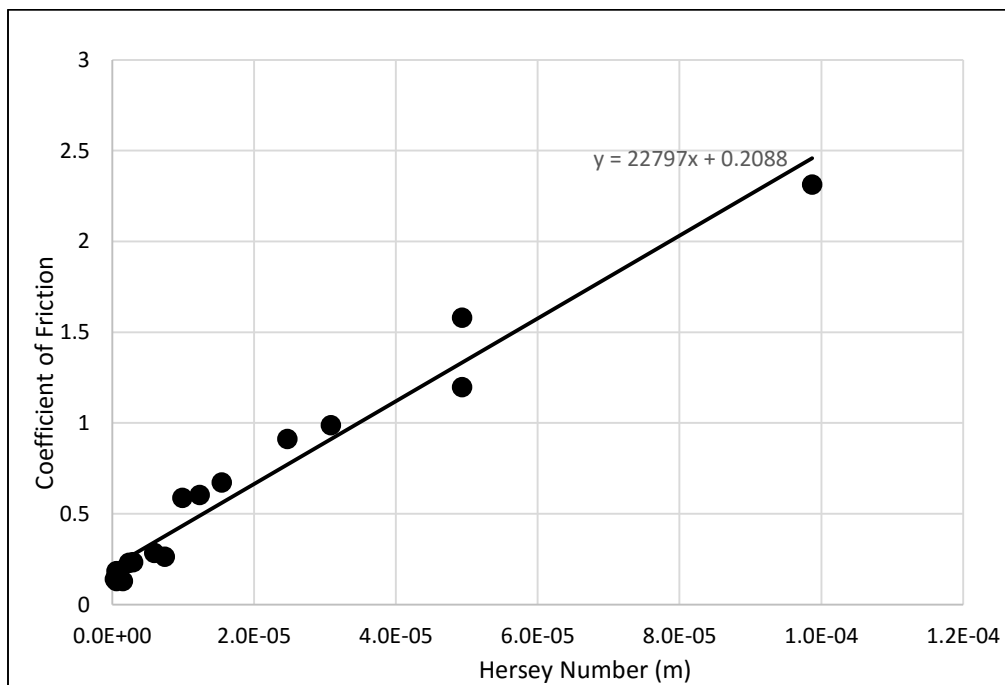


**Figure 5.18 Experimental Stribeck curve for unidirectional carbon/epoxy prepreg oriented at 75° to the direction of slippage**

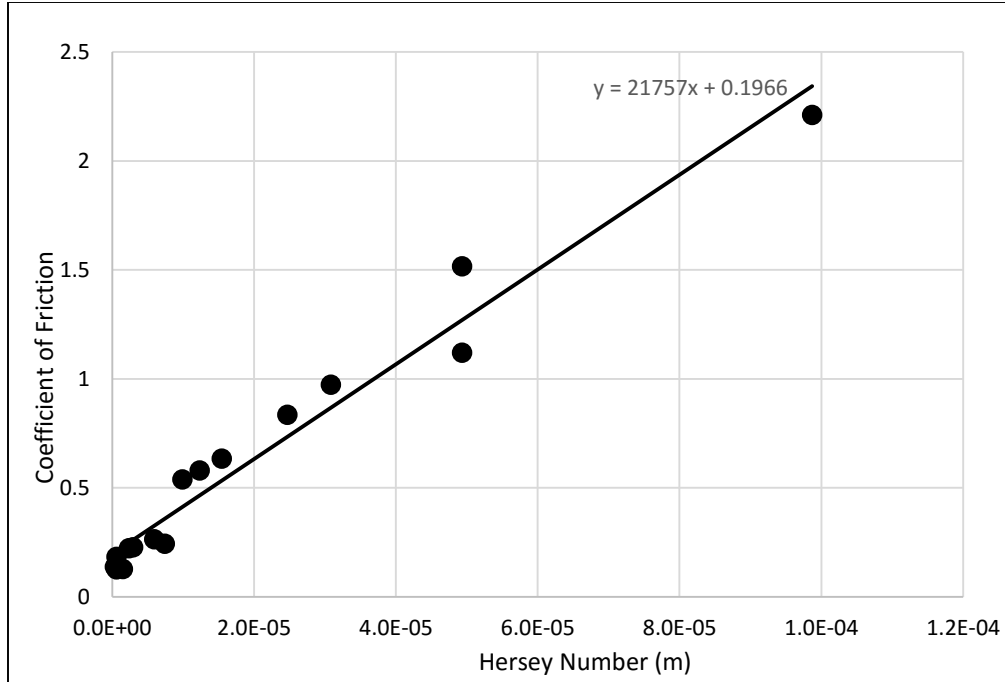


**Figure 5.19 Experimental Stribeck curve for unidirectional carbon/epoxy prepreg oriented at 90° to the direction of slippage**

Similar to 8HS and 5HS, it is noticed that linear equations obtained from the Stribeck curves for UD are in the form

$$\mu = a . H + b$$

where variables a and b have different values for each set of fabric orientation. Figures 5.20 and 5.21 show the variables a and b plotted against fabric angle  $\theta$ . The lines are fitted through the intersecting points. The equations of these fitted lines are given below:

$$a = 0.9042 \theta^2 - 155.95 \theta + 28951$$

$$b = 1E-05 \theta^2 - 0.0026 \theta + 0.3216$$

A general equation was developed which could be used to predict coefficient of friction for any set of processing conditions for UD at any fabric orientation, as given by equation 5.4.

$$\mu = (0.9042 \theta^2 - 155.95 \theta + 28951).H + (1E-05 \theta^2 - 0.0026 \theta + 0.3216) \quad (5.4)$$

where  $\theta$  is the fabric orientation angle in degrees.

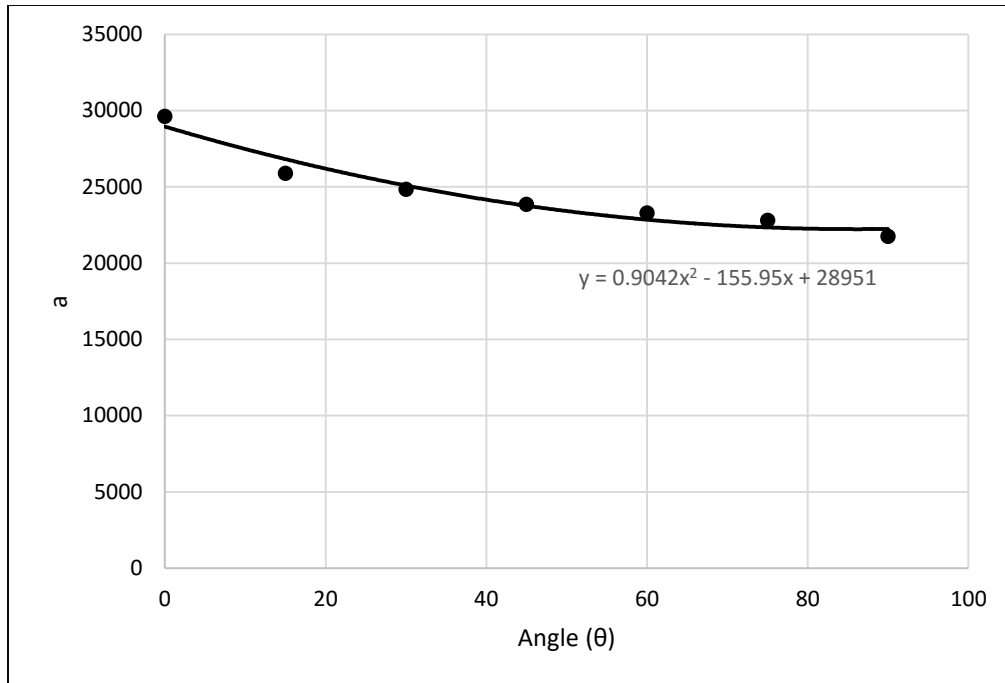


**Figure 5.20 Relationship between “a” and fabric angle “ $\theta$ ” for UD**

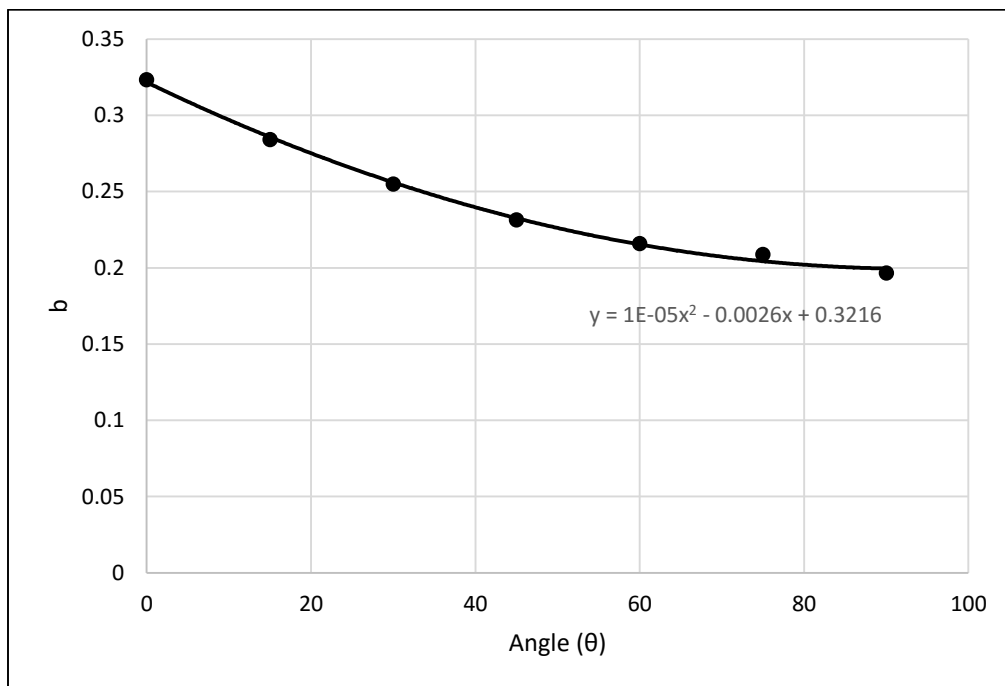


**Figure 5.21 Relationship between “b” and fabric angle “ $\theta$ ” for UD**

### 5.3 Friction Models of Other Prepreg Configurations

To characterize tool/ply friction, Stribeck curves for 8-harness/vacuum bag and 5-harness/vacuum bag were drawn as shown in figures 5.22 and 5.23. Figure 5.24 shows the Stribeck curve for the inter-ply friction between 5-harness/8-harness OOA prepregs.

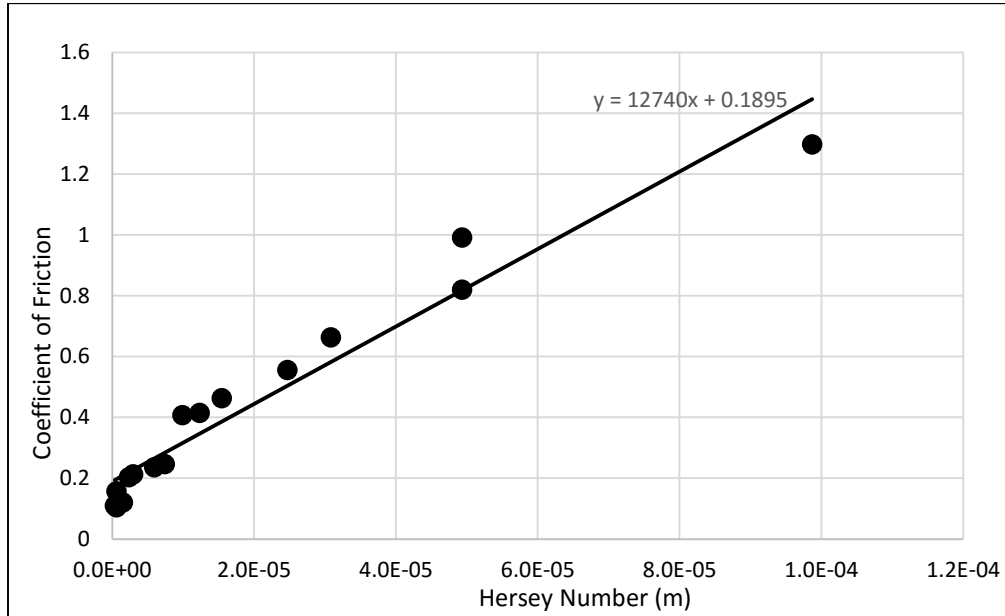


Figure 5.22 Experimental Stribeck curve for 8HS/Vacuum Bag

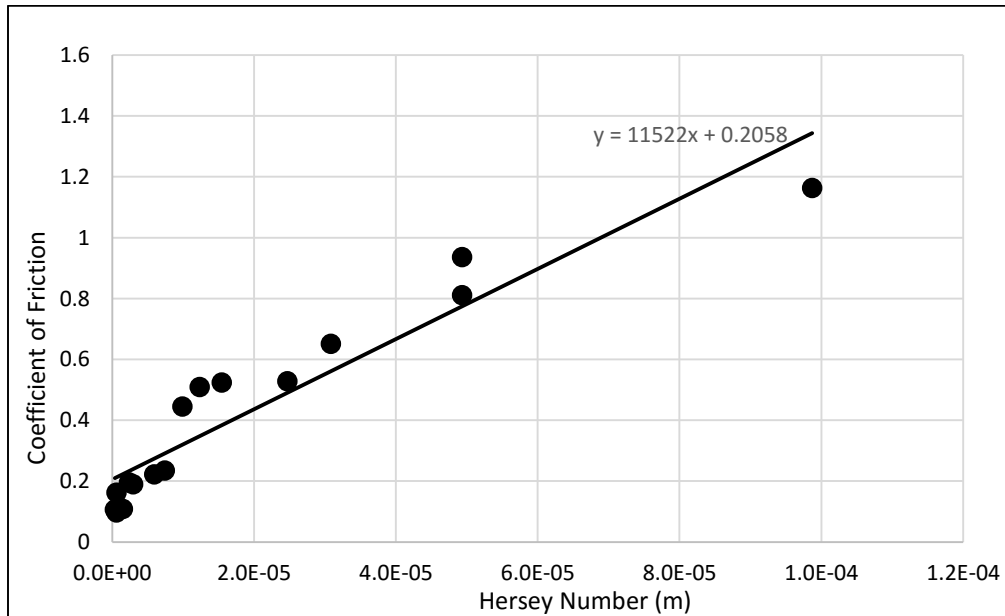
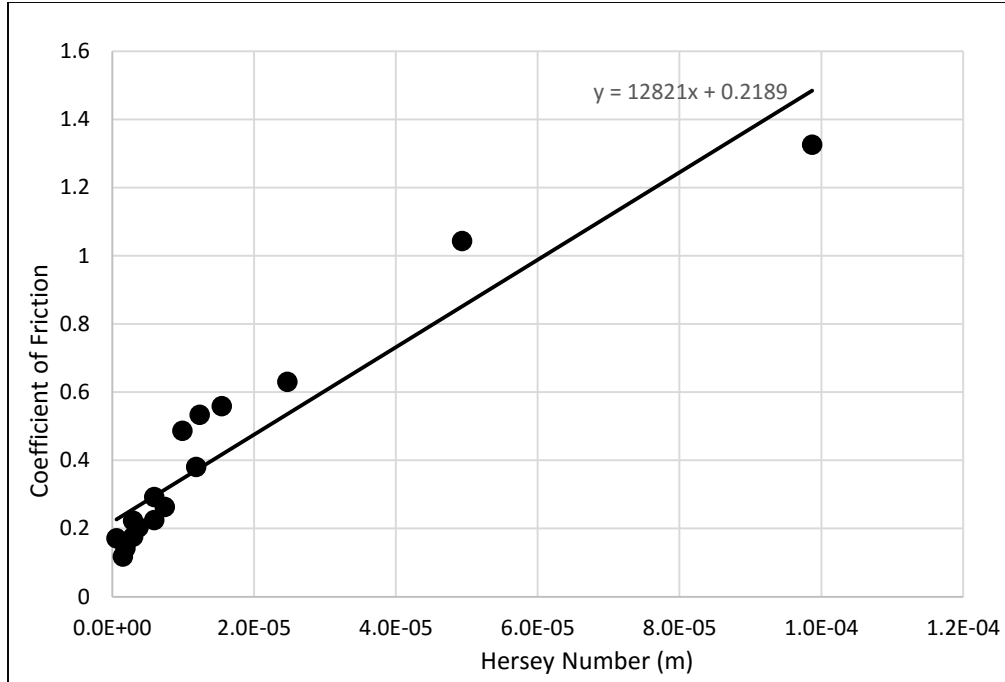


Figure 5.23 Experimental Stribeck curve for 5HS/Vacuum Bag



**Figure 5.24 Experimental Stribeck curve for 5HS/8HS preregs**

Table 5.5 shows the linear relationships between friction coefficients and Hersey numbers for 8HS/Vacuum Bag, 5HS/Vacuum and 5HS/8HS.

**Table 5.5 Linear equations for 8HS/Vacuum Bag, 5HS/Vacuum Bag and 5HS/8HS**

Fiber Orientations	Linear Equations
8HS/Vacuum Bag	$\mu = 12740.H + 0.1895$
5HS/Vacuum Bag	$\mu = 11522.H + 0.2058$
5HS/8HS	$\mu = 12821.H + 0.2189$

Steady state value of frictional force, from load-displacement graphs, is also important in developing the friction model for interply shear. Stribeck curves for state values of friction were developed, that are shown in the appendices.

### 5.4 Optimization Techniques

We have investigated and discussed in detail, in the previous chapters, about the influence of various process parameters on the inter-ply shear of carbon/epoxy preregs. A numerical approach

is required to come to the conclusion about which processing condition effects the inter-ply slippage phenomenon by how much amount. This section describes the optimization of the results obtained from the friction tests. The statistical techniques used in this study are Taguchi method and Analysis of Variance (ANOVA) method. The ANOVA method explains the percentagewise influence of parameters on the occurrence of the wrinkling. The primary aim of the optimization is to characterize the inter-ply friction of out-of-autoclave prepregs at different process parameter combinations through less number of trials.

## 5.5 Taguchi Method

Taguchi provided a new statistical approach in which a modified form of design of experiments (DOE) is used. Taguchi method involves the use of special orthogonal arrays to study the entire range of parameters by performing few experiments only [52]. A signal-to-noise (S/N) ratio is then calculated from the experimental results. Signal-to-noise ratio is the measure of quality characteristics diverging from or approaching to the desired values. The term ‘signal’ stands for the desirable effect and ‘noise’ stands for the undesirable effect to the output characteristic. There are three categories of signal-to-noise that are commonly used which are smaller-the-better, larger-the-better and nominal-the-best.

**SMALLER-THE-BETTER:** It is used for all undesirable characteristics for which the ideal value is zero.

$$\text{S/N ratio, } \eta = -10 \log_{10} \frac{1}{n} \sum_{i=1}^n y_i^2 \quad (5.5)$$

where  $n$  = number of repetitions and  $y_i$  = observed data

**LARGER-THE-BETTER:** It is used for all desired characteristics.

$$\text{S/N ratio, } \eta = -10 \log_{10} \frac{1}{n} \sum_{i=1}^n \frac{1}{y_i^2} \quad (5.6)$$

where  $n$  = number of repetitions and  $y_i$  = observed data

NOMINAL-THE-BEST: It is used when a specific value is desired and variation about the value is minimum.

$$\text{S/N ratio, } \eta = -10 \log_{10} \frac{\mu^2}{\sigma^2} \quad (5.7)$$

where  $\mu$  = mean and  $\sigma$  = variance

### 5.5.1 Standard Procedure

Taguchi proposed a standard procedure for applying his method for optimizing any process. The steps are as follow.

- Identification of the main function, side effects and failure mode.
- Identification of the noise factors and test conditions.
- Identification of the objective function to be optimized.
- Identification of the control factors and their levels.
- Designing the orthogonal array matrix experiment.
- Conducting the matrix experiment.
- Analyzing the data and determining the optimum levels of the control factors.
- Predicting the performance at these levels.

### 5.5.2 Selection of Process Parameters

Before doing the optimization, process parameters which influence the inter-ply shear mechanism the most are selected. The process parameters taken into consideration are normal pressure, temperature and pulling rate. According to design of experiments three levels for each parameter were chosen as shown in Table 5.6. Most of the levels for process parameters were selected considering the data in literature and composite forming handbooks.

**Table 5.6. Different levels for each parameter**

Symbols	Parameters	Units	Level 1	Level 2	Level 3
P	Normal Pressure	atm	0.5	0.8	1
T	Temperature	°C	50	70	90
R	Pulling Rate	mm/sec	0.5	1	2

### 5.5.3 Selection of Orthogonal Array

The next step needed is to select an orthogonal array for performing the experiments. An appropriate orthogonal array for conducting experiments can be selected based on the degrees of freedom of process parameters. Degrees of freedom are calculated as follow.

$$\text{Degree of freedom} = 1 \text{ (for Mean Value)}$$

$$+ 3 \times 2 \text{ (two for each parameter)}$$

$$\text{Total degrees of freedom} = 7$$

The most appropriate orthogonal array  $L_9$ , as shown in Table 5.7, was selected.

**Table 5.7  $L_9$  Orthogonal Array**

Experiment No.	Parameter Levels		
	P	T	R
	Normal Pressure	Temperature	Pulling Rate
1	0.5	50	0.5
2	0.5	70	1
3	0.5	90	2
4	0.8	50	1
5	0.8	70	2
6	0.8	90	0.5
7	1	50	2
8	1	70	0.5
9	1	90	1

**Table 5.8 Signal-To-Noise (S/N) Ratio for Each Experiment**

Experiment No.	Parameter Levels			Inter-Ply Friction (N)		Signal-to-Noise Ratios (dB)	
	P	T	R	8HS	5HS	8HS	5HS
1	0.5	50	0.5	1103	775	-60.85	-57.79
2	0.5	70	1	411	320	-52.28	-50.10
3	0.5	90	2	334	280	-50.47	-48.94
4	0.8	50	1	2268	1392	-67.11	-62.87
5	0.8	70	2	629	540	-55.97	-54.65
6	0.8	90	0.5	270	228	-48.63	-47.16
7	1	50	2	3405	2113	-70.64	-66.49
8	1	70	0.5	418	330	-52.42	-50.37
9	1	90	1	386	287	-51.73	-49.16

#### 5.5.4 Signal-to-Noise (S/N) Ratios

In this study, main objective is to reduce the inter-ply friction by playing with the processing conditions. During the forming operation of composite prepregs, occurrence of wrinkles is one of the unwanted outcomes. Smaller-the-Better formula, as given by equation 5.5, was selected as inter-ply friction is the undesirable characteristic. To calculate S/N values, peak values of friction from load-displacement graphs were selected. Tests were performed at different levels of normal pressure, temperature and pulling rate according to the orthogonal array as shown in table 5.7 on 8HS and 5HS carbon/epoxy prepregs. Results from the experiments were then converted into signal-to-noise ratio (S/N) using equation 5.5. The signal-to-noise ratio values for all the responses are shown in Table 5.8. Higher the S/N ratio, more favorable are the processing conditions for interply-slippage. It was observed that experiment 6 had highest S/N ratio, for both 8-harness and 5-harness prepregs, with normal pressure of 0.8 atm, temperature of 90 °C and pulling rate of 0.5 mm/sec

#### 5.5.5 Influence of Processing Parameters

As the experimental design is orthogonal, separate influence of each parameter at different levels can be found. For example, the mean signal-to-noise ratios for the normal pressure at levels 1, 2 and 3 can be calculated by finding average signal-to-noise ratios for experiments 1-3, 4-6 and 7-9 respectively. Similarly, mean signal-to-noise ratios at each level for all other parameters can be calculated. Tables 5.9 and 5.10 show the mean signal-to-noise ratios for each level of parameters and is called signal-to-noise response table. It was observed that normal pressure at level 1, temperature at level 3 and pulling rate at level 1 appeared as the optimum conditions for forming process for both 8HS and 5HS. Last columns of the tables show the difference between the maximum and minimum values of mean S/N ratios.

**Table 5.9 Signal-To-Noise (S/N) Response for Each Parameter for 8HS**

Symbols	Parameters	Level 1	Level 2	Level 3	Difference
P	Normal Pressure	-54.53	-57.24	-58.27	3.73
T	Temperature	-66.20	-53.56	-50.28	15.92
R	Pulling Rate	-53.97	-57.04	-59.03	5.06

**Table 5.10 Signal-To-Noise (S/N) Response for Each Parameter for 5HS**

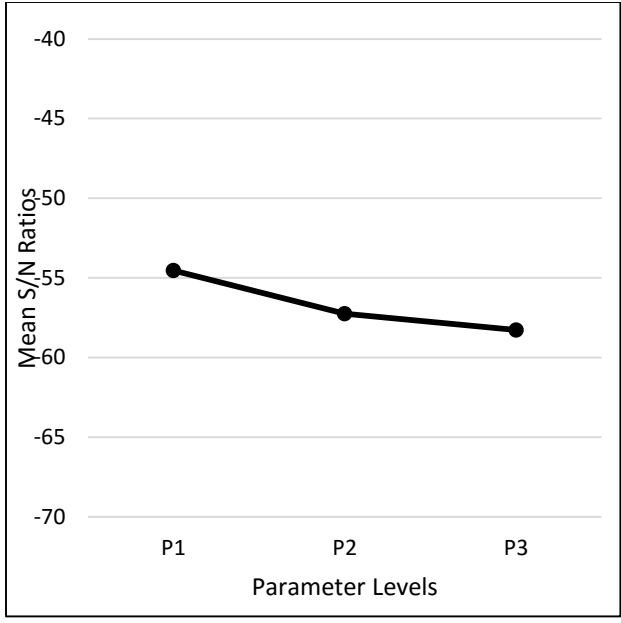
<b>Symbols</b>	<b>Parameters</b>	<b>Level 1</b>	<b>Level 2</b>	<b>Level 3</b>	<b>Difference</b>
P	Normal Pressure	-52.28	-54.89	-55.34	3.06
T	Temperature	-62.39	-51.70	-48.42	13.97
R	Pulling Rate	-51.77	-54.04	-56.69	4.92

The best process parameter combinations, based on the results obtained from Taguchi method, recommended to decrease the inter-ply friction and to reduce the chances of wrinkles in the final product are shown in table 5.11. The effect of ply-ply and tool-ply friction on the occurrence of wrinkles and other defects is taken into consideration in these results.

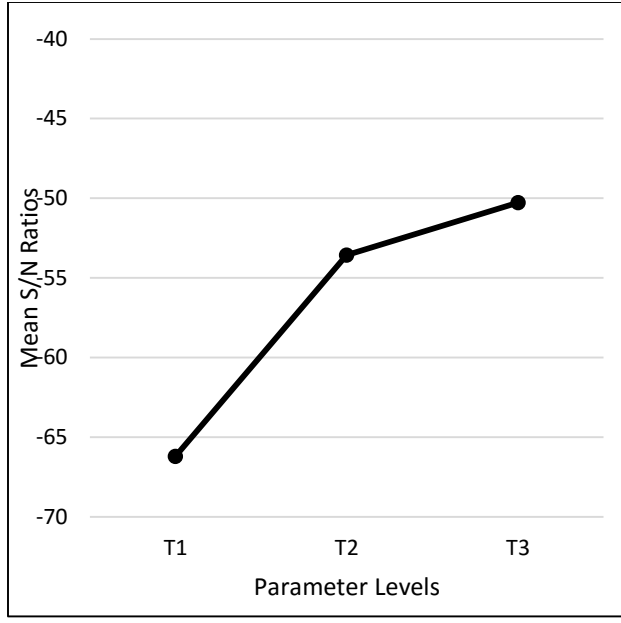
**Table 5.11 Optimum process parameter combinations**

<b>Parameters</b>	<b>Units</b>	<b>Values</b>
Normal Pressure	atm	0.5
Temperature	°C	90
Pulling Rate	mm/sec	0.5

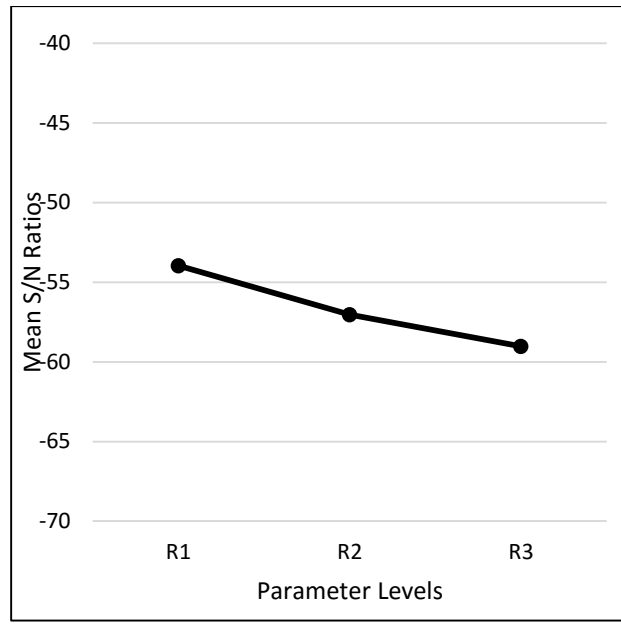
Signal-to-noise responses were plotted on the graph as shown in Figures 5.25 and 5.26. It was observed that inter-ply friction increases with the increase in normal pressure which is consistent with the previous works [25,31,32]. Processing temperature has the largest influence on forming of composite plies as difference between maximum and minimum value of mean S/N ratio for temperature is the largest. Inter-ply friction appeared to be at lowest value at 90 °C. This result is in agreement with the fact that viscosity of the resin reduces with the increase in temperature. Figures 5.25 (c) and 5.26 (c) show the influence of pulling rate on inter-ply friction. Inter-ply friction increases with the increase in pulling rate which shows the hydrodynamic nature of inter-ply friction.



(a)

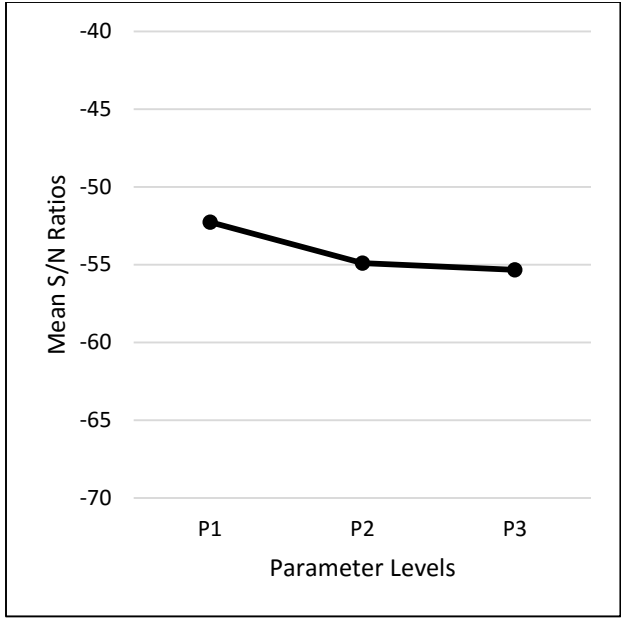


(b)

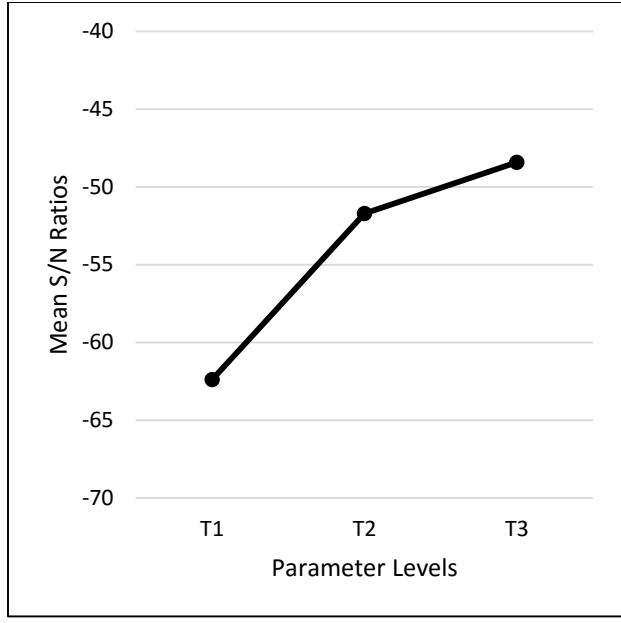


(c)

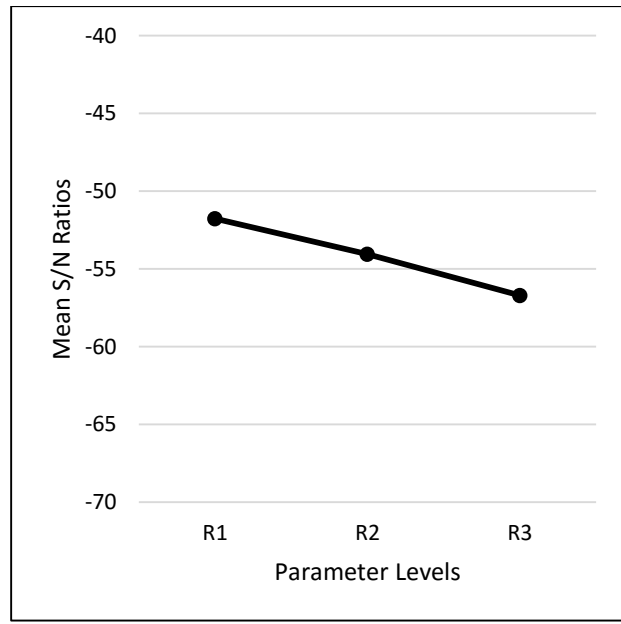
**Figure 5.25 Signal-to-noise (S/N) response graph for 8HS at different levels of (a) Normal Pressure (b) Temperature and (c) Pulling Rate**



(a)



(b)



(c)

**Figure 5.26 Signal-to-noise (S/N) response graph for 5HS at different levels of (a) Normal Pressure (b) Temperature and (c) Pulling Rate**

## 5.6 Analysis of Variance (ANOVA)

ANOVA is a statistical technique for determining influence of any given input parameter from a group of experimental results by design of experiments and it can be used to interpret experimental data [52][51][50][49][49][49,50]. The influence of a parameter level is calculated as the deviation it causes from the overall mean. The overall mean S/N ratio is expressed as

$$\bar{\eta} = \frac{1}{n} \sum_{i=1}^n \eta_i \quad (5.8)$$

where  $n$  is number of experiments and  $\eta_i$  is S/N ratio for  $i$ th experiment

The sum of squares due to deviation about the overall mean is expressed as

$$SS = \sum_{i=1}^n (\eta_i - \bar{\eta})^2 \quad (5.9)$$

where  $\eta_i$  is S/N ratio for  $i$ th experiment and  $\bar{\eta}$  is the overall mean S/N ratio

To find the relative importance among the processing parameters for forming of composite plies Analysis of Variance method was used. Overall mean signal-to-noise ratio was calculated using equation 5.8.

For 8HS,

$$\begin{aligned} \bar{\eta} &= \frac{1}{n} \sum_{i=1}^n \eta_i \\ &= \frac{1}{9} (-60.85 - 52.28 - 50.47 - 67.11 - 55.97 - 48.63 - 70.64 - 52.42 - 51.73) \\ &= -56.68 \end{aligned}$$

For 5HS,

$$\begin{aligned} \bar{\eta} &= \frac{1}{n} \sum_{i=1}^n \eta_i \\ &= \frac{1}{9} (-57.79 - 50.10 - 48.94 - 62.87 - 54.65 - 47.16 - 66.49 - 50.37 - 49.16) \\ &= -54.17 \end{aligned}$$

The sum of squares due to deviation about the overall mean was calculated using equation 5.9. Tables 5.12 and 5.13 are the ANOVA tables for 8HS and 5HS respectively. The degrees of freedom for each parameter which are equal to 2 for normal pressure, temperature and pulling rate. Column 3 shows the sum of squares for each processing parameters and the total sum of squares. Variance was calculated by dividing sum of square for each parameter by its degree of freedom.

Percentage contribution of each parameter in inter-ply slippage is shown in the last columns of the tables 5.12 and 5.13. Processing temperature appeared as the most contributing parameter with percentage of 87.37% for 8HS and 85.81% for 5HS. Pulling rate and normal pressure have percentage contribution of 8.04% and 4.59% respectively for 8HS. And for 5HS, pulling rate and normal pressure contribute 9.78% and 4.41% respectively.

**Table 5.12 ANOVA Table for 8HS**

<b>Parameters</b>	<b>Degrees of freedom</b>	<b>Sum of Squares, S</b>	<b>Variance, V</b>	<b>Percent Contribution, P (%)</b>
Normal Pressure (atm)	2	22.29	11.14	4.59
Temperature (°C)	2	424.22	212.11	87.37
Pulling Rate (mm/sec)	2	39.03	19.52	8.04
Total		485.54		100

**Table 5.13 ANOVA Table for 5HS**

<b>Parameters</b>	<b>Degrees of freedom</b>	<b>Sum of Squares, S</b>	<b>Variance, V</b>	<b>Percent Contribution, P (%)</b>
Normal Pressure (atm)	2	16.44	8.22	4.41
Temperature (°C)	2	319.88	159.94	85.81
Pulling Rate (mm/sec)	2	36.45	18.23	9.78
Total		372.77		100

### **5.6.1 Confirmation Test**

Optimum processing conditions were selected as 0.5 atm normal pressure, 90 °C temperature and 0.5 mm/sec pulling rate. The value of signal-to-noise ratio under optimum condition was calculated using the following equation.

For 8HS,

$$\begin{aligned}\eta_{opt} &= \bar{\eta} + (\eta_{Popt} - \bar{\eta}) + (\eta_{Topt} - \bar{\eta}) + (\eta_{Ropt} - \bar{\eta}) \\ &= -56.68 + (-54.53 + 56.68) + (-50.28 + 56.68) + (-53.97 + 56.68) \\ &= -45.42\end{aligned}$$

For 5HS,

$$\begin{aligned}\eta_{opt} &= \bar{\eta} + (\eta_{Popt} - \bar{\eta}) + (\eta_{Topt} - \bar{\eta}) + (\eta_{Ropt} - \bar{\eta}) \\ &= -54.17 + (-52.28 + 54.17) + (-48.42 + 54.17) + (-51.77 + 54.17) \\ &= -44.13\end{aligned}$$

Confirmation test was conducted to verify the estimated result for optimum processing conditions. Result from the confirmation test was converted into signal-to-noise ratio.

For 8HS,

$$\eta_{exp} = -47.46$$

For 5HS,

$$\eta_{exp} = -45.80$$

The difference between S/N ratios of estimated and experimental result was found to be 2.04 dB and 1.67 dB for 8HS and 5HS respectively.

## 5.7 Summary

This chapter explained that a linear friction model could be developed between coefficient of friction and Hersey number for different prepreg configurations. The Stribeck curves were developed by plotting friction coefficient against Hersey number. The linear models developed in this study could be used in simulation operations for the prediction of actual forming operations before performing them.

Optimization techniques were explained in this chapter to find out the ideal conditions for the manufacturing of composite products without wrinkles. The ANOVA method tells us about the percentage contribution of each process parameter in the inter-ply friction mechanism.

# Chapter 6 : Conclusions and Contributions

The conclusions drawn from the research work presented in this dissertation are encapsulated below:

- The interply friction behaviors of out-of-autoclave (OOA) 8HS, 5HS and UD carbon/epoxy prepregs were investigated at different processing conditions using a friction test-rig developed for this study. It was concluded that the occurrence of wrinkles in the final composite product could be eliminated by reducing the ply/ply and tool/ply friction. Results show that temperature, pulling rate and normal pressure have different impacts on interply friction. Increase in temperature and decrease in the pulling rate can enhance slipping between prepreg plies. With the increase in normal pressure, frictional force increases slightly but the coefficient of friction, which is the ratio of force of friction to the normal force, decreases.
- It was observed that friction mechanism between prepreg plies is mixed friction type i.e., combination of both coulomb and hydrodynamic friction. The presence of stick-slip peaks in load-displacement graphs indicate that it is a coulomb dominated friction while dependence of inter-ply friction on the pulling velocity shows friction is hydrodynamic in nature. By comparing the 8HS, 5HS and UD prepregs, frictional resistance was found to be the largest in unidirectional composites, followed by 8-harness and 5-harness composites respectively.
- In a composite laminate consisting of layers of 8HS, 5HS and UD, packed inside bagging material, slippage first takes place at the interface of bagging material and composite plies followed by 5-harness, 8-harness and unidirectional prepregs.
- The change in fiber orientation of the prepreg plies has influence on the frictional resistance between layers of the composite laminate. The frictional resistance was found maximum at 0° fiber orientation and it decreases when orientation of fiber was changed to 15°, 30° and 45°. As the angle of warp yarn increases, the force of friction decreases and reached the minimum value as the warp fiber angle reaches 45°.
- Microscopic analysis showed the visualization of the micro-structures of the cured composite laminates. Fiber volume fraction for 8-harness composite is observed more than 5-harness composite. Void contents for 8HS is 0.993 % and for 5HS is 0.925%. Less voids

in 5HS are because of more resin content in it as compared to 8HS. The laminate thickness for 8HS is 1381.06  $\mu\text{m}$  and for 5HS is 1402.88  $\mu\text{m}$ .

- An analytical friction model for ply/ply and tool/ply friction was developed on the basis of Stribeck curves. To draw Stribeck curves, Hersey number was calculated and plotted against the coefficient of friction. A linear relationship between friction coefficient and Hersey number was calculated. As Hersey number ( $H$ ) is the function of viscosity of resin, normal pressure and pulling rate, so using the viscosity values at any given temperature and using other processing conditions, coefficient of friction could be easily calculated.
- A general equation was developed which could be used to predict coefficient of friction for any set of processing conditions (temperature, pulling rate, normal pressure) at any fabric (fiber) orientation.
- Optimization process for the reduction of interply friction of out-of-autoclave carbon/epoxy prepregs was investigated using Taguchi method. Overall mean signal-to-noise ratio show that high processing temperature is favorable for low inter-ply friction. Low normal pressure is favorable for forming process as it has highest signal-to-noise (S/N) ratio out of three levels. The optimum processing parameter combinations for forming operation were concluded as follows:

Normal Pressure = 0.5 atm

Temperature = 90 °C

Pulling Rate = 0.5 mm/sec

- Analysis of variance (ANOVA) technique showed that processing temperature is the most influencing parameter, by determining the percentage of contribution of each parameter on the interply friction, for forming of composite followed by pulling rate and normal pressure. It was observed that percentage contribution of temperature is 87.37% for 8HS and 85.81% for 5HS which is the highest of all other parameters.

## **Chapter 7 : Future Scope**

To improve the quality characteristics of composite products, other modes of deformation must be investigated such as intra-ply shear, intra-ply tensile loading, consolidation, ply bending etc. A model should be developed taking into consideration all the modes of deformation during forming operation to characterize the thermoforming operation of prepregs before performing the actual operation. The simulation of the actual process could be developed using software technology on the basis of the data obtained from the friction test results. Additionally, various drawbacks of the hot drape forming technology need to be rectified. By considering all these recommendations, superior quality composite products could be manufactured.

## REFERENCES

- [1] Y. Ma, T. Centea, G. Nilakantan, and S. R. Nutt, "Vacuum Bag Only Processing of Complex Shapes: Effect of Corner Angle, Material Properties and Process Conditions," *Proc. 29th Tech. Conf. Am. Soc. Compos. US-Japan Conf. Compos. Mater. D-30 Meet.*, pp. 2–17, 2014.
- [2] "The use of composites in aerospace: Past, present and future challenges." [Online]. Available: <https://avaloncsl.files.wordpress.com/2013/01/avalon-the-use-of-composites-in-aerospace-s.pdf>.
- [3] K. S. Madhok, "COMPARATIVE CHARACTERIZATION OF OUT-OF- AUTOCLAVE MATERIALS MADE BY AUTOMATED FIBER PLACEMENT AND HAND-LAY-UP PROCESSES," Masters Thesis, Concordia University, 2013.
- [4] A. C. Long, *Composites forming technologies*. CRC Press, 2007.
- [5] P. Harrison, R. T. Thije, R. Akkerman, and a. C. Long, "Characterising and modelling tool-ply friction of viscous textile composites," vol. 7, no. December, pp. 5–22, 2010.
- [6] J. Wang, "Predictive modelling and experimental measurement of composite forming behaviour," no. August, 2010.
- [7] S. V Hoa, *Principles of the Manufacturing of Composite Materials*. Destech Publication, 2009.
- [8] K. Vanclooster, "Forming of Multilayered Fabric Reinforced Thermoplastic Composite," Katholeike University, Belgium, 2009.
- [9] R. Parambath Mohan, "Investigation of Intra/ply Shear Behavior of Out-of-Autoclave Carbon/Epoxy Prepreg," Concordia University, Montreal, 2015.
- [10] A. C. Long, *Design and Manufacture of Textile Composites*. CRC Press, 2006.
- [11] S. B. Truslow, "Permanent Press, No Wrinkles: Reinforced Double Diaphragm Forming of Advanced Thermoset Composites," p. 105, 2000.
- [12] C. E. Wilks, "Processing technologies for woven glass/polypropylene composites," PhD Thesis, University of Nottingham, 2000.

- [13] C. Mack and H. M. Taylor, "The Fitting of Woven Cloth to Surfaces," *J. Text. Inst. Trans.*, vol. 47, no. 9, pp. T477–T488, 1956.
- [14] B. Zhu, T. X. Yu, and X. M. Tao, "Large deformation and slippage mechanism of plain woven composite in bias extension," *Compos. Part A Appl. Sci. Manuf.*, vol. 38, no. 8, pp. 1821–1828, 2007.
- [15] G. Lebrun, M. N. Bureau, and J. Denault, "Evaluation of bias-extension and picture-frame test methods for the measurement of intraply shear properties of PP/glass commingled fabrics," *Compos. Struct.*, vol. 61, no. 4, pp. 341–352, 2003.
- [16] M. Aono, D. E. Breen, and M. J. Wozny, "Fitting a Woven-Cloth Model to a Curved Surface: Mapping Algorithms," *Comput. Des.*, vol. 26, no. 4, pp. 278–292, 1994.
- [17] P. Harrison, M. J. Clifford, and A. C. Long, "Shear characterisation of viscous woven textile composites: A comparison between picture frame and bias extension experiments," *Compos. Sci. Technol.*, vol. 64, no. 10–11, pp. 1453–1465, 2004.
- [18] E. de Bilbao, D. Soulat, G. Hivet, and a. Gasser, "Experimental Study of Bending Behaviour of Reinforcements," *Exp. Mech.*, vol. 50, no. 3, pp. 333–351, 2010.
- [19] K. Bilisik and G. Yolacan, "Experimental determination of bending behavior of multilayered and multidirectionally-stitched E-Glass fabric structures for composites," *Text. Res. J.*, vol. 82, no. 10, pp. 1038–1049, 2012.
- [20] R. H. W. ten Thije and R. Akkerman, "Design of an experimental setup to measure tool-ply and ply-ply friction in thermoplastic laminates," *Int. J. Mater. Form.*, vol. 2, no. SUPPL. 1, pp. 197–200, 2009.
- [21] A. M. Murtagh, "Characterisation of Shearing and Frictional Behaviour during Sheet Forming of Thermoplastic Composites," PhD Thesis, University of Limerick, May, 1995.
- [22] K. Vanclooster, S. V. Lomov, and I. Verpoest, "Simulation of multi-layered composites forming," *Int. J. Mater. Form.*, vol. 3, no. SUPPL. 1, pp. 695–698, 2010.
- [23] K. A. Fetfatsidis, D. Jauffrès, J. A. Sherwood, and J. Chen, "Characterization of the tool/fabric and fabric/fabric friction for woven-fabric composites during the thermostamping process," *Int. J. Mater. Form.*, vol. 6, no. 2, pp. 209–221, 2013.
- [24] J. Sun, M. Li, Y. Gu, D. Zhang, Y. Li, and Z. Zhang, "Interply friction of carbon fiber/epoxy prepreg stacks under different processing conditions," *J. Compos. Mater.*, vol. 48, no. 5, pp. 515–526, 2013.

- [25] Y. R. Larberg and M. Åkermo, "On the interply friction of different generations of carbon/epoxy prepreg systems," *Compos. Part A Appl. Sci. Manuf.*, vol. 42, no. 9, pp. 1067–1074, 2011.
- [26] L. Briançon, H. Girard, and J. P. Gourc, "A new procedure for measuring geosynthetic friction with an inclined plane," *Geotext. Geomembranes*, vol. 29, no. 5, pp. 472–482, 2011.
- [27] A. M. Murtagh, J. J. Lennon, and P. J. Mallon, "Surface friction effects related to pressforming of continuous fibre thermoplastic composites," *Compos. Manuf.*, vol. 6, no. 3–4, pp. 169–175, 1995.
- [28] R. Scherer and K. Friedrich, "Inter- and intraply-slip flow processes during thermoforming of cf/pp-laminates," *Compos. Manuf.*, vol. 2, no. 2, pp. 92–96, 1991.
- [29] S. Chow, "Frictional interaction between blank holder and fabric in stamping of woven thermoplastic composites," Masters Thesis, University of Massachusetts Lowell, 2002.
- [30] I. M. Hutchings, *Tribology: Friction and Wear of Engineering Materials*. CRC Press, 1992.
- [31] C. J. Martin, J. C. Seferis, and M. A. Wilhelm, "Frictional resistance of thermoset prepregs and its influence on honeycomb composite processing," *Compos. Part A Appl. Sci. Manuf.*, vol. 27, no. 10, pp. 943–951, 1996.
- [32] J. L. Gorczyca-Cole, J. a. Sherwood, and J. Chen, "A friction model for thermostamping commingled glass-polypropylene woven fabrics," *Compos. Part A Appl. Sci. Manuf.*, vol. 38, no. 2, pp. 393–406, 2007.
- [33] N. A. Kalebek and O. Babaarslan, "Effect of weight and applied force on the friction coefficient of the spunlace nonwoven fabrics," *Fibers Polym.*, vol. 11, no. 2, pp. 277–284, 2010.
- [34] V. M. Drakonakis, J. C. Seferis, and C. C. Doumanidis, "Curing pressure influence of out-of-autoclave processing on structural composites for commercial aviation," *Adv. Mater. Sci. Eng.*, vol. 2013, 2013.
- [35] C. Garschke, C. Weimer, P. P. Parlevliet, and B. L. Fox, "Out-of-autoclave cure cycle study of a resin film infusion process using in situ process monitoring," *Compos. Part A Appl. Sci. Manuf.*, vol. 43, no. 6, pp. 935–944, 2012.
- [36] S. L. Agius and B. L. Fox, "Rapidly cured out-of-autoclave laminates: Understanding and controlling the effect of voids on laminate fracture toughness," *Compos. Part A Appl. Sci. Manuf.*, vol. 73, pp. 186–194, 2015.

- [37] L. Liu, B. M. Zhang, D. F. Wang, and Z. J. Wu, "Effects of cure cycles on void content and mechanical properties of composite laminates," *Compos. Struct.*, vol. 73, no. 3, pp. 303–309, 2006.
- [38] P. Olivier, J. P. Cottu, and B. Ferret, "Effects of cure cycle pressure and voids on some mechanical properties of carbon/epoxy laminates," *Composites*, vol. 26, no. 7, pp. 509–515, 1995.
- [39] H. Huang and R. Talreja, "Effects of void geometry on elastic properties of unidirectional fiber reinforced composites," *Compos. Sci. Technol.*, vol. 65, no. 13, pp. 1964–1981, 2005.
- [40] M. D. Hersey, *Theory and Research in Lubrication*. John Wiley & Sons, Inc., 1966.
- [41] E. Buckingham, *On Physically Similar Systems: Illustrations of the Use of Dimensional Equations*. 1914.
- [42] J. Lee, S. Cho, Y. Hwang, C. Lee, and S. H. Kim, "Enhancement of lubrication properties of nano-oil by controlling the amount of fullerene nanoparticle additives," *Tribol. Lett.*, vol. 28, no. 2, pp. 203–208, 2007.
- [43] R. Akkerman, R. Ten Thije, U. Sachs, and M. De Rooij, "Friction in textile thermoplastic composites forming," *Proc. 10th Int. Conf. Text. Compos.*, vol. 10, pp. 271–279, 2010.
- [44] R. H. W. ten Thije, R. Akkerman, L. van der Meer, and M. P. Ubbink, "Tool-ply friction in thermoplastic composite forming," *Int. J. Mater. Form.*, vol. 1, no. SUPPL. 1, pp. 953–956, 2008.
- [45] "CYCOM 5320-1 Technical Data Sheet." [Online]. Available: [http://cytec.com/sites/default/files/datasheets/CYCOM\\_5320-1\\_031912.pdf](http://cytec.com/sites/default/files/datasheets/CYCOM_5320-1_031912.pdf).
- [46] L. Sun, "Thermal Rheological analysis of Cure Process of Epoxy Prepreg," PhD Thesis, Louisiana State University, 2002.
- [47] H. S. Grewal and M. Hojjati, "Thermoforming Process Optimization for Reduction of Inter-Ply Friction of Out-of-Autoclave Material," 2015.
- [48] H. S. Grewal and M. Hojjati, "INTER-PLY FRICTION MEASUREMENT OF OUT-OF-AUTOCLAVE THERMOSETTING PREPREG COMPOSITES," pp. 1–10, 2015.
- [49] S. R. Morris and C. T. Sun, "An investigation of interply slip behaviour in AS4/PEEK at forming temperatures," *Compos. Manuf.*, vol. 5, no. 4, pp. 217–224, 1994.

- [50] S. H. Chang, S. B. Sharma, and M. P. F. Sutcliffe, "Microscopic investigation of tow geometry of a dry satin weave fabric during deformation," *Compos. Sci. Technol.*, vol. 63, no. 1, pp. 99–111, 2003.
- [51] J. Kratz, K. Hsiao, F. Goran, and P. Hubert, "Thermal models for MTM45-1 and Cycom 5320 out-of-autoclave prepreg resins," *J. Compos. Mater.*, 2012.
- [52] K. Palanikumar, "Experimental investigation and optimisation in drilling of GFRP composites," *Meas. J. Int. Meas. Confed.*, vol. 44, no. 10, pp. 2138–2148, 2011.
- [53] S. Kamaruddin, Z. A. Khan, and S. H. Foong, "Quality characteristic improvement of an injection moulding product made from blends plastic by optimizing the injection moulding parameters using Taguchi method," *Int. J. Plast. Technol.*, vol. 14, no. 2, pp. 152–166, 2010.

## APPENDICES

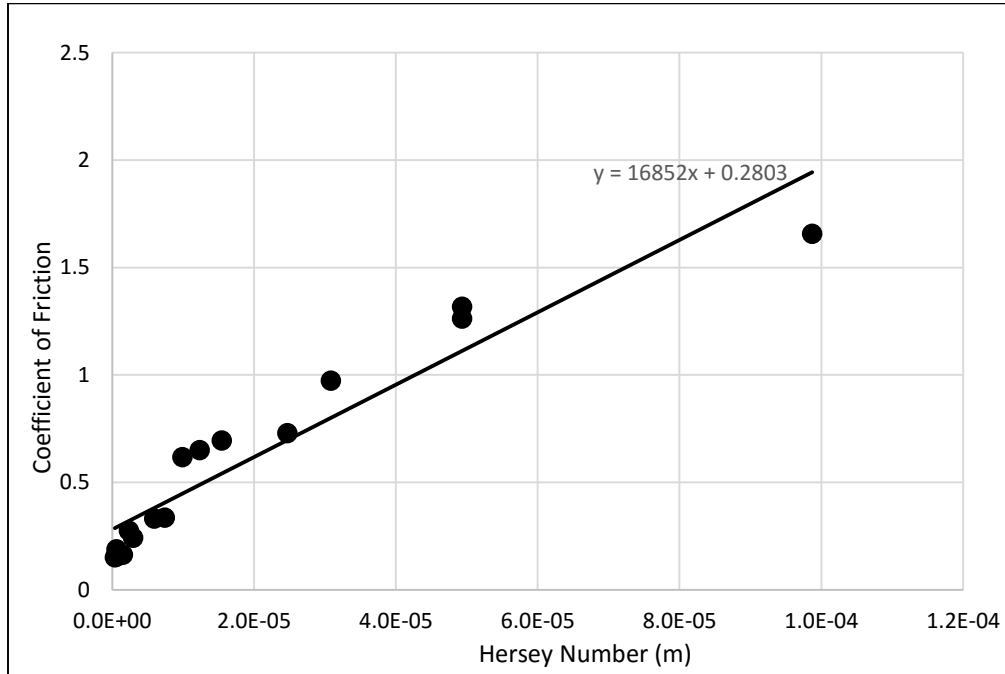


**Figure 1. Experimental Stribeck curve for 8-harness satin carbon/epoxy prepreg oriented at 60° to the direction of slippage**

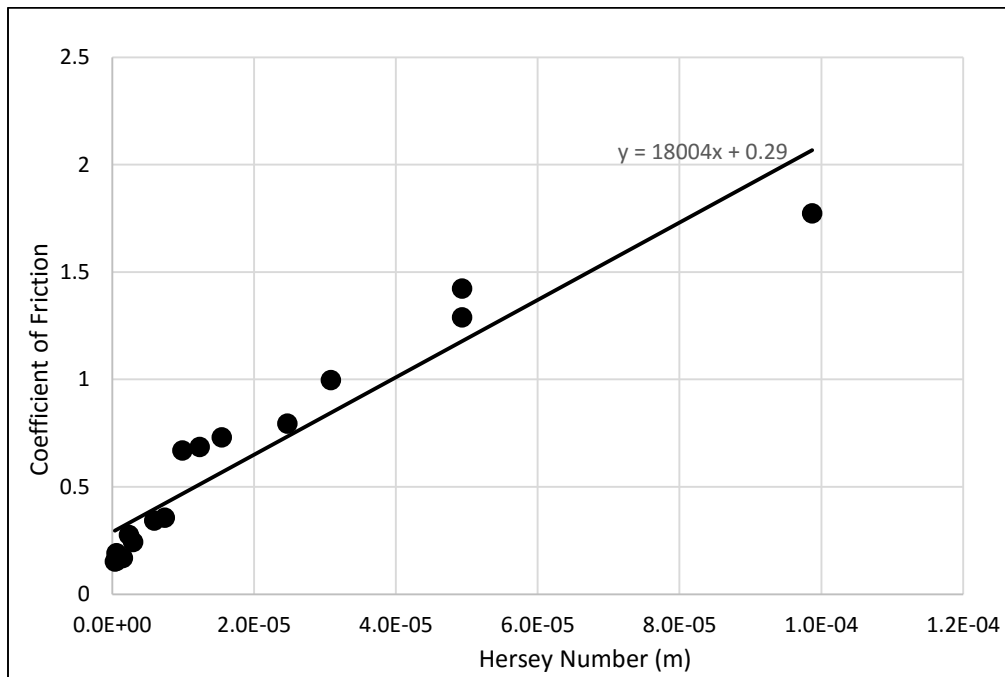


**Figure 2. Experimental Stribeck curve for 8-harness satin carbon/epoxy prepreg oriented at 75° to the direction of slippage**

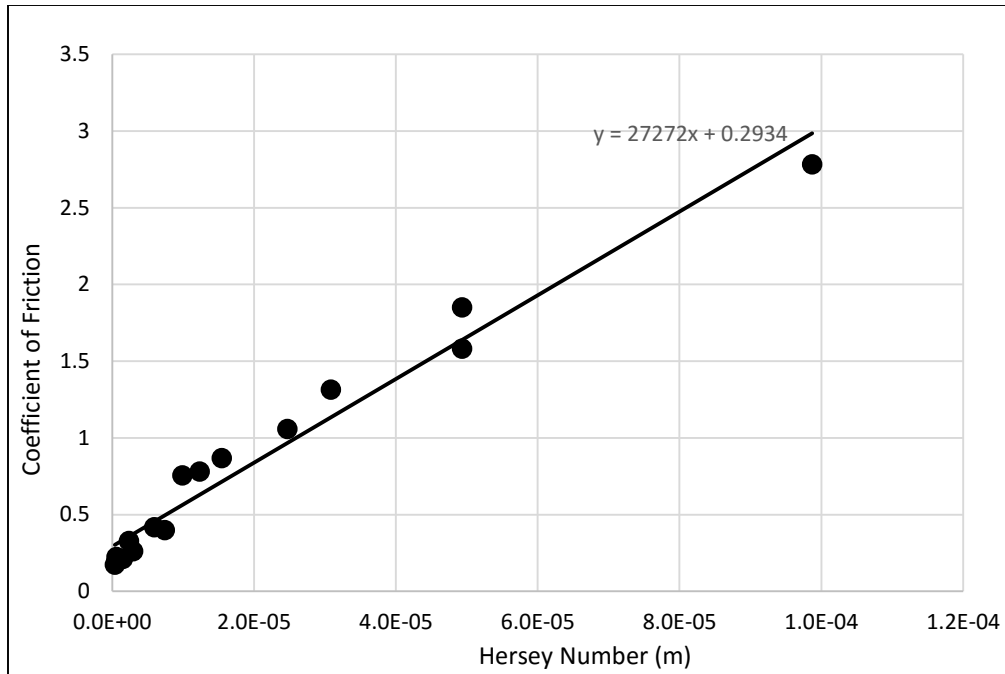


**Figure 3. Experimental Stribeck curve for 8-harness satin carbon/epoxy prepreg oriented at 90° to the direction of slippage**

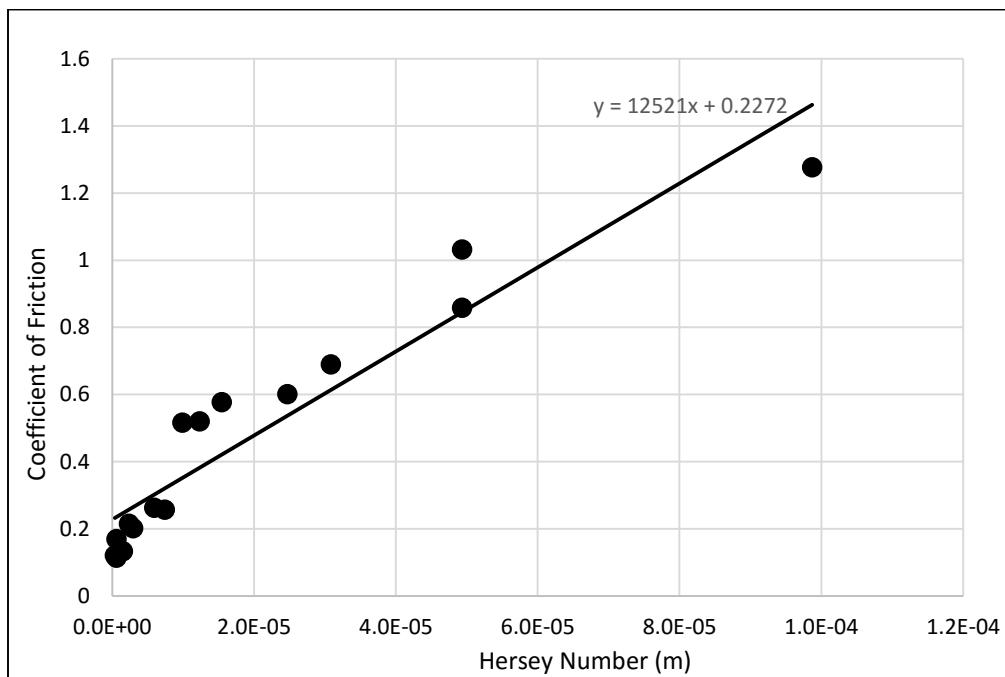


**Figure 4. Experimental Stribeck curve for 5-harness satin carbon/epoxy prepreg oriented at 60° to the direction of slippage**

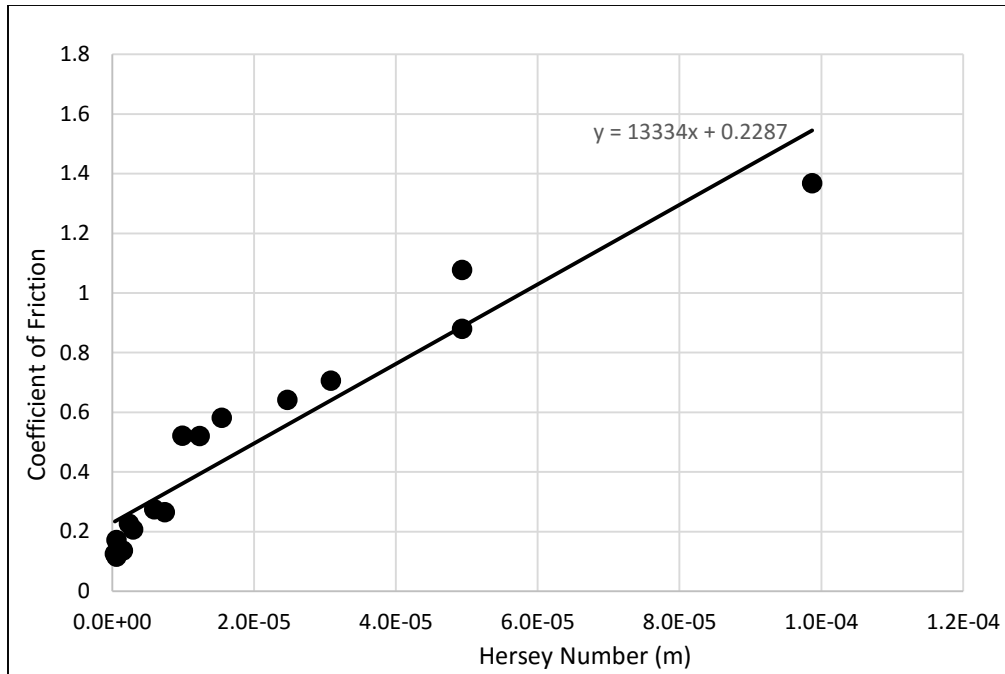


**Figure 5. Experimental Stribeck curve for 5-harness satin carbon/epoxy prepreg oriented at 75° to the direction of slippage**

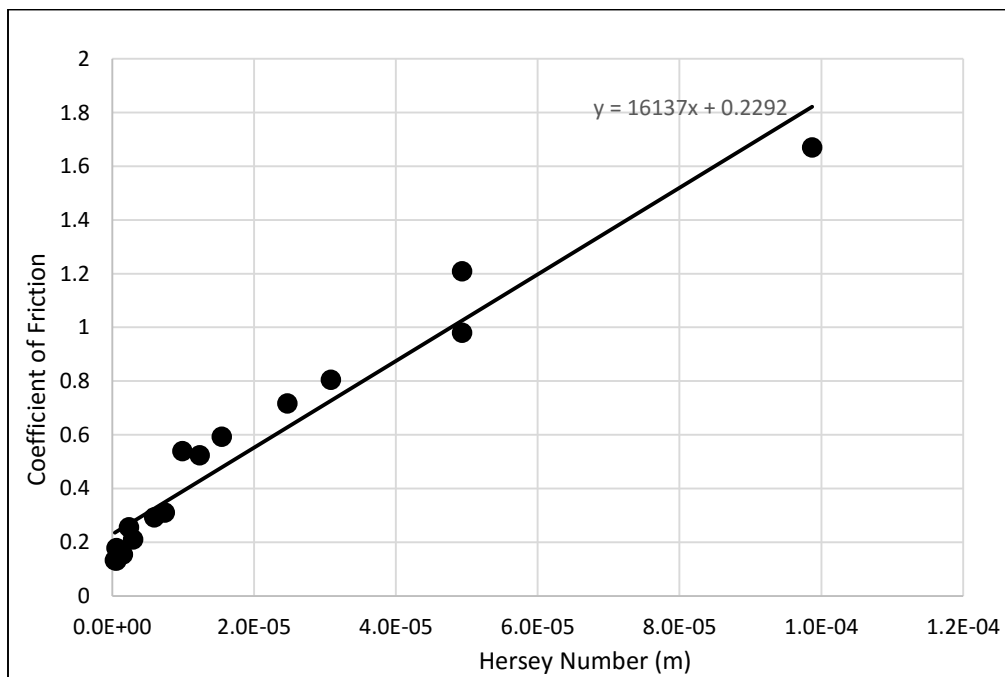


**Figure 6. Experimental Stribeck curve for 5-harness satin carbon/epoxy prepreg oriented at 90° to the direction of slippage**

The Stribeck curves based on the steady state values of frictional resistance, from load-displacement graphs, are shown below.

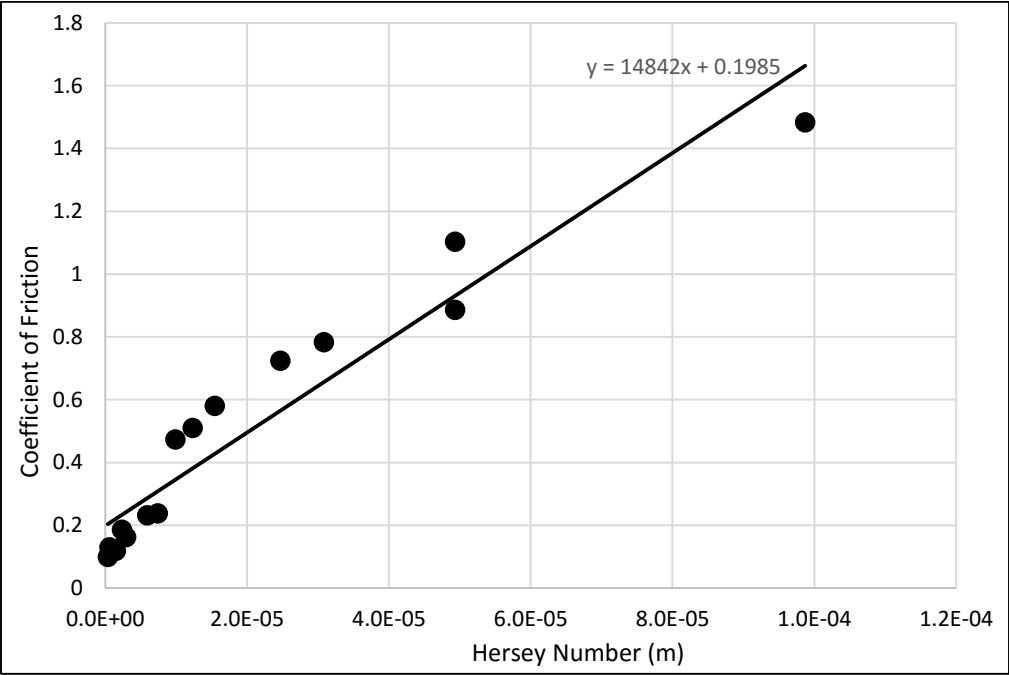


Figure 7. Experimental Stribeck curve for 8HS oriented at 0° to the direction of slippage

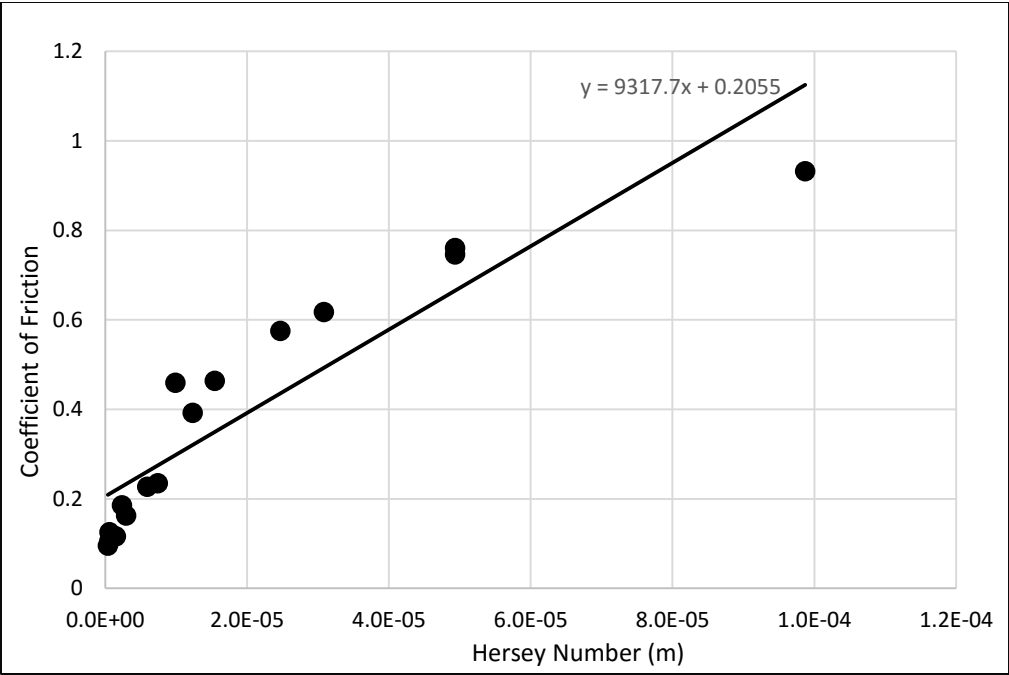
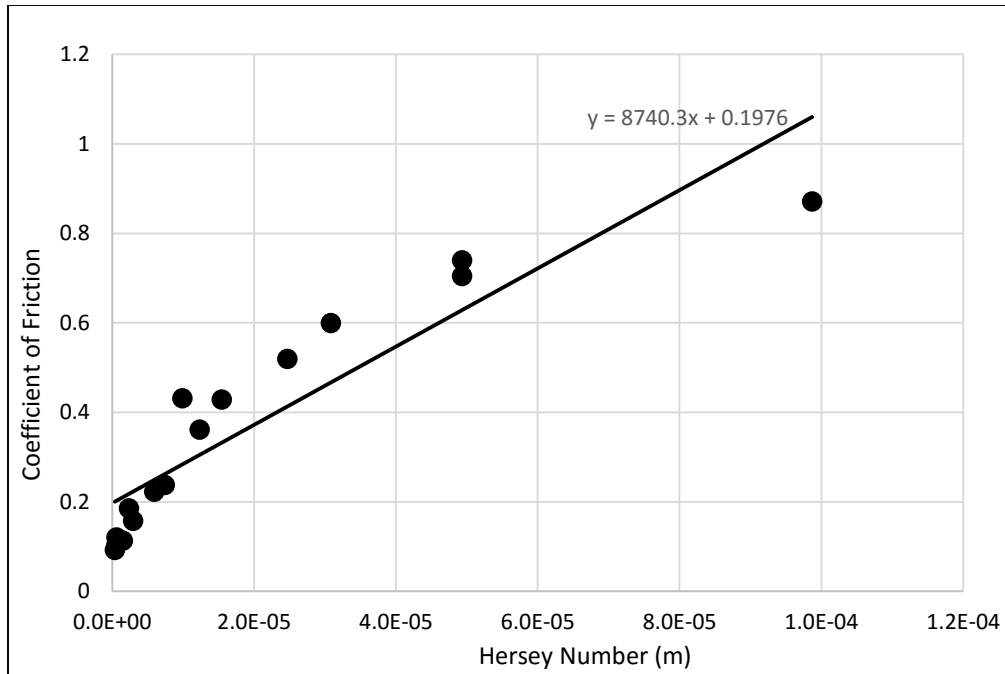
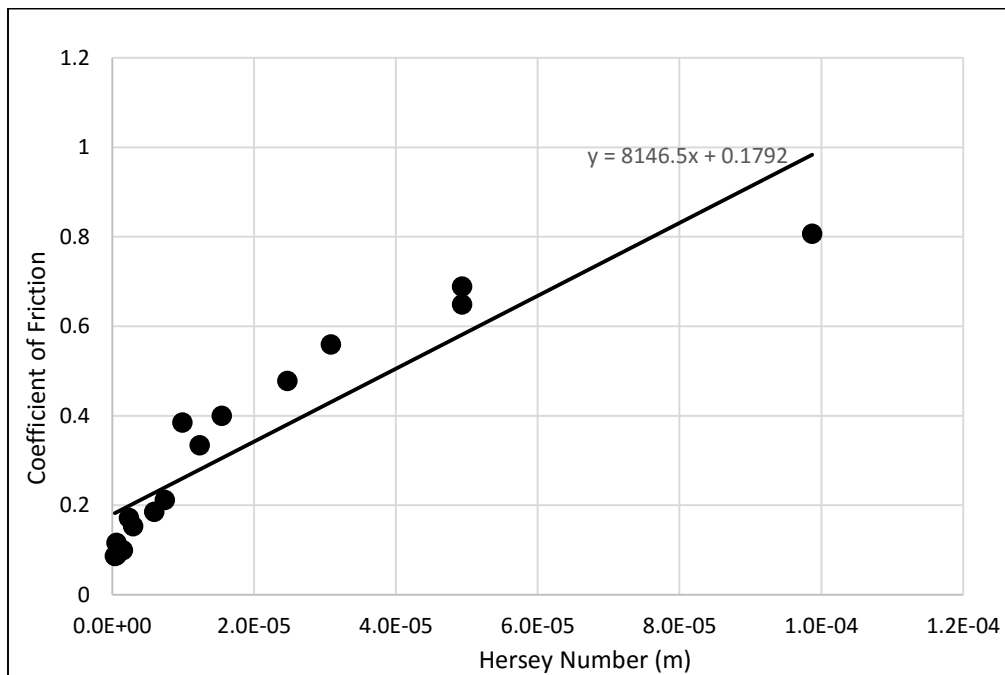


Figure 8. Experimental Stribeck curve for 8HS oriented at 15° to the direction of slippage



**Figure 9. Experimental Stribeck curve for 8-harness satin carbon/epoxy prepreg oriented at 30° to the direction of slippage**



**Figure 10. Experimental Stribeck curve for 8-harness satin carbon/epoxy prepreg oriented at 45° to the direction of slippage**

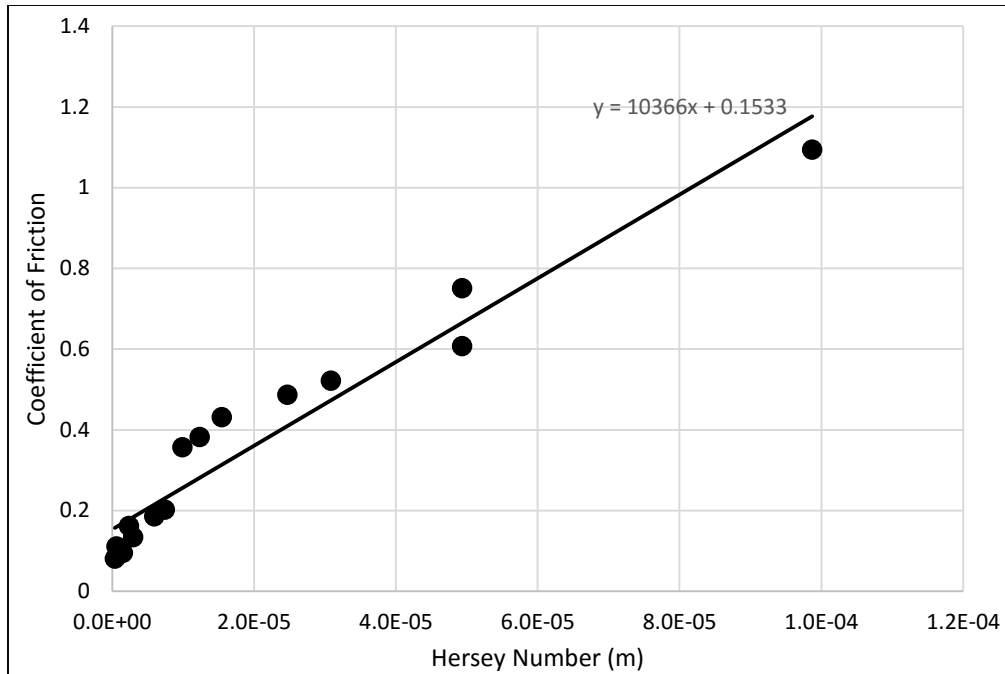


**Figure 11. Experimental Stribeck curve for 5-harness satin carbon/epoxy prepreg oriented at 0° to the direction of slippage**

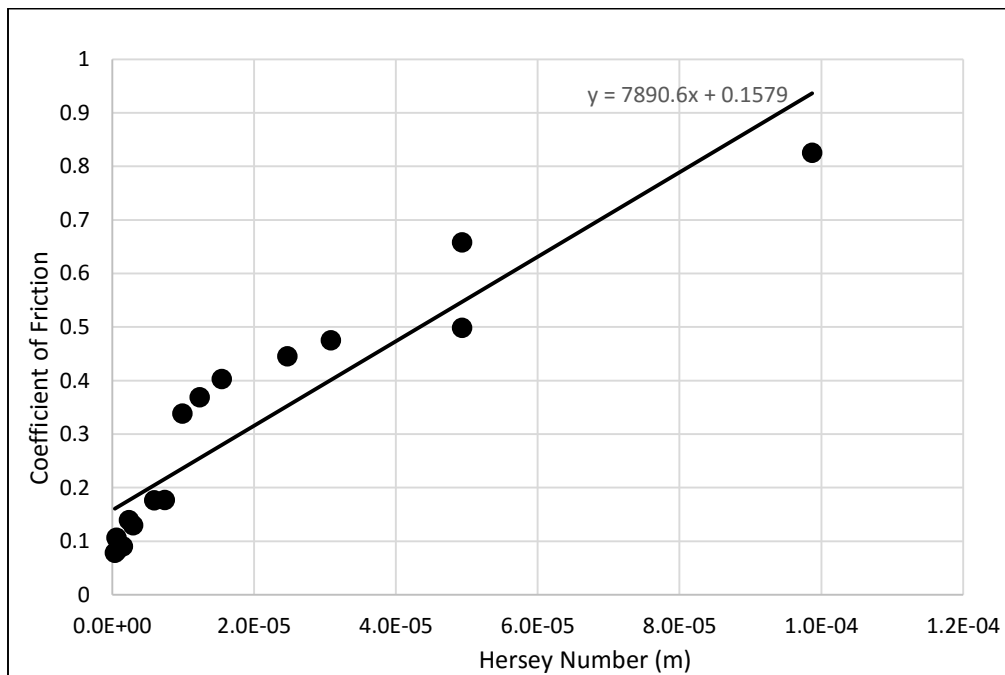


**Figure 12. Experimental Stribeck curve for 5-harness satin carbon/epoxy prepreg oriented at 15° to the direction of slippage**

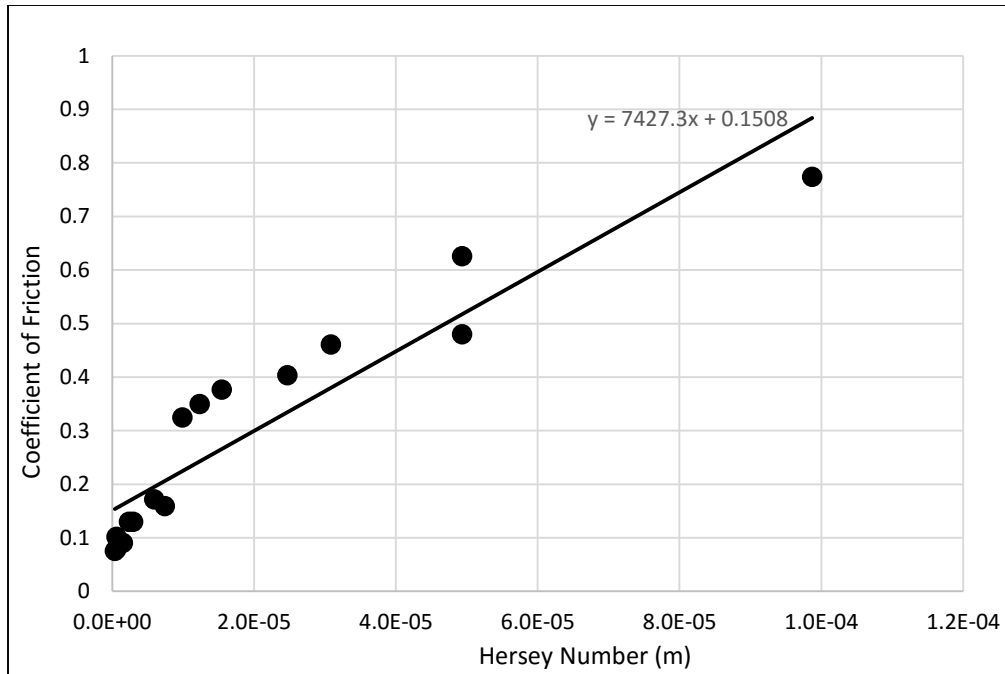


**Figure 13. Experimental Stribeck curve for 5-harness satin carbon/epoxy prepreg oriented at 30° to the direction of slippage**

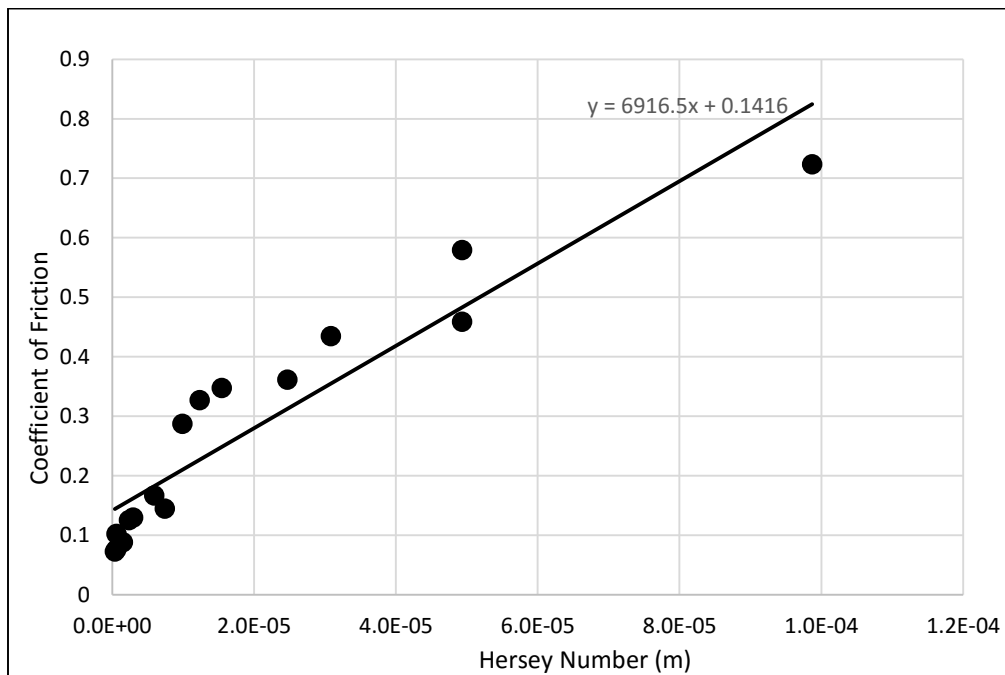


**Figure 14. Experimental Stribeck curve for 5-harness satin carbon/epoxy prepreg oriented at 45° to the direction of slippage**

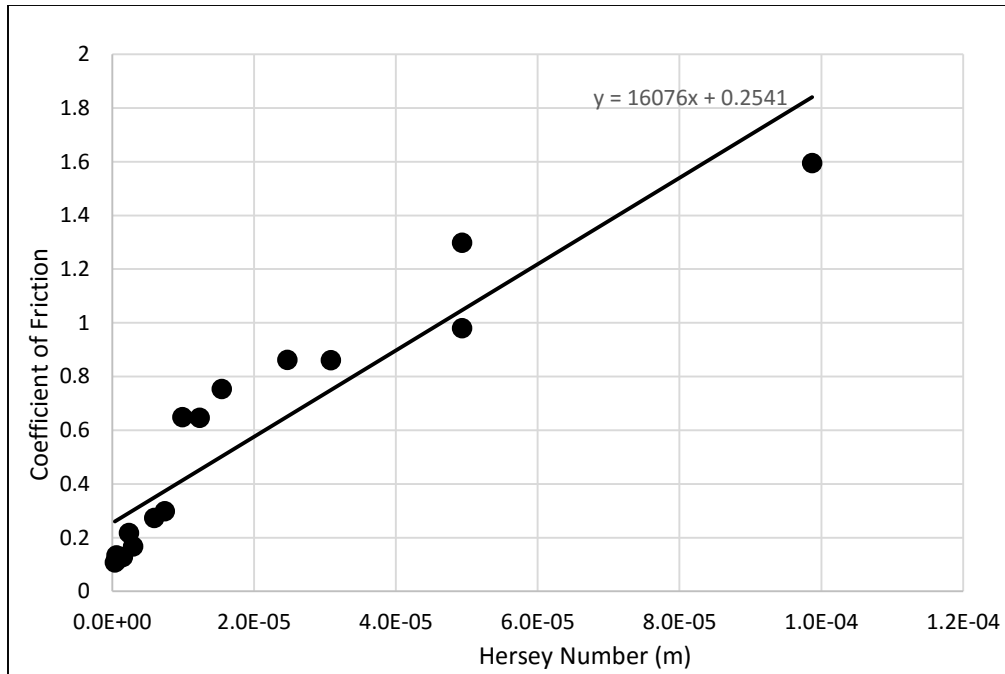


**Figure 15. Experimental Stribeck curve for unidirectional carbon/epoxy prepreg oriented at 0° to the direction of slippage**

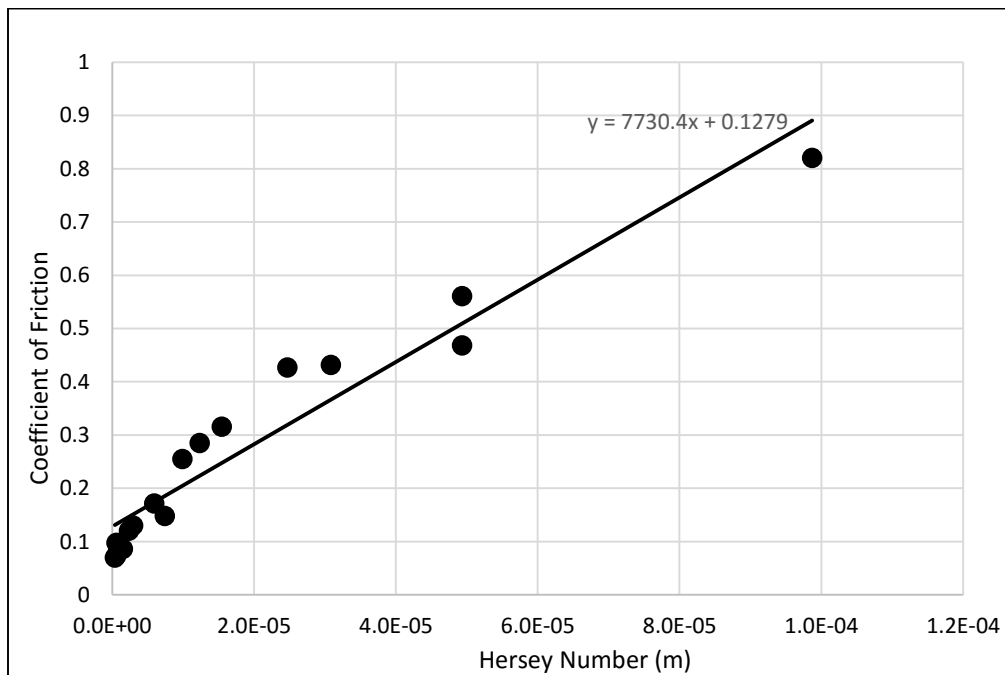


**Figure 16. Experimental Stribeck curve for 8HS/Vacuum Bag**

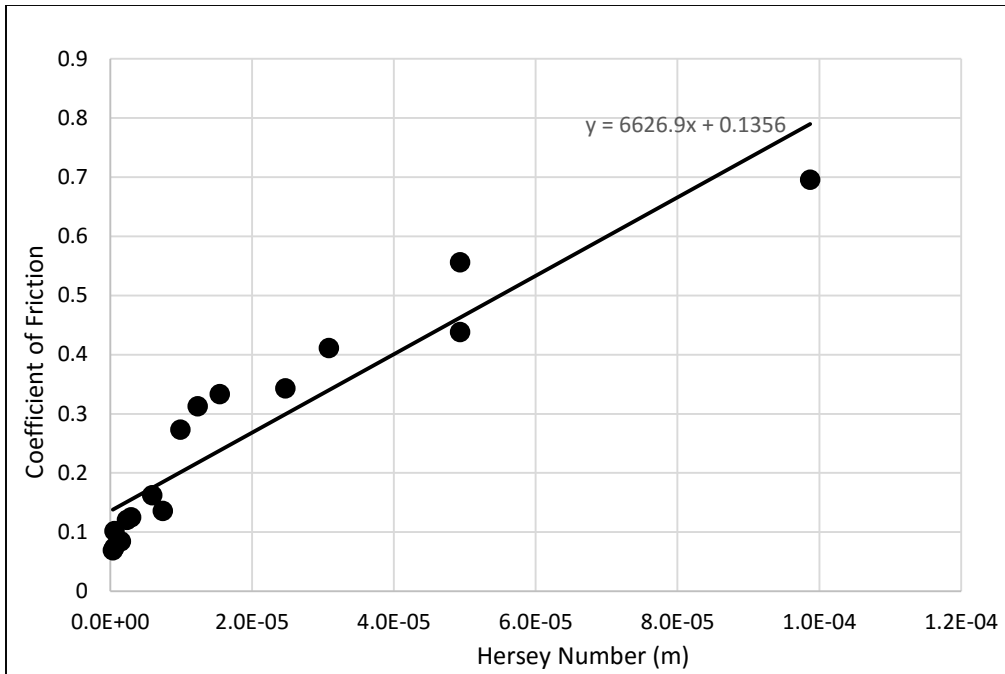


**Figure 17. Experimental Stribeck curve for 5HS/Vacuum Bag**

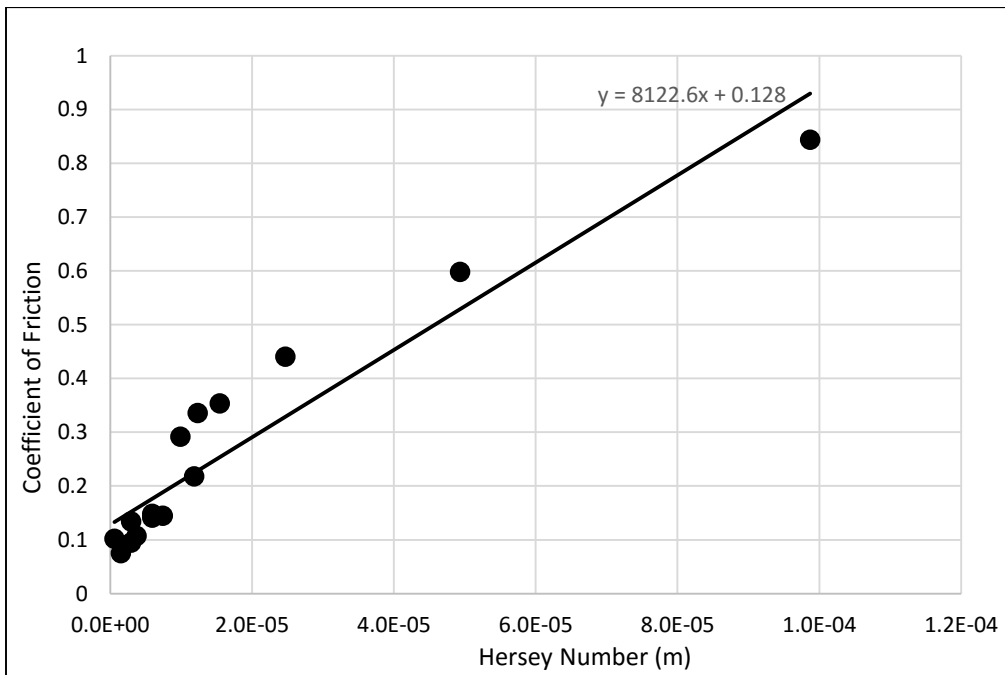


**Figure 18. Experimental Stribeck curve for 5HS/8HS Prepregs**